A STUDY OF THE POLARIZATION OF LIGHT SCATTERED BY VEGETATION

by

Paul Norman Woessner

B. S., University of Maryland, 1982

Submitted to the Graduate Faculty of

Arts and Sciences in partial fulfillment

of the requirements for the degree of

Masters of Science

University of Pittsburgh

1985

A STUDY OF THE POLARIZATION OF LIGHT SCATTERED BY VEGETATION

Paul Woessner, M.S.
University of Pittsburgh, 1985

This study was undertaken in order to better understand the factors that govern the polarization of light scattered from vegetation and soils. This phenomenon is not well understood but is potentially of interest for remote sensing of the earth. The intensity and polarization of light scattered by clover and grass *in vivo* and soil were measured at a number of different angles of incidence and reflectance. Both individual leaves and natural patches of leaves were measured. The light transmitted through the leaves was found to be negatively polarized. The light scattered from the upper leaf surfaces was found to be positively polarized in a manner which could be accounted for qualitatively but not quantitatively by the Fresnel reflection coefficients modified by a shadowing function of the form $\cos^2(g/2)$, where g is the phase angle. Our findings indicate that the polarization of light scattered by vegetation is a more complex process than previously thought, and that besides the surface-scattered component of light, the volume-scattered and multiply-scattered components also contribute significantly to the polarization.

TABLE OF CONTENTS

1. Introduction

A series of measurements of the polarization of a variety of soil and vegetative surfaces has been undertaken. This study is in support of the multilinear array (MLA) project for future earth resources remote sensing missions, such as Landsat. It is of importance to these types of projects for two reasons: 1) it is necessary to know the amount of polarization which is present in natural scenes in order to specify the amount of internal polarization which can be tolerated by the instrument and the accuracy to which the polarization has to be known, and 2) information concerning various properties (e.g. albedo and roughness) of the surface can be obtained using polarization. Also, we would like to test the following hypotheses: 1) Can we predict the bidirectional reflectance of a vegetative surface using the same reflectance laws that describe soils? 2) Can the positive branch of the polarization curve be predicted by simple models that consider only singly-scattered light reflected from the outer surface of the leaf as contributing to the polarization? Finally, we want to see what the relation is between the reflectance and polarization of an individual leaf and of many leaves.

In order to study these questions we measured the reflectance and polarization of a single live leaf at a variety of angles and wavelengths in the near UV, visible and near IR. We compared this data with similar measurements of the reflectance and polarization of leaves in the aggregate. Finally, we attempted to match the data to the theoretical predictions of some simple models.

2. Background

2.1 Polarization of light by planetary regoliths

The seminal work on polarization of light reflected by planetary surfaces was conducted by Lyot (1929). He discovered that the polarization of sunlight scattered from planetary surfaces is only weakly dependent on i, the zenith angle of the incident ray, and e, the zenith angle of the emerging ray. It is determined mainly by the phase angle g, the angle between the source and detector seen from the surface, and the orientation of the scattering plane, the plane containing the source, detector and surface element. The light was found to be linearly polarized in a direction either perpendicular or parallel to the scattering plane.

The scattering plane is characterized by i, e and either g or φ, where φ is the azimuth angle (figure 1). The azimuth angle is defined as the angle between the planes formed by i and e and the normal to the surface. Many workers use φ instead of g, but we chose to use g because it simplifies the equations mathematically. The relation between these four angles is: $\cos g = (\cos i)(\cos e) + (\sin i)(\sin e)(\cos \varphi)$.

We denote the component of any quantity when the direction of polarization is perpendicular to the scattering plane by a (+) subscript and when parallel to the scattering plane by a (-) subscript. Then, denoting the scattered intensity by $I=I_+ - I_-$, the vector polarization P may be written as a scalar: $P=(I_+ - I_-)/(I_+ + I_-)$. Thus, if $P<0$, then P is in the scattering plane, and if $P>0$, then P is

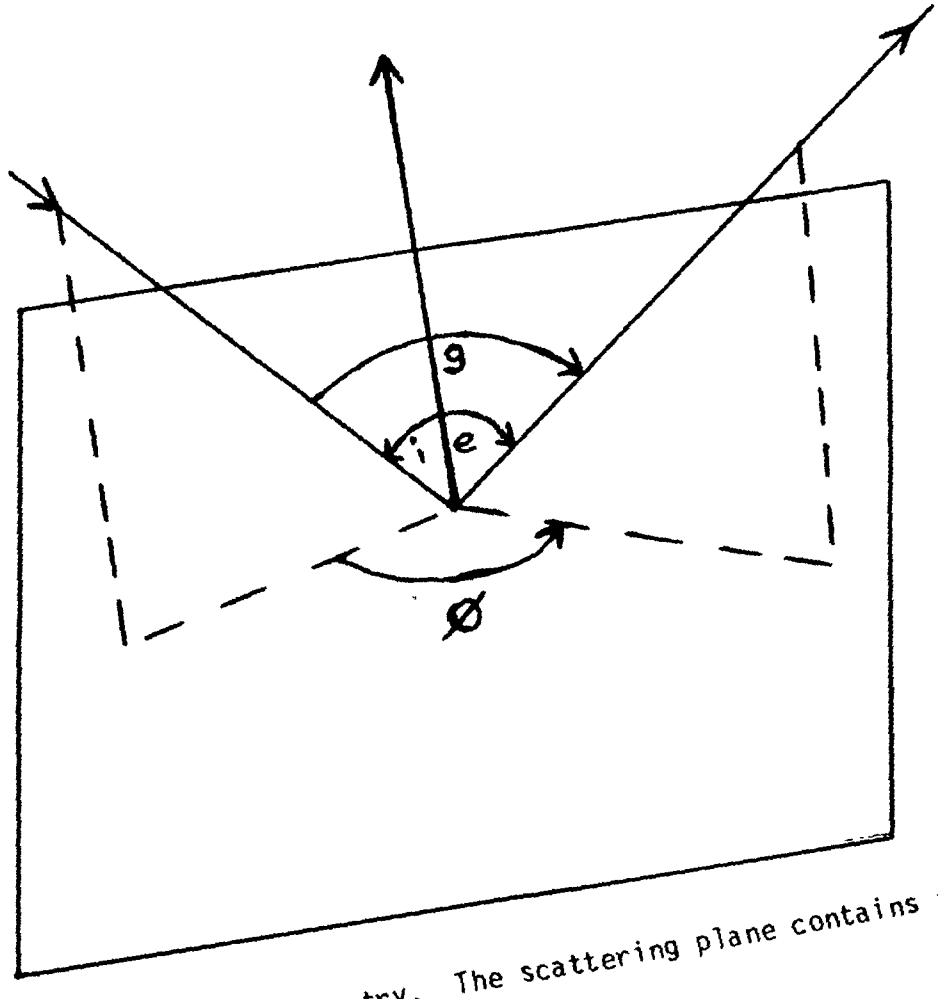

Figure 1: Scattering Geometry. The scattering plane contains the incident and reflected rays.

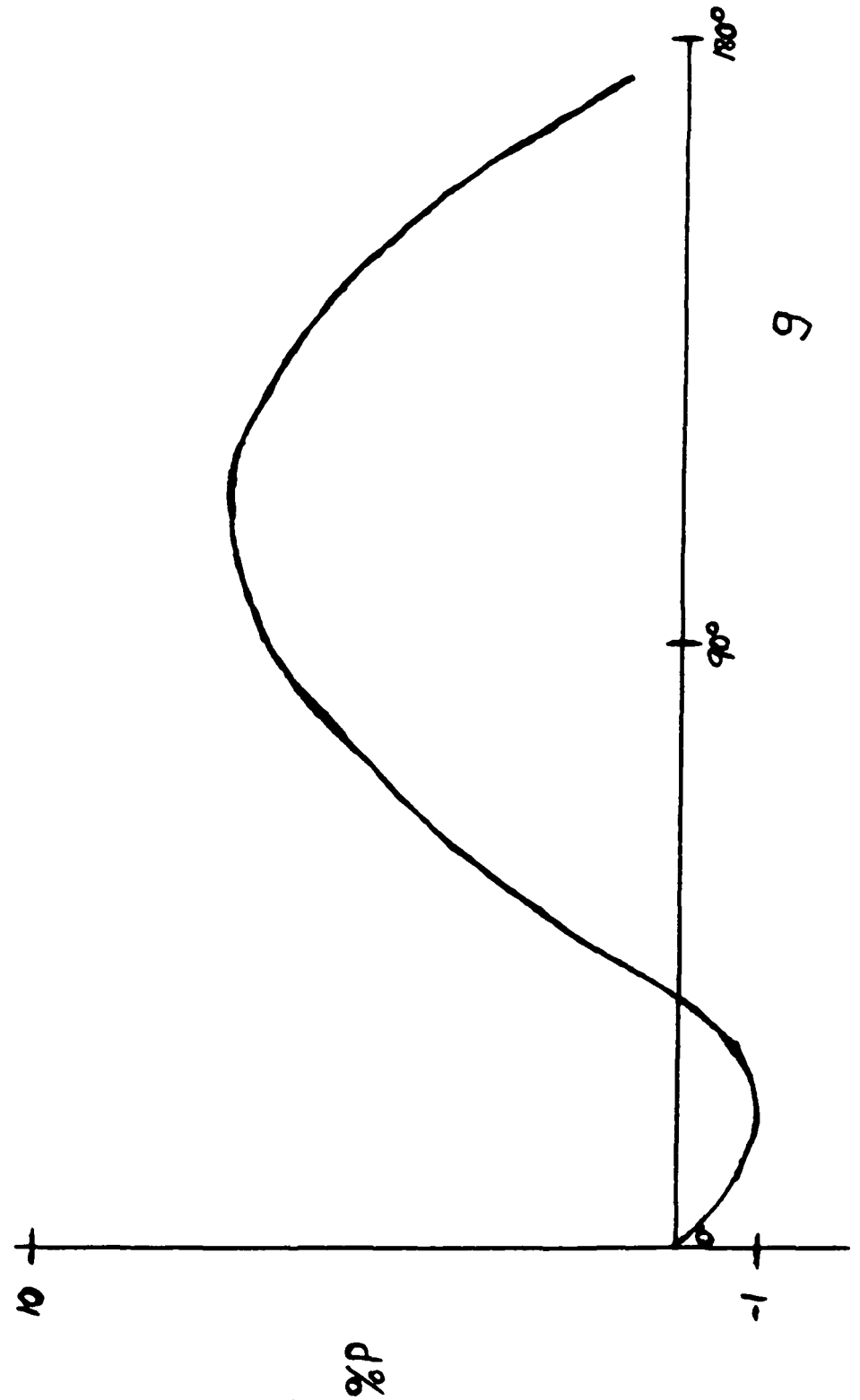

Figure 2: Typical Percent Polarization vs. Phase Angle curve for a planetary surface.

perpendicular to the scattering plane. Lyot found that for particulate surfaces P is determined mainly by g and only secondarily by i and e. A typical curve of P vs. g is shown in figure 2.

The positive branch of the curve may be understood qualitatively as follows (Hapke, 1971). The scattered intensity I is made up of the following components: singly-scattered light reflected from the outer surface of the particles (surface scattered rays) I_s, singly-scattered light that has penetrated into the particles and scattered back out via internal structures (volume scattered rays) I_v, and light that has been scattered by more than one leaf or particle (multiply scattered rays) I_m. Thus, $I=I_s+I_v+I_m$; I_v and I_m should be weakly polarized, but I_s is described approximately by the Fresnel expressions for specular reflection, and its two components perpendicular and parallel to the scattering plane, I_{s+} and I_{s-} respectively, may be quite different. Thus in the first approximation, if the illuminance J is unpolarized:

$$I_+=J_+r_+=.5J(I_{s+}+I_v+I_m),$$

$$I_-=J_-r_-=.5J(I_{s-}+I_v+I_m),$$

$$P=(I_+-I_-)/(I_++I_-)$$

$$=.5J[(I_{s+}+I_v+I_m)-(I_{s-}+I_v+I_m)]/\ .5J[(I_{s+}+I_v+I_m)+(I_{s-}+I_v+I_m)]$$

$$=[(I_{s+}-I_{s-})/2]/[((I_{s+}+I_{s-})/2)+I_v+I_m].$$

It can be shown (Hapke, 1981; also see section 4 of this thesis) that I_s and I_v consist of functions of g multiplied by the same functions of i and e. Therefore, for low albedo surfaces, where I_m is negligible, the i and e dependence cancels in the numerator and denominator, and P is rigorously a function of g only. As the albedo increases, I_m becomes important, and since I_m has a different

dependence on i and e than I_s and I_v, P becomes somewhat dependent on i and e. Also, P will be large when only I_s is important, but as the albedo increases, so do I_v and I_m and the polarization decreases. Thus, there is an inverse relation between the amplitude of the positive branch and the albedo; this general relation is known as the "Umov effect" after a Russian astronomer who first noted it on the moon.

The negative branch of the curve, on the other hand, is poorly understood. It seems to be present if a surface is particulate and porous. It is not present or weakly developed if the particles are too close together or too far apart. It is thought to involve double surface scattering in which the plane of polarization is rotated preferentially by 90° (Wolff, 1975), but may also involve light transmitted by the particles, which tends to be negatively polarized because of the differences between the Fresnel transmission coefficients at the particle surfaces.

2.2 Polarization of light by vegetative surfaces

One of the main objectives of this study is to see whether models developed for the polarization of light by vegetative surfaces are compatible with those developed to interpret astrophysical planetary data. The astrophysical models make no assumptions about the nature of the particles, only that the surface consists of discrete, irregularly shaped scatterers that are large compared with the wavelength. For example, the leaves, stalks and heads of the

vegetation could be considered as "particles" of the surface. Lyot (1929) first made polarization measurements of vegetation with the thought of possible application to Mars.

More recently, several studies have shown that the vegetative models seem to be compatible with the astrophysical ones. Egan and Hallock (1966) made measurements of broad-leaved evergreens because they were interested in being able to identify trees that were hard to distinguish individually. They made measurements on rhododendron, pine, holly and also grass in two bands, green (540 nm) and IR (1000 nm). Their curves were quite similar to those of various minerals (e.g. rose quartz, pumice, ilmenite) that they measured. They concluded that the most significant features of the polarization curve are: the phase angle at which inversion of P takes place and the general slope and maxima of both positive and negative P. Finally, they remarked that when color measurements (e.g. spectral bidirectional reflectance) are added as clues it seems quite possible that the presence and state of growth of pine, deciduous trees and grass, among other features, may be analyzed much beyond the image resolution capability of the observing optical system.

Curran (1982) has recently undertaken an aerial reconnaissance study of the polarization from an area of heathland, which includes the following vegetative types: open heath, birch scrub, woodland, bog and grass. He states that it is known from previous laboratory and field studies that the degree to which light is linearly polarized is negatively correlated with surface roughness, and to a lesser extent radiance; i.e., light, rough and diffusely

reflecting surfaces polarize radiation less than dark, smooth and specularly reflecting surfaces. He further states that polarized visible light (PVL) has been used by researchers to discriminate between rough and smooth vegetation canopies. He concludes by saying that his experiment clearly demonstrates that PVL is a valuable source of remotely sensed data for the discrimination of land cover.

Vanderbilt (1980) presented a model that attempts to explain the amount of linearly polarized light reflected by a plant canopy. This model is similar to astrophysical models in that it assumes the polarization comes from reflectance off the surface of a leaf, although it is more complicated mathematically since it uses φ instead of g. Vanderbilt states that examination of the model suggests that, potentially, satellite polarization measurements may be used to monitor crop development stage, leaf water content, leaf area index, hail damage and certain plant diseases. He goes on to say that such information is needed for use with models which predict crop grain yield.

Vanderbilt et. al. (1982) investigated how visible light is linearly polarized and reflected by a wheat canopy as a function of sun-view directions, crop development stage and wavelength. They found that the linearly polarized light from the canopies is generally greatest in the azimuth direction of the sun and trends toward zero as the angle of incidence of sunlight trends toward zero degrees. They claim that the variation of the angle of incidence of sunlight on the leaf explains almost all of the variation of the amount of polarized light with sun-view direction. However, this conclusion is

very difficult to understand if the discussion in section 2.1 above is valid.

2.3 Landsat

Landsat is an earth resources satellite collecting data for use in the following areas: oil and mineral exploration, agriculture, land use planning, forestry, water management, map making, etc. The spacecraft is in a near-polar, sun-synchronous orbit of 920 km with an inclination of 99° and period of 103 minutes; this allows the spacecraft to map the entire planet every 18 days (Lintz and Simonett, 1976). The detectors on the satellite are: Return Beam Vidicon (RBV), Multispectral Scanner (MSS) and starting with Landsat 3, the Thematic Mapper (TM). The wavelength channels used by the detectors can be found in table 1.

Using the TM, the following vegetative properties can be distinguished (Myers, 1983):

1) TM-1: This band is used mainly for differentiation between soils and vegetation and deciduous or coniferous foliage.
2) TM-2: Low pigment content, which include chlorophyll, carotenoids and anthocyamins, often results in higher reflectance. Senescence and nitrogen status of vegetation are two of the properties studied in this region.

Table 1: Landsat Bands

Detector	band #	wavelength interval (nm)
RBV	1	475 - 575
	2	580 - 680
	3	698 - 830
MSS	1	500 - 600
	2	600 - 700
	3	700 - 800
	4	800 - 1100
TM	1	450 - 520
	2	520 - 600
	3	630 - 690
	4	760 - 900
	5	1550 - 1750
	6	10,400 -12,500
	7	2080 - 2350

3) TM-3: Relative radiance spectra for agricultural scenes, including soils and agriculture cover types, show the greatest contrast in this band.

4) TM-4: The near-IR wavelength region is the best spectral band in which to distinguish plants and plant conditions. Reflectance in the 700-1350 nm wavelength interval is controlled by the lack of pigment absorption and by the lack of absorption by liquid water. Reflectance changes are associated primarily with changes in the size and shape of cells and intercellular spaces, and perhaps, with other physiological changes in leaf structures. Healthy leaves have high IR reflectance as compared with low IR reflectance with unhealthy leaves.

5) TM-5: Plant stresses have been detected in the 750-2500 nm band in the near-IR region through changes in leaf structure and water content.

6) TM-6: Thermal emission data is obtained in this band.

7) TM-7: Reflectance from 2080-2350 nm decreases as leaf-tissue content increases.

2.4 The Leaf

2.4a Internal Structure

The following description of the internal structure of a leaf was taken from van Nostrand's Encyclopedia (Considine, 1983). Covering the entire surface of the leaf is the epidermis, a layer of tabular cells

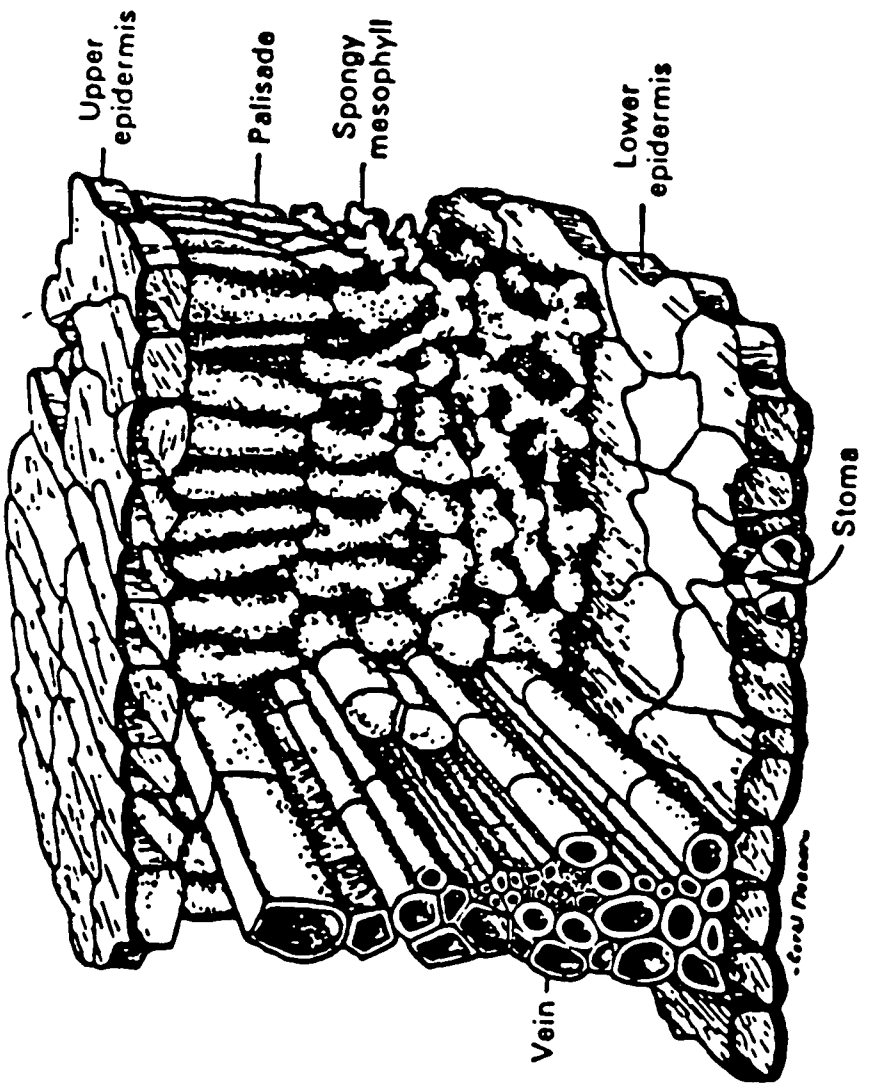

Figure 3: A portion of the blade of a leaf cut so as to show the internal structure. The cell contents are not shown (after Considine, 1983).

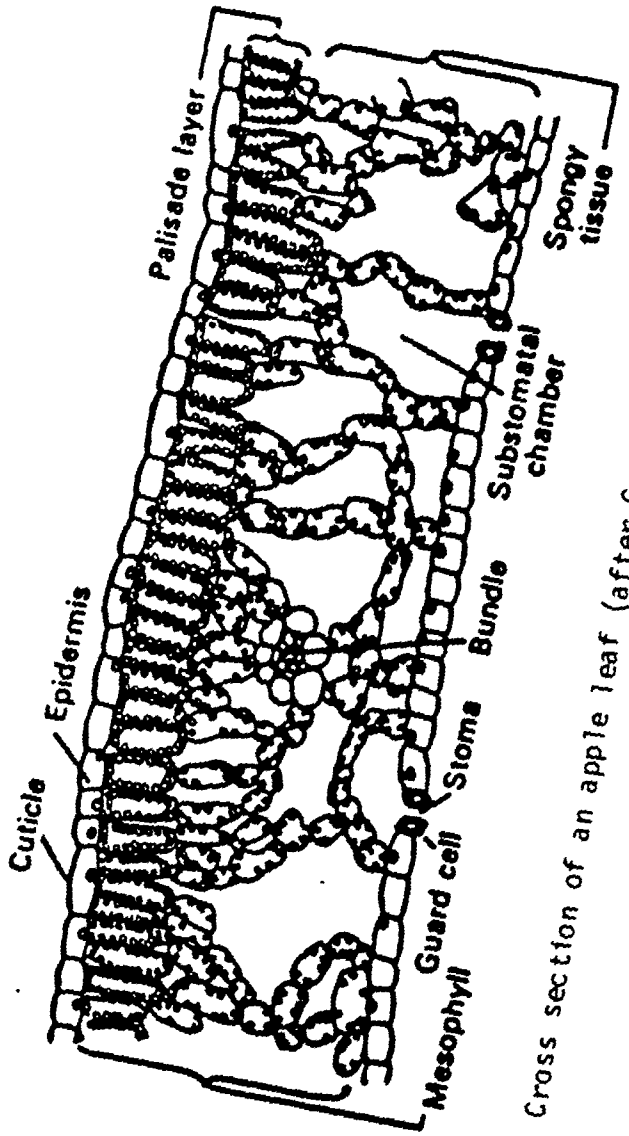

Figure 4: Cross section of an apple leaf (after Considine, 1983).

(cf. figure 3). On the upper surface of the leaf, the epidermal cells are frequently covered with a layer of cutin, a waxy substance which is impervious to water. Usually, there are no chloroplasts present in the epidermal cells. In the epidermis of the leaf, particularly the lower surface, there are many minute openings, called stomata, which permit a ready exchange of gases between the interior of the leaf and external air. Each stoma is surrounded by a pair of guard cells containing chloroplasts. These cells close the stoma by collapsing and open it by expanding. All cells occurring between the upper and lower epidermal layers are called mesophyll cells (cf. figure 4). Beneath the upper epidermis the mesophyll cells form a very distinct layer, called the palisade mesophyll, which are elongated cells with their long axis perpendicular to the surface of the leaf. They contain large numbers of chloroplasts. Occupying the rest of the leaf is a loose tissue composed of irregularly arranged rounded cells known as the spongy mesophyll. Numerous intercellular spaces separate these cells from one another.

Occurring throughout the leaf, just below the palisade cells, are the veins. Each vein is composed of three types of cells: 1) thick-walled xylem cells (towards the top of the leaf) that carry water and dissolved mineral matter to all parts of the leaf, 2) phloem cells (towards the bottom of the leaf) that carry food away from the green cells of the leaf where they are elaborated and 3) outside these, and often forming a conspicuous tissue are the masses of fibers called collenchyma, which are thick-walled cells that give support to the leaf.

2.4b Light Interaction with Leaves

The spectral reflectance properties (Raines and Carey, 1980) of a leaf in the 400-2500 nm region of the spectrum are a function of the leaf pigments, primarily the chlorophyll pigments, the leaf cell morphology, internal refractive index discontinuities and the water content.

The pigments of the chlorophyll group are the primary control from 400-700 nm, the cell morphology and internal refractive index discontinuities are the primary controls from 700-1300 nm and the water content is the major control in the 1300-2500 nm region.

On a spectral absorptance curve (figure 5) of a leaf the maxima near 450 nm and 680 nm are due primarily to absorption by chlorophyll a; however, absorption bands may also be broadened due to other chlorophyll bands. Various other leaf pigments (e.g. carotenoids) also may contribute to broadening the absorption bands near 450 nm. The high reflectance region from 700-1300 nm is due to lack of absorption bands plus refractive index discontinuities within the leaf. The primary type of discontinuity is the internal air-cell interfaces of a leaf. However, leaf components, stomata, nuclei, cell walls, crystals and cytoplasm also produce significant refractive index discontinuities that contribute to the reflectance of a leaf. In the region from 1300-2500 nm the spectral reflectance curve of a leaf is similar to a transmission spectrum of pure water, and the curve can be matched to that of an equivalent thickness of water.

Described below (Myers, 1983) are several other properties of leaves that may affect their reflectance of light. It has been shown

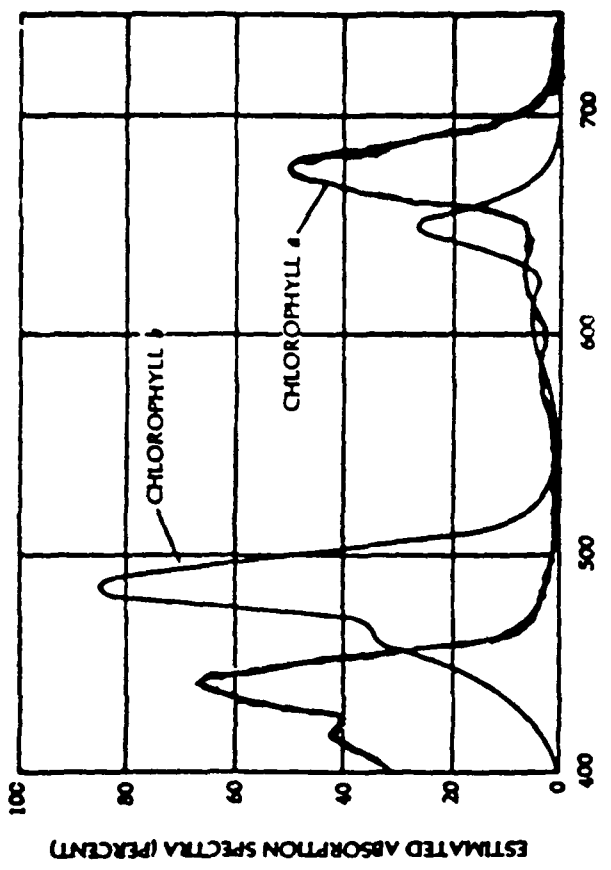

Figure 5: The estimated absorption spectra of chlorophyll a and chlorophyll b within the chloroplast (after Curtis, 1983).

that lower leaf surfaces of dorsiventral leaves (e.g. clover) have higher reflectance values than upper leaf surfaces, which indicates two things: 1) the spongy parenchyma contribute more to light scattering than the palisade parenchyma and 2) that the chloroplasts in the palisade cells absorb light.

The absorption, reflection and transmission of electromagnetic radiation by leaves is a function of the wavelength of that radiation (Tucker and Garratt, 1977). Four principal leaf characteristics determine the related three final states:

1) Internal leaf structure or the histological arrangement of tissues and cells is responsible in part for the diffusion or internal scattering of incident solar irradiance. Spectral absorptance, reflectance and transmittance are thereby greatly determined by the mean optical pathlength of incident radiation.
2) The pigment composition, concentrations and distributions control the absorption of UV and visible radiation.
3) The concentration and distribution of leaf water control the absorption of radiation in the IR region of the spectrum.
4) The surface roughness characteristics and the refractive index of the cuticular wax of the upper epidermis control the spectral reflectance from this surface.

Scattering of electromagnetic radiation in leaves is a complex phenomenon (figure 6) caused by the cytoplasmic contents, refractive index differences, irregular cellular shapes and various geometric organizations of tissues. Scattering, possibly analagous to Rayleigh scattering, may occur for particles of the incident radiation;

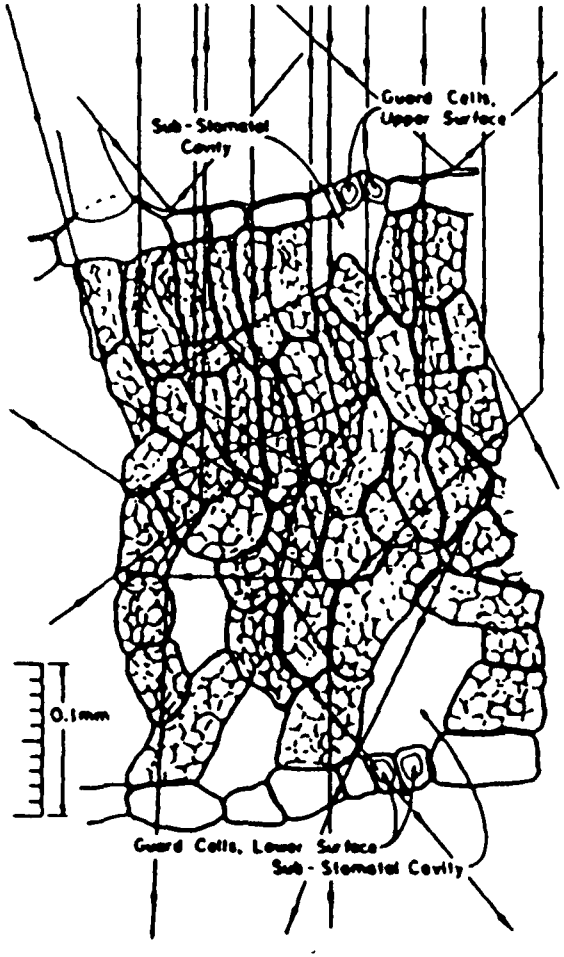

Figure 6: Cross section of a Mimulus cardinalis leaf showing possible paths for light rays which are critically reflected at cell walls within the leaf. The chloroplasts can be seen within the mesophyll cells (after Gates et. al., 1965).

e.g., the long, slender strands called grana, which are in chloroplasts and contain chlorophyll. Finally, Tucker and Garratt state that refractive-reflective scattering predominates in the leaf scattering mechanism and is principally due to cell wall-air space refractive index differences.

Senescence is deterioration in plant leaves, flowers, fruits, stems and roots as they near the end of their functional life (Myers, 1983). As a leaf senesces it suffers a loss of water and pigments, which increases the volume-scattered component of light in the leaf. Also, the increase in the refractive index of the leaf due to water loss increases the surface-scattered component of light. Therefore, we expect the reflectance to increase in all bands, particularly red and blue. According to Myers, as broad leaves senesce, their light reflectance usually increases markedly in the 550 nm (green) wavelength region because of chlorophyll degradation. Finally, since nitrogen nutrition of plants markedly affects pigment concentration, it has been found (Myers, 1983) that a reduced amount of nitrogen in a plant causes a reduction in pigment concentrations and therefore an increase in reflectivity in the chlorophyll bands because of decreased radiation absorptance.

3. Experimental

3.1 Apparatus

The measurements of the polarization of the various soils and vegetation were undertaken using a photo-polarimetric goniometer in the planetary surfaces laboratory at the University of Pittsburgh. This goniometer uses a photomultiplier with an S-20 photocathode as the detector, a quartz-iodine incandescent lamp as the source, plus interference filters which allow it to cover the range from about 350-820 nm. The filters used were: 448 nm (blue), 554 nm (green), 690 nm (red) and 820 nm (IR). A UV filter (353 nm) was found to have a red leak and was not used. The blue and red filters are centered on the chlorophyll a absorption bands, with the green filter lying between these two bands, and the IR band lying to the long wavelength side of the chlorophyll bands. The source, detector and the normal to the surface all lie in one plane. The laboratory instrument is not portable and has a field of view of about one inch. Therefore, it can be used to study only those soils and vegetation with small physical elements.

3.2 Vegetation chosen

Ordinary clover, trifolium repens (white or Dutch), was chosen for a detailed investigation. This plant was chosen because we wished to investigate the scattering properties of individual leaves,

as well as leaves in the aggregate, and the leaves are small enough that one can fit into the field of view of the photo-polarimeter. Also, this vegetation is of widespread occurrence. A patch of grass was also examined. Finally, part of a leaf of corn (Zea mays) was examined because corn is a widely grown crop. We also examined the soil that the clover was growing in.

3.3 Method

Pressed halon was used as a standard for the measurements. Halon is the trade name for polytetrafluoroethylene powder. It has a reflectance of 99% or higher in the wavelength region of interest here and is commonly used in diffuse reflectance spectrophotometry (Weidner and Hsia, 1981). Before each set of measurements were made through a given filter, halon was observed with the instrument set at e=0° and i=5°, and the polarizer at 45°. The high voltage power supply and db gain were set so that the output from the halon standard was approximately 10 volts.

Unless otherwise stated, all leaves and patches of plants were measured *in vivo*, with the leaf attached to its parent plant and the plant growing in the soil. When a leaf was measured lying horizontally, it was pressed flat and then taped to black velvet cloth covering the top of the specimen stand using black tape. This was done to minimize spurious background light. When the leaf was measured vertically its stem was positioned so the top of the leaf faced horizontally in the direction of the source. When

Table 2: Measurement Configurations

Sample	e (°)	i (°)
Clover		
leaf horiz.	80 to -80 (every 10°)	0, 30, 60
leaf vert.	"	0, 45, 90
patch	"	0, 30, 60
dry leaf	"	0, 60
Grass patch	"	0, 60
Corn leaf, horiz.	"	0, 60
Soil		
Baked	0, 60	70 to -70 (every 10°)
Natural	"	"
Moist	"	"

measurements were taken on the clover patch, the stand was removed and the patch placed naturally so that the light fell near its center. Black velvet was placed over the soil in which the plant was growing. Measurements were also made on a clover patch that had gone for a week without water so the clover leaves would dry out and turn brown. Then I cut one of the dry leaves off and measured it in the horizontal position. The polarization of a patch of grass was also measured and the grass handled in the same manner as the patch of clover. A part of a corn leaf was studied in the horizontal position. Finally, we examined the soil that the clover grew in. It was studied in a natural state, baked to a temperature between 100-250° C, and moistened by water.

The measurements were taken according to table 2. At each angle, all four filters were used. Each measurement was taken with the polarizer in the 0° (I+) and 90° (I_) position. The percent polarization was then calculated using $\%P = [(I_+ - I_-)/(I_+ + I_-)] \times 100\%$, and the reflectance, relative to the standard, from $r = (I_+ + I_-)/(2I_{standard})$.

4. Results

4.1 Data

The reflectance and polarization of the clover, grass, corn and soil data are presented in figures 7-15. In the figures, e is positive when the detector is on the same side of the normal as the source

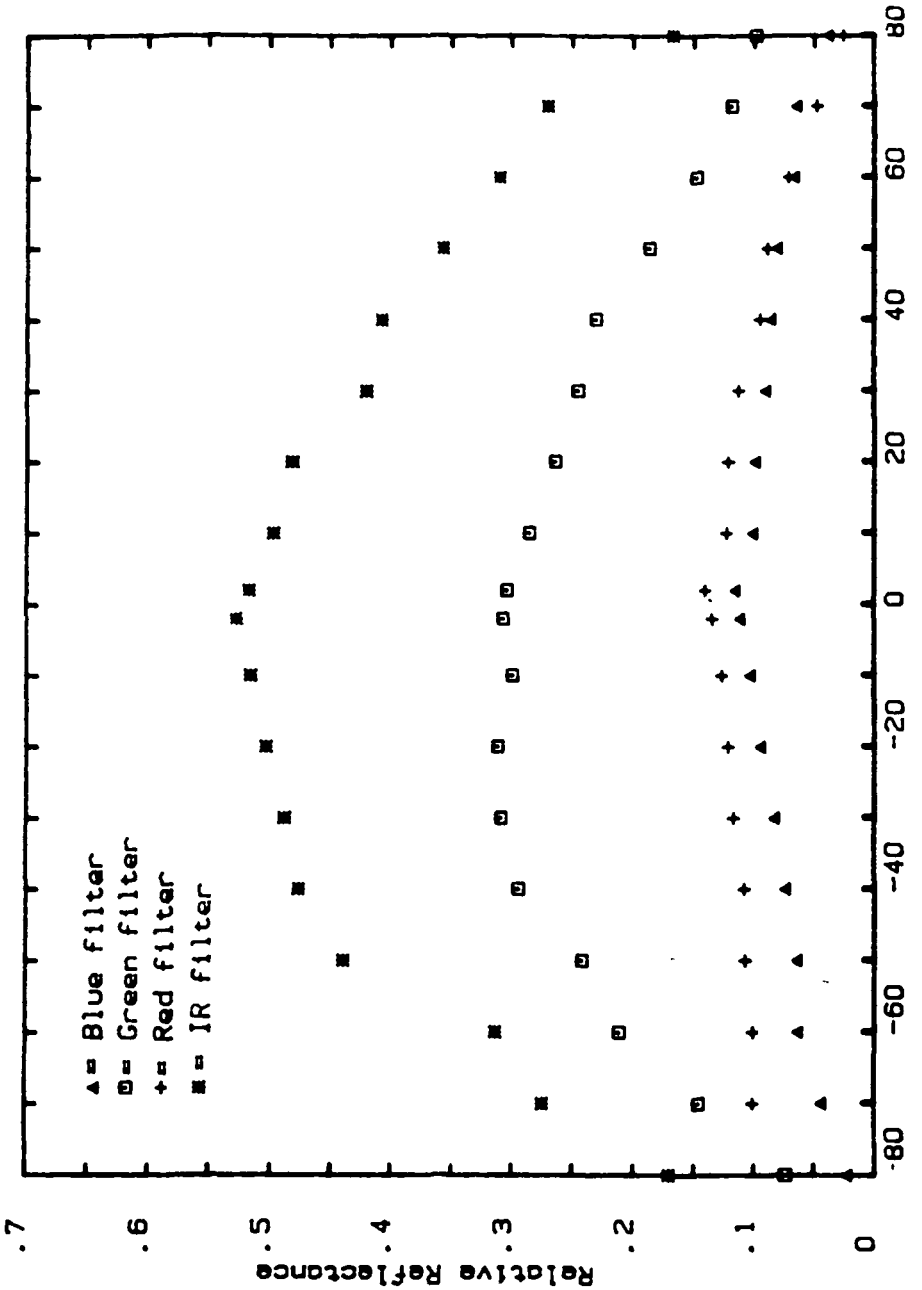

Figure 7a: Relative Reflectance vs. Angle of Emergence. Looking at a live clover leaf in the horizontal position at i=0°.

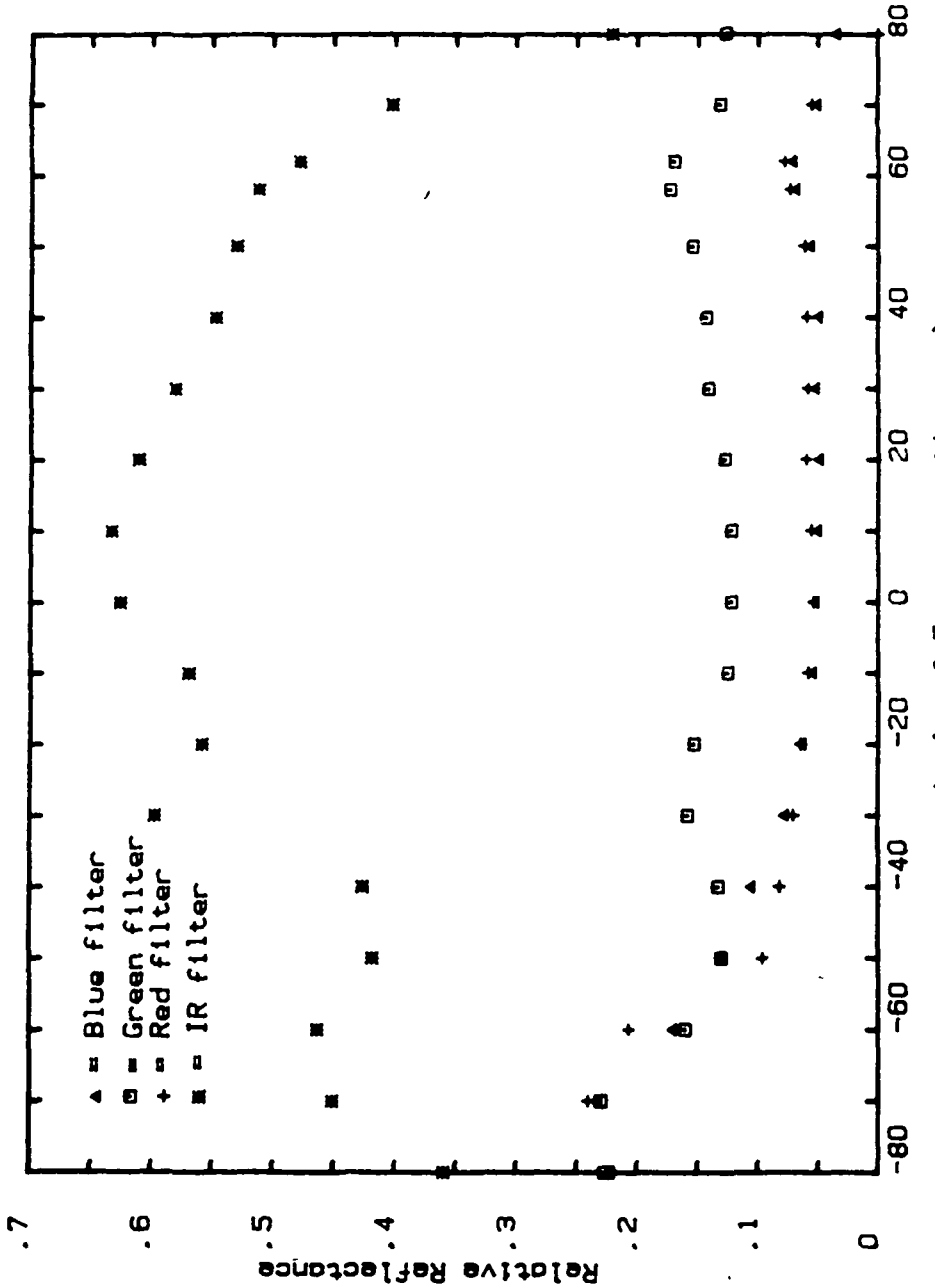

Figure 7b: Relative Reflectance vs. Angle of Emergence. Looking at a live clover leaf in the horizontal position at i=60°.

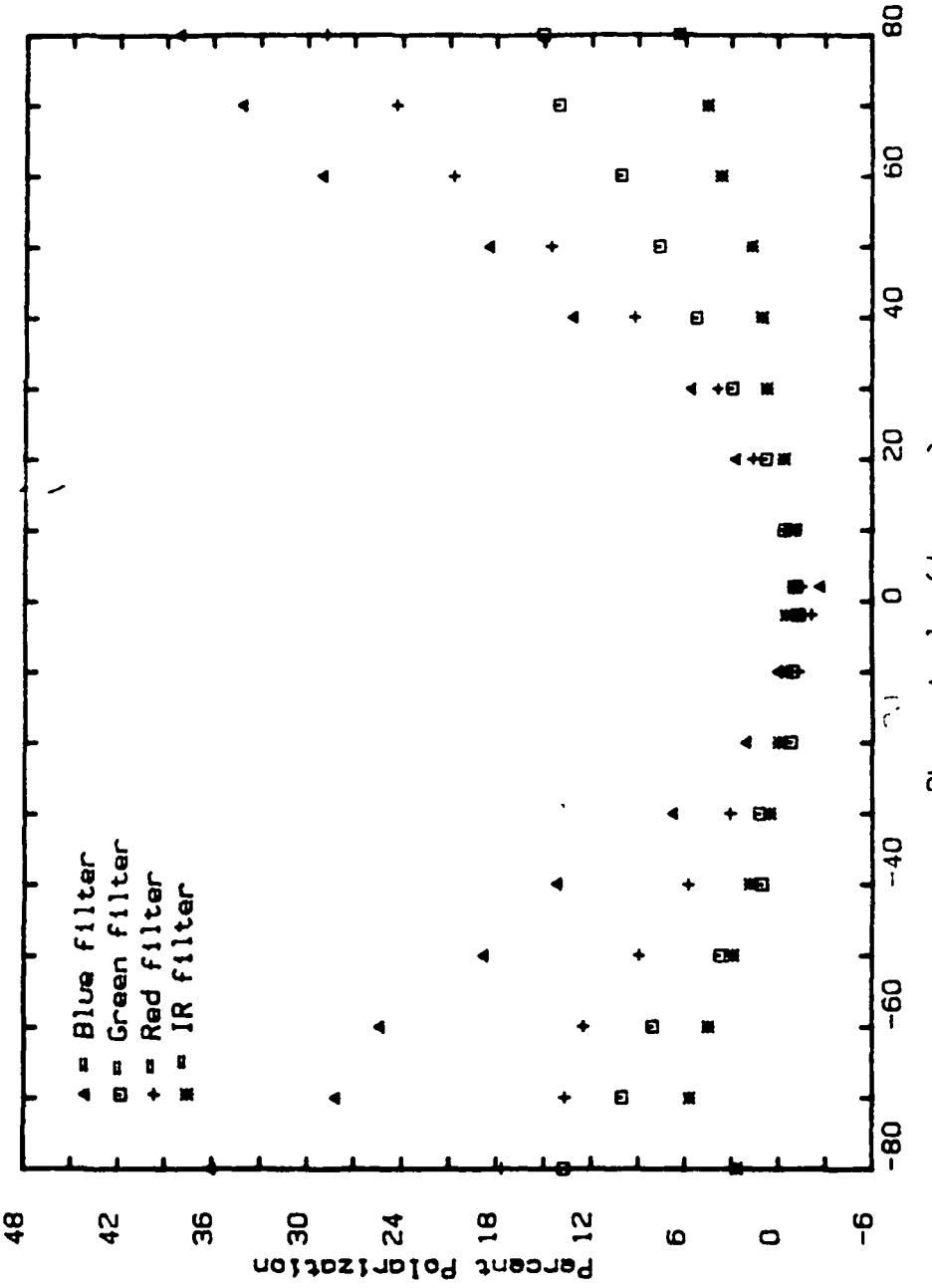

Figure 7c: Percent Polarization vs. Phase Angle. Looking at a live clover leaf in the horizontal position at i=0°.

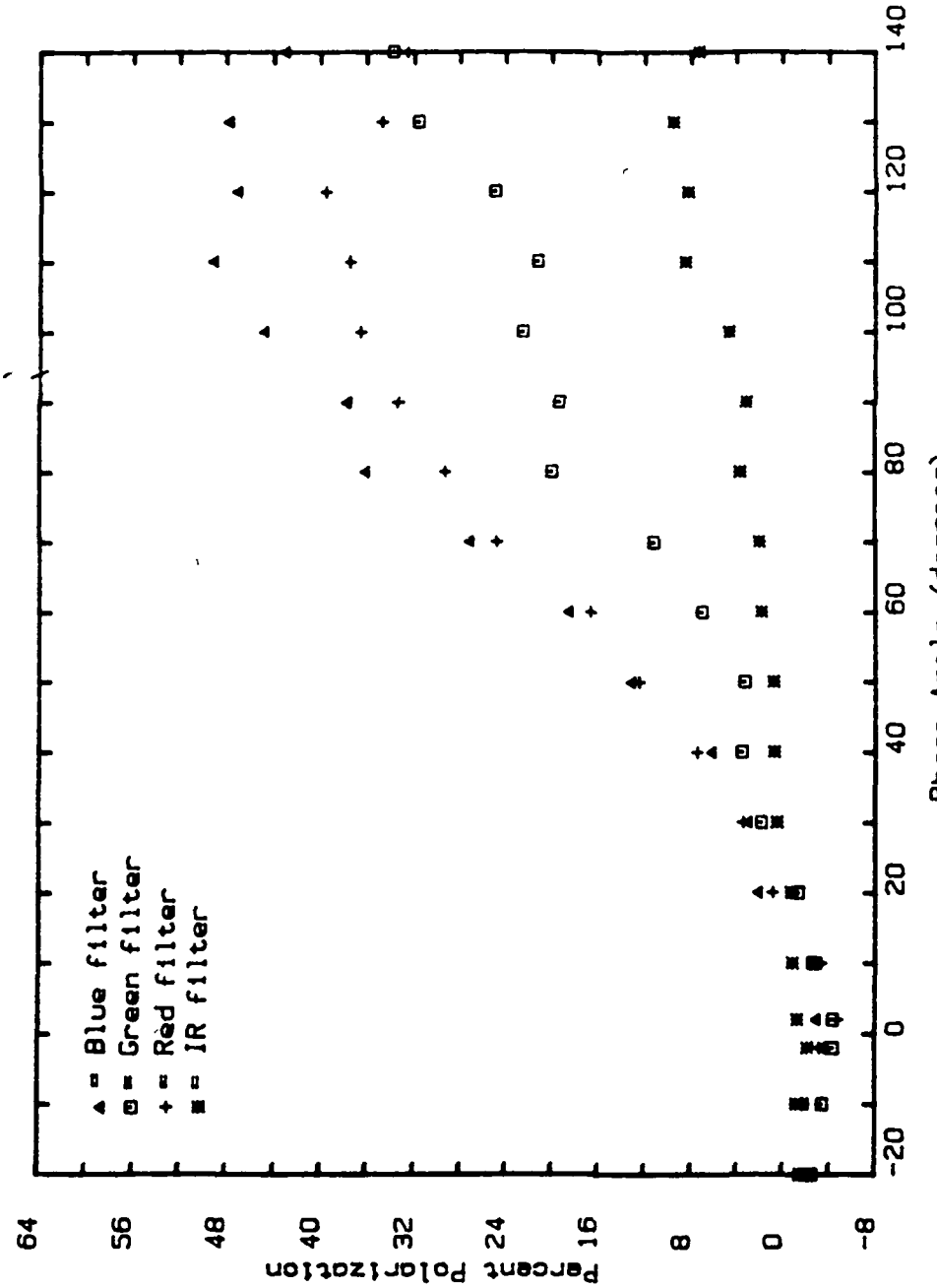

Figure 7d: Percent Polarization vs. Phase Angle. Looking at a live clover leaf in the horizontal position at i=60°.

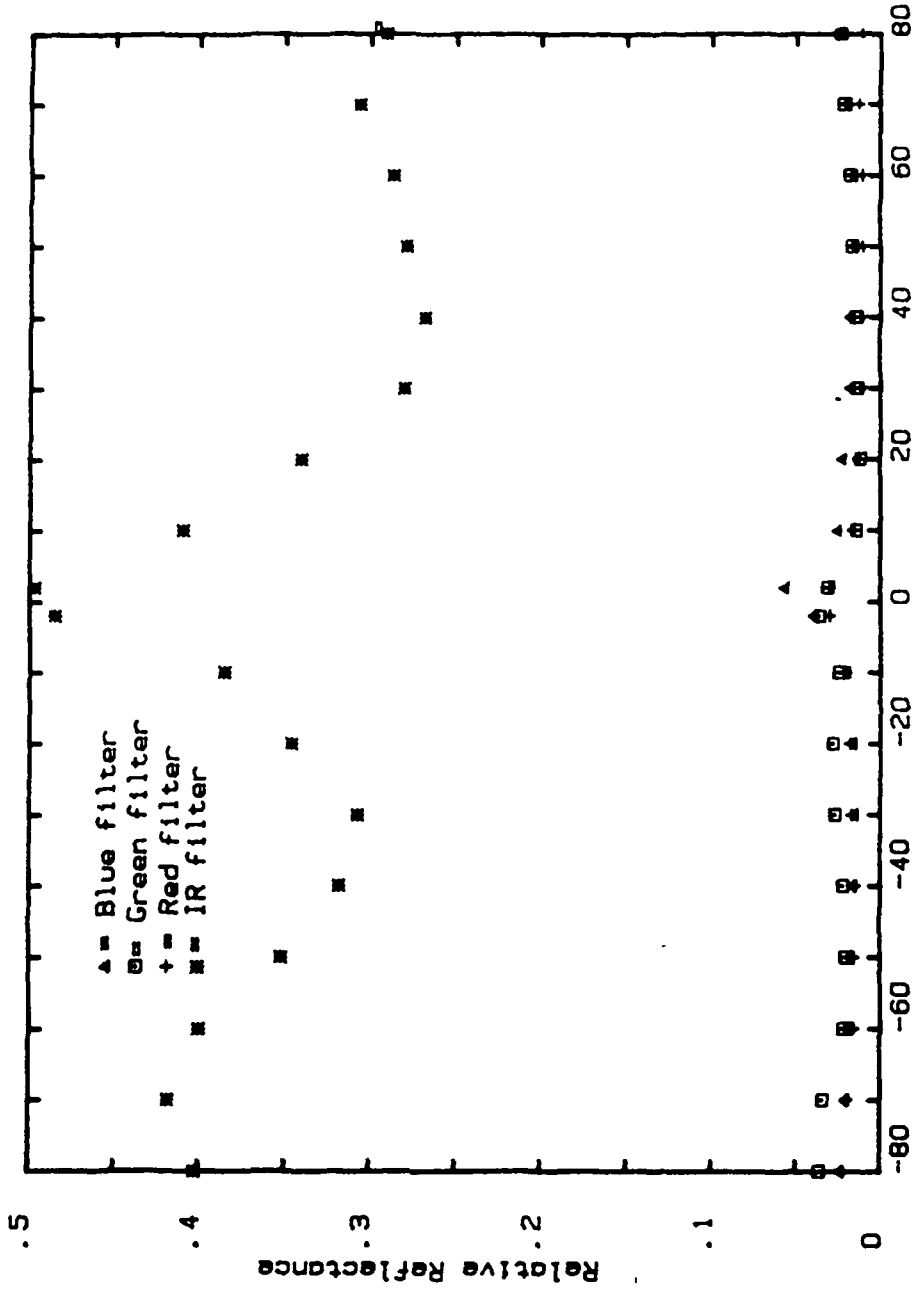

Figure 8a: Relative Reflectance vs. Angle of Emergence. Looking at a live clover leaf in the vertical position at i=0°.

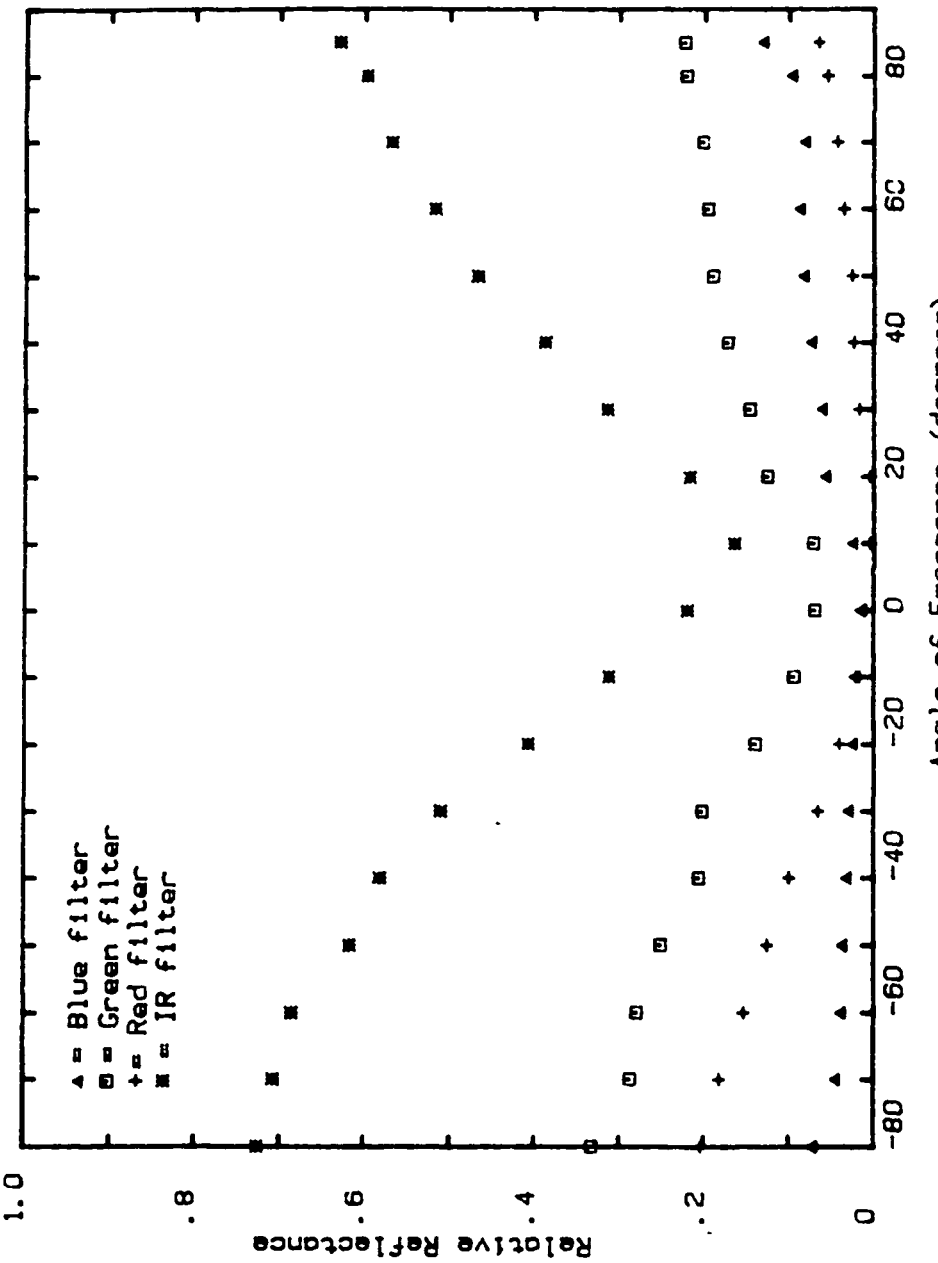

Figure 8b: Relative Reflectance vs. Angle of Emergence. Looking at a live clover leaf in the vertical position at i=90°.

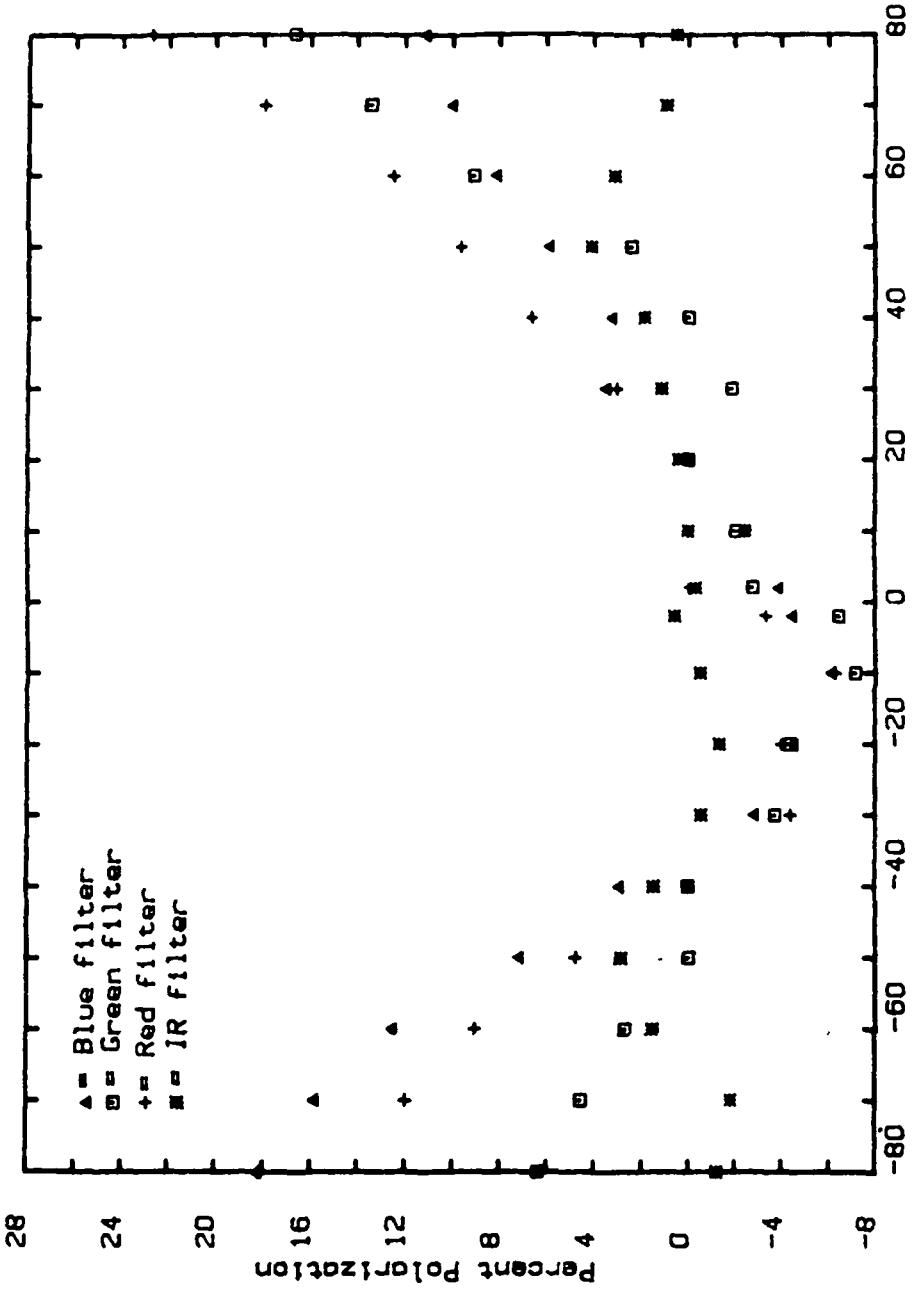

Figure 8c: Percent Polarization vs. Phase Angle Looking at a live clover leaf in the vertical position at i=0°.

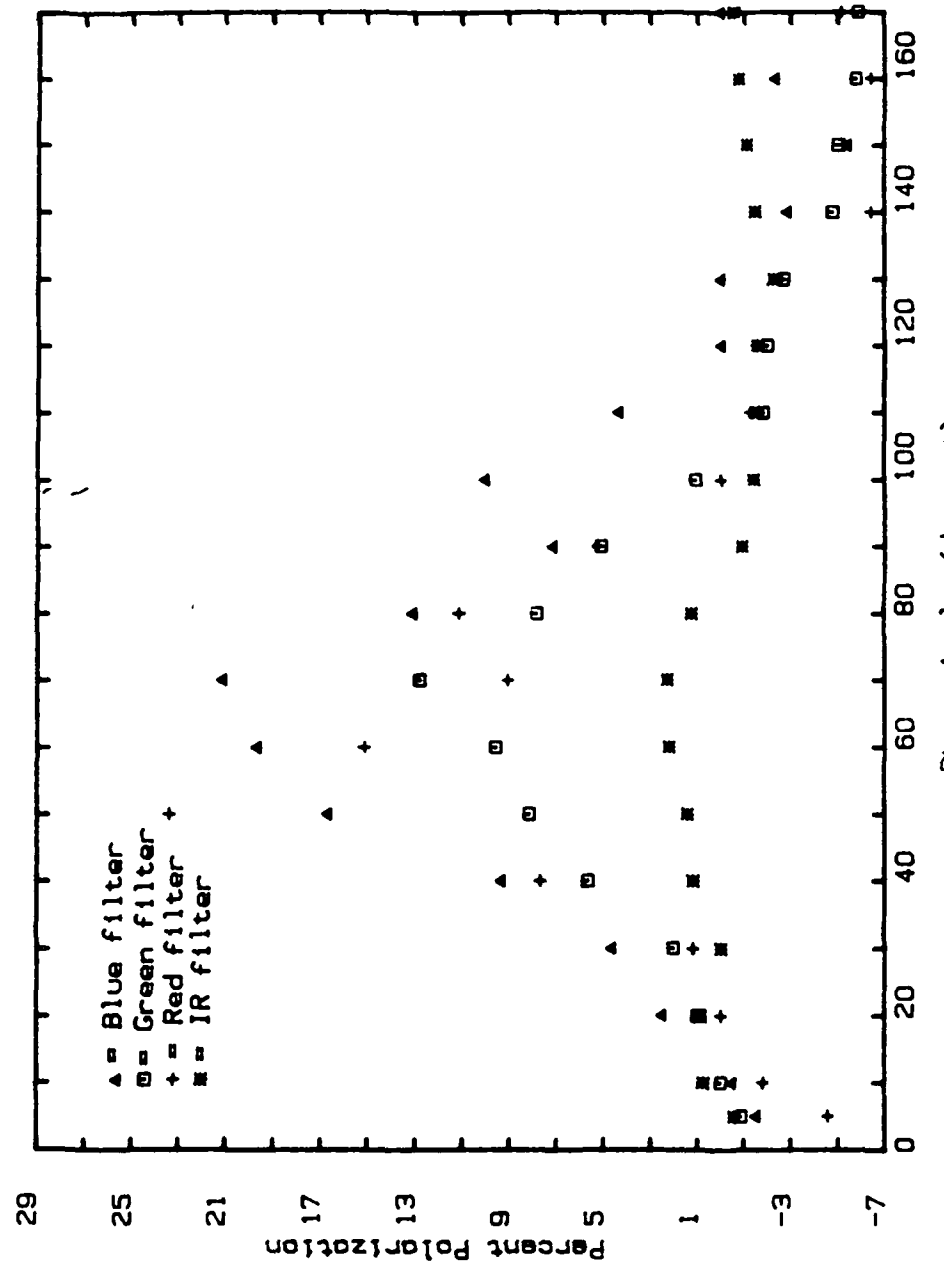

Figure 6d: Percent Polarization vs Phase Angle. Looking at a live clover leaf in the vertical position at i=90°.

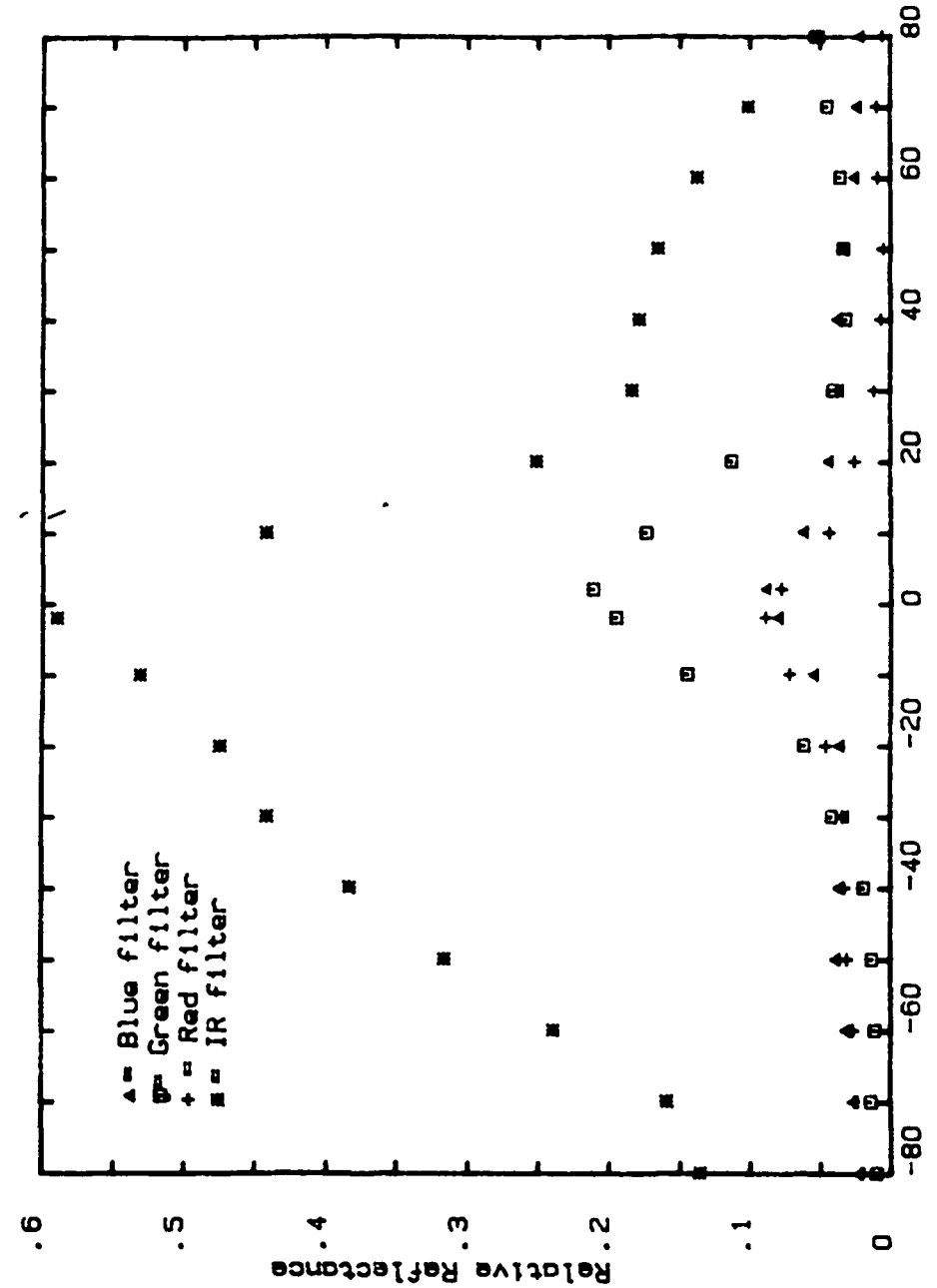

Figure 9a: Relative Reflectance vs. Angle of Emergence. Looking at a live clover patch at i=0°.

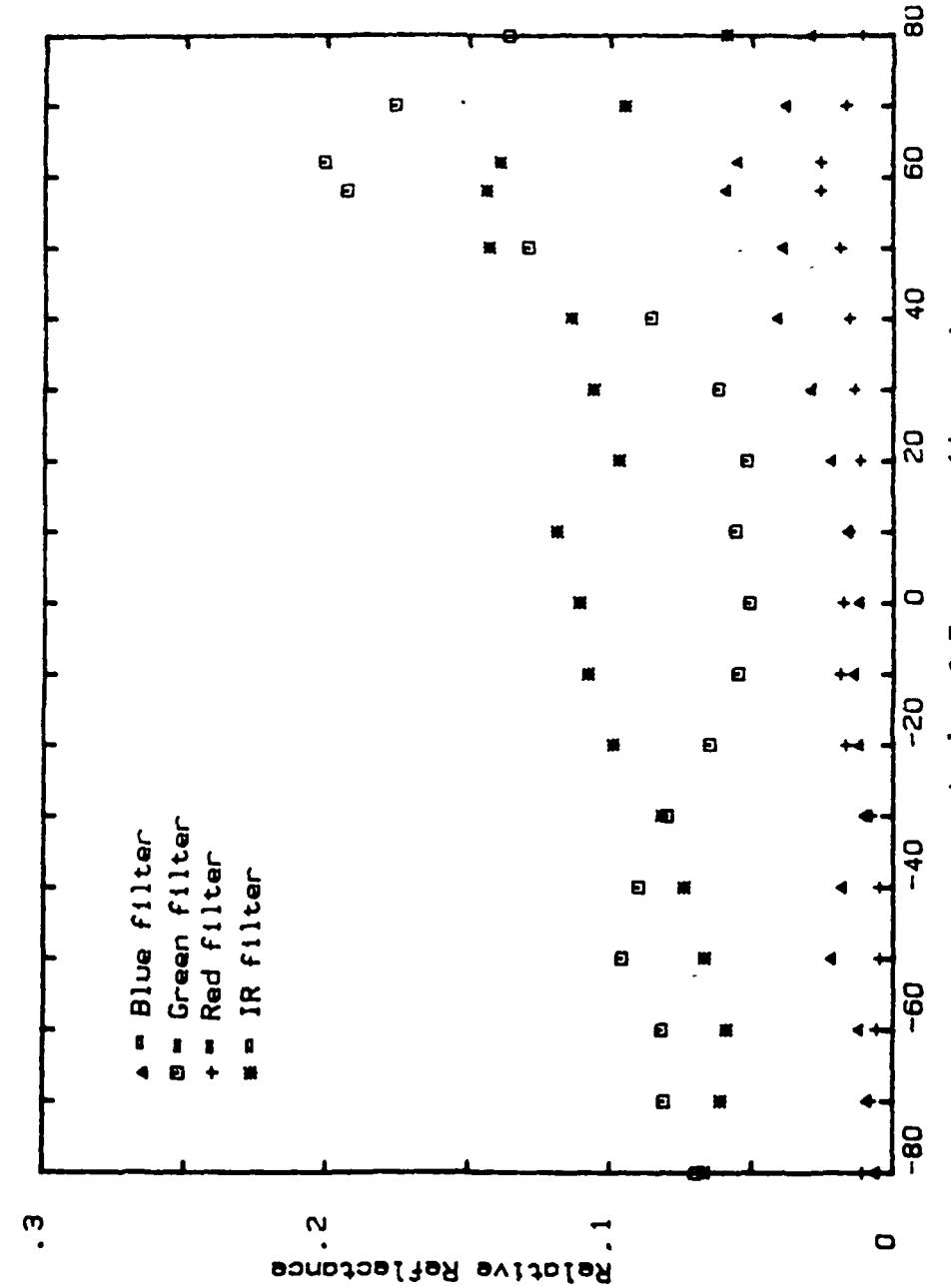

Figure 9b: Relative Reflectance vs. Angle of Emergence. Looking at a live clover patch at $i=60^{\circ}$.

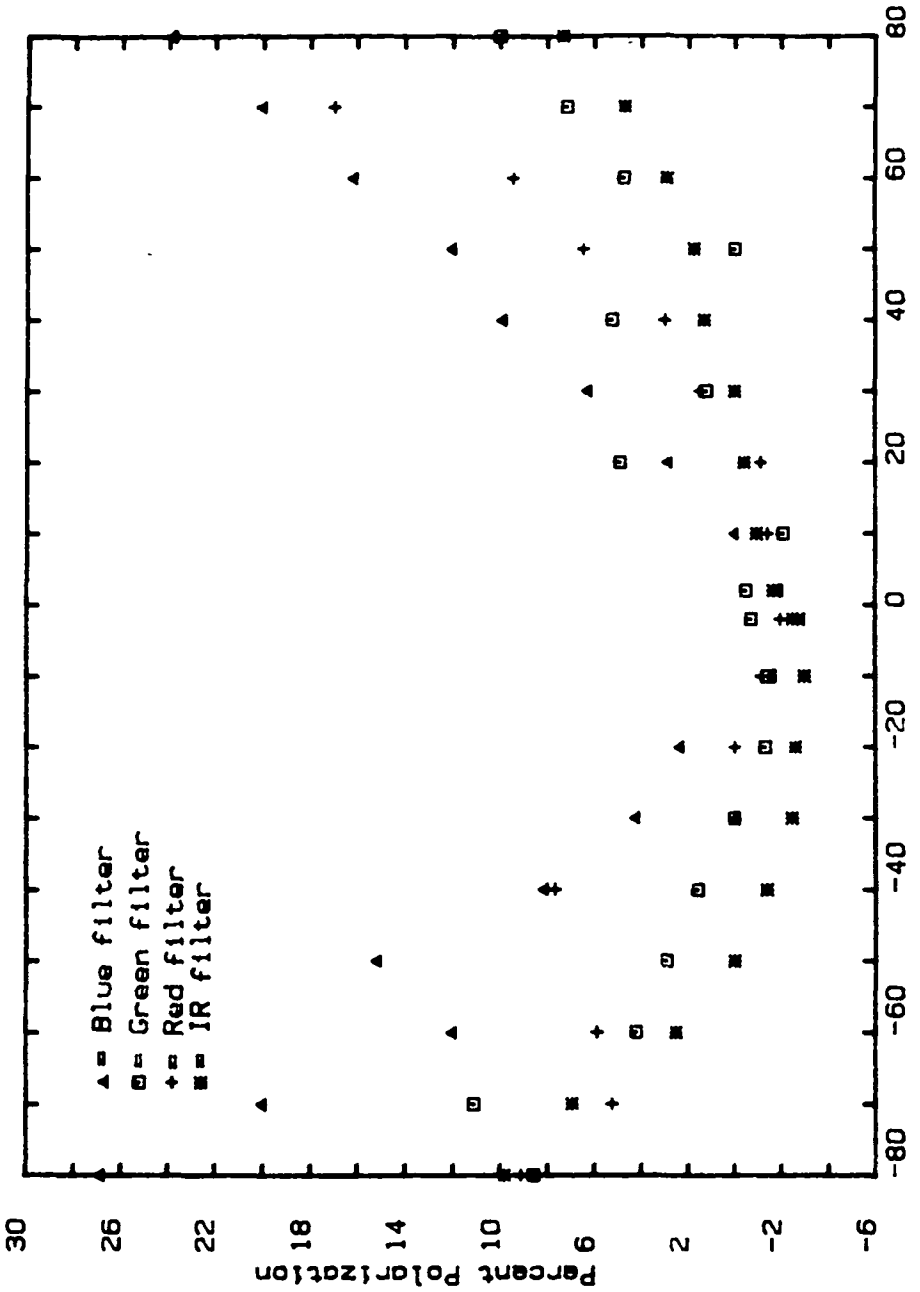

Figure 9c: Percent Polarization vs. Phase Angle. Looking at a live clover patch at i=0°.

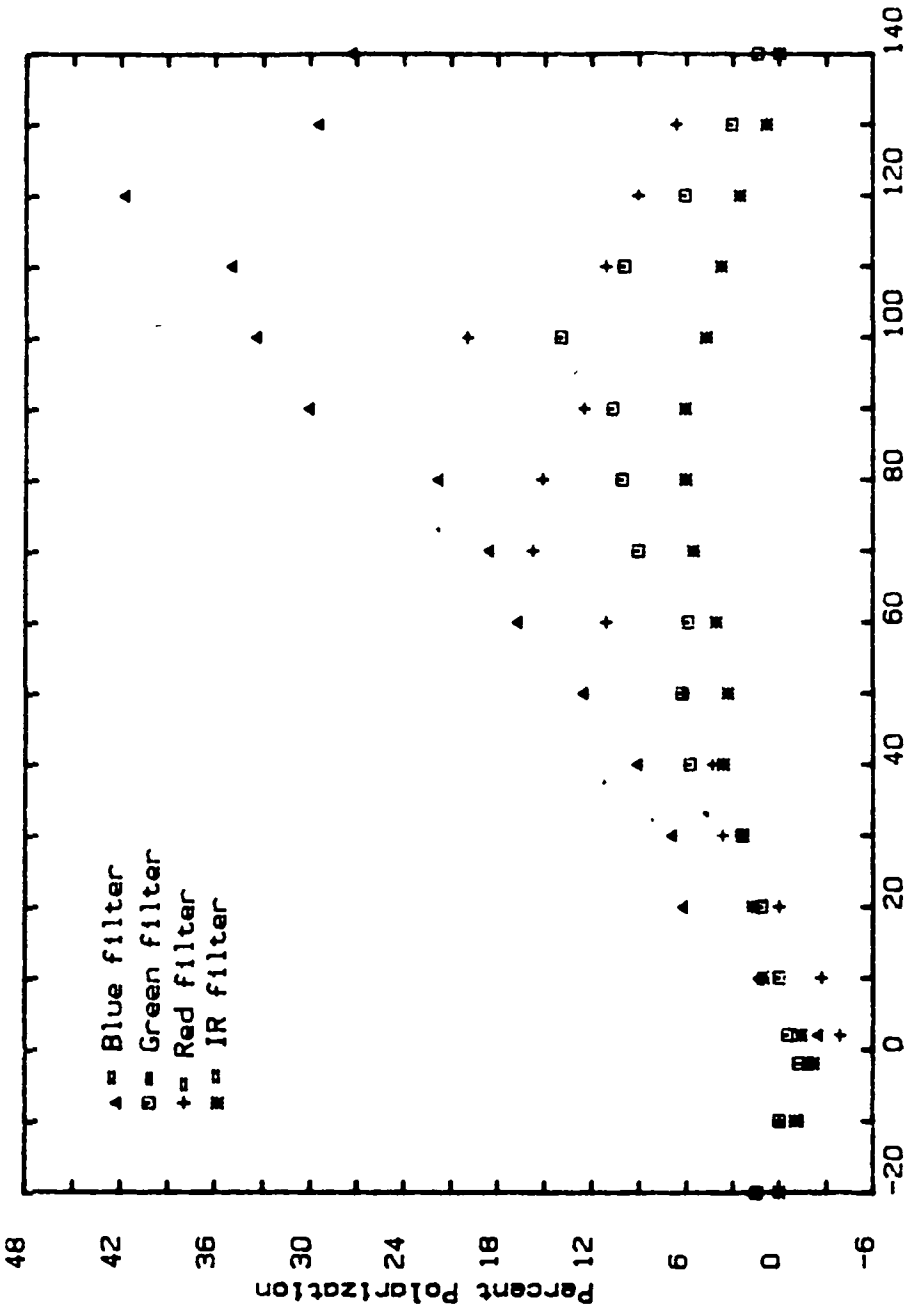

Figure 9d: Percent Polarization vs. Phase Angle. Looking at a live clover patch at i=60°.

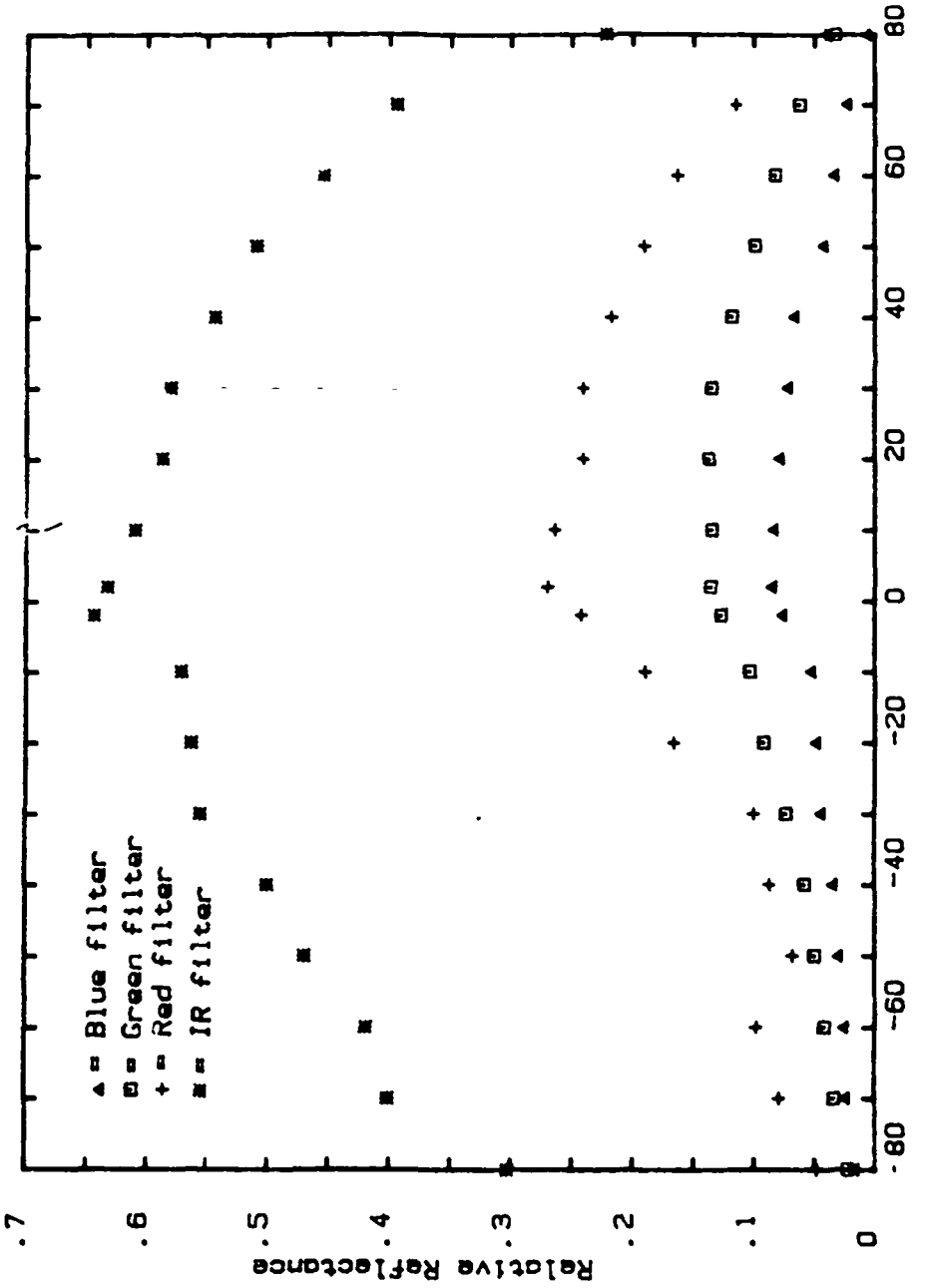

Figure 10a: Relative Reflectance vs. Angle of Emergence. Looking at a dry clover leaf in the horizontal position at i=0°.

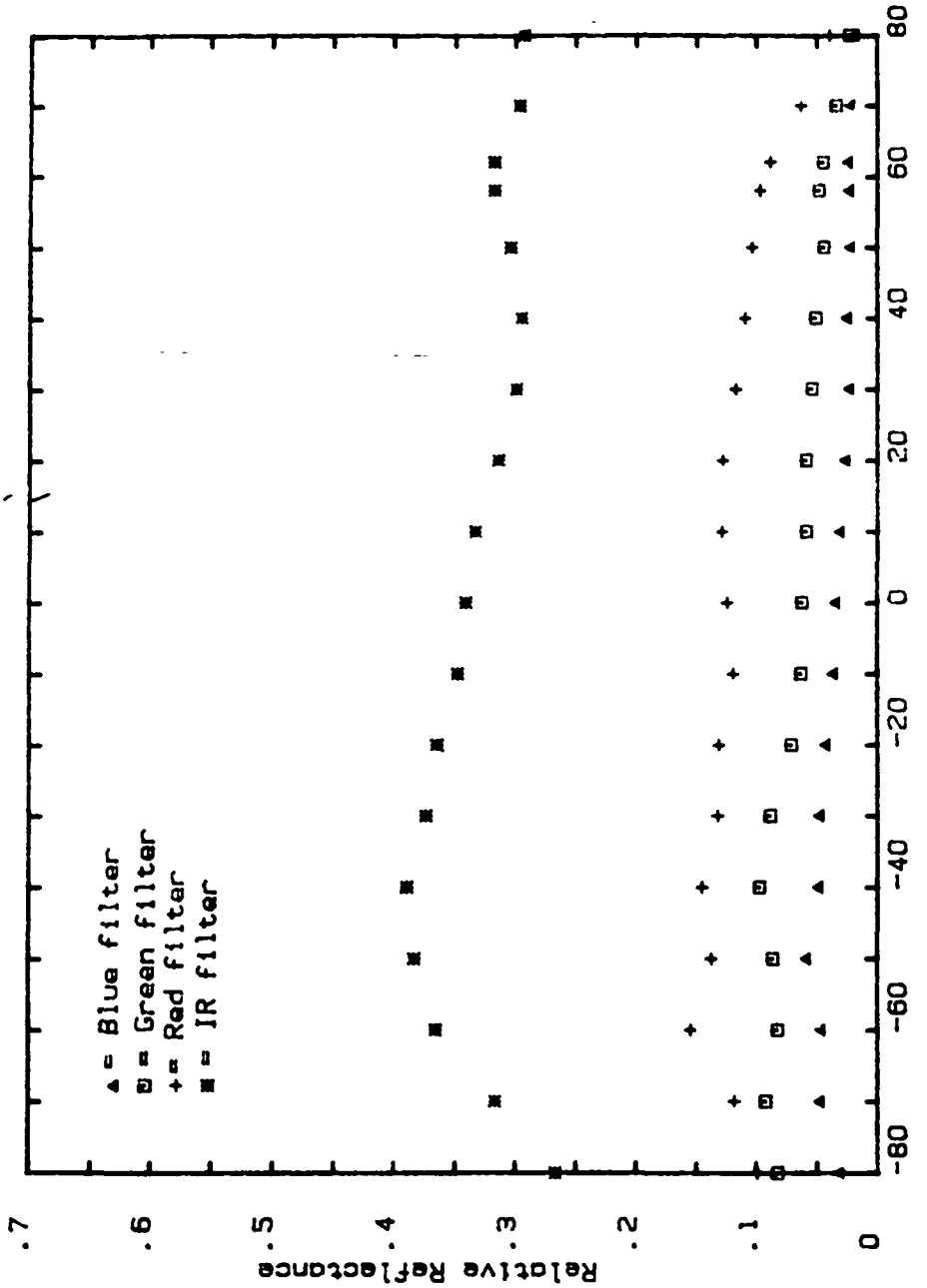

Figure 10b: Relative Reflectance vs. Angle of Emergence. Looking at a dry clover leaf in the horizontal position at i=60°.

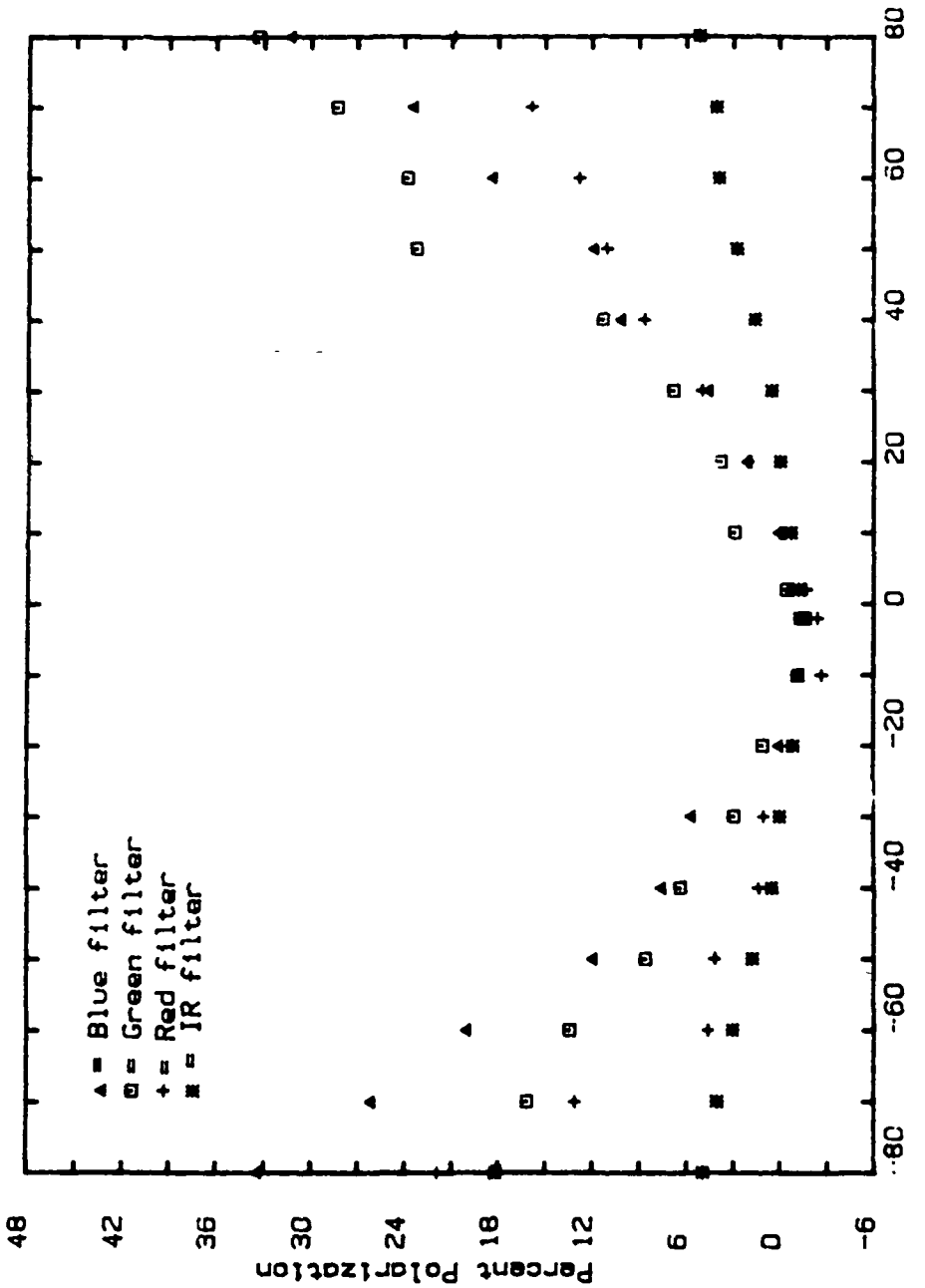

Figure 10c: Percent Polarization vs. Phase Angle. Looking at a dry clover leaf in the horizontal position at i=0°.

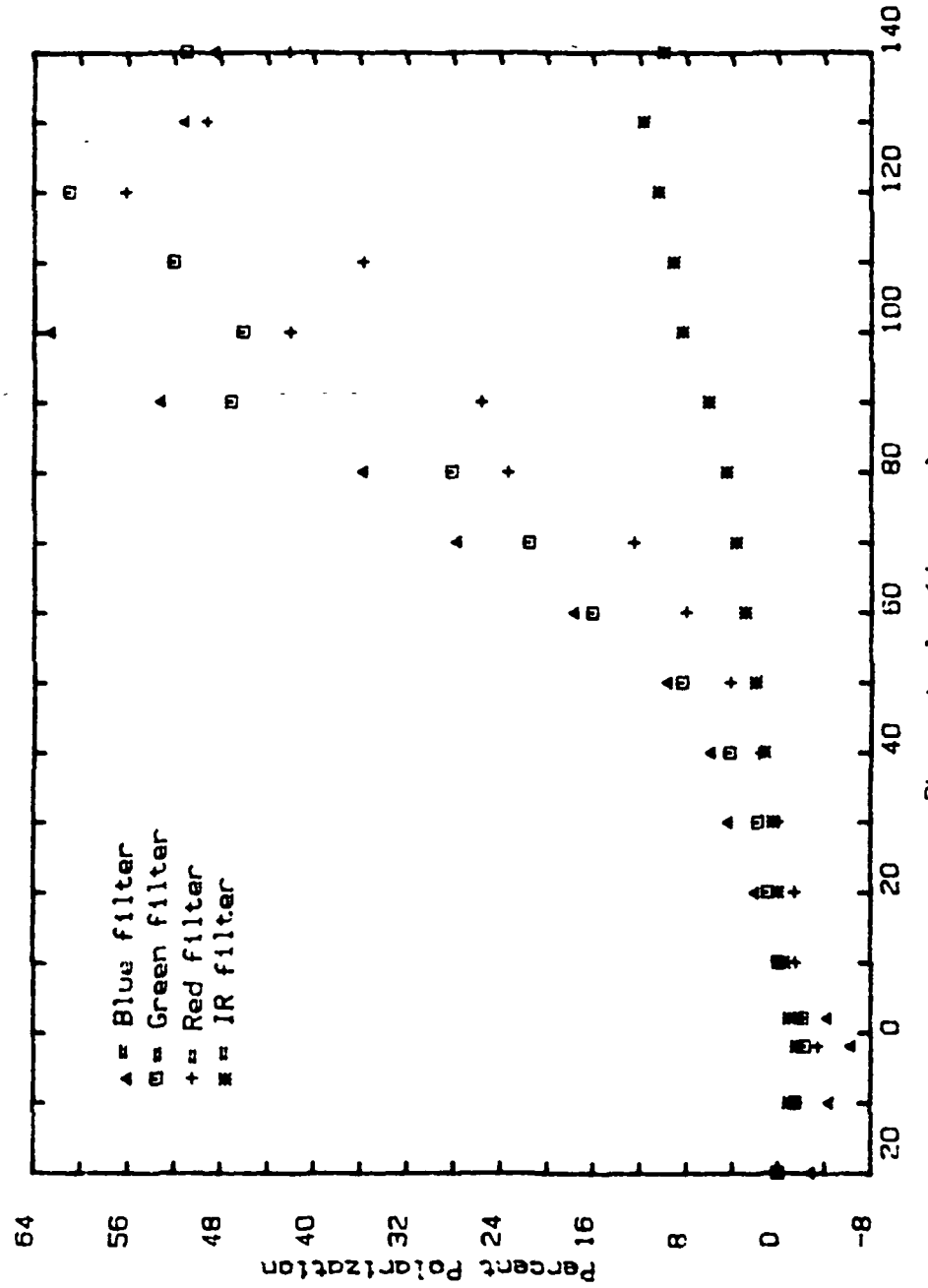

Figure 10d: Percent Polarization vs. Phase Angle. Looking at a dry clover leaf in the horizontal position at i=60°.

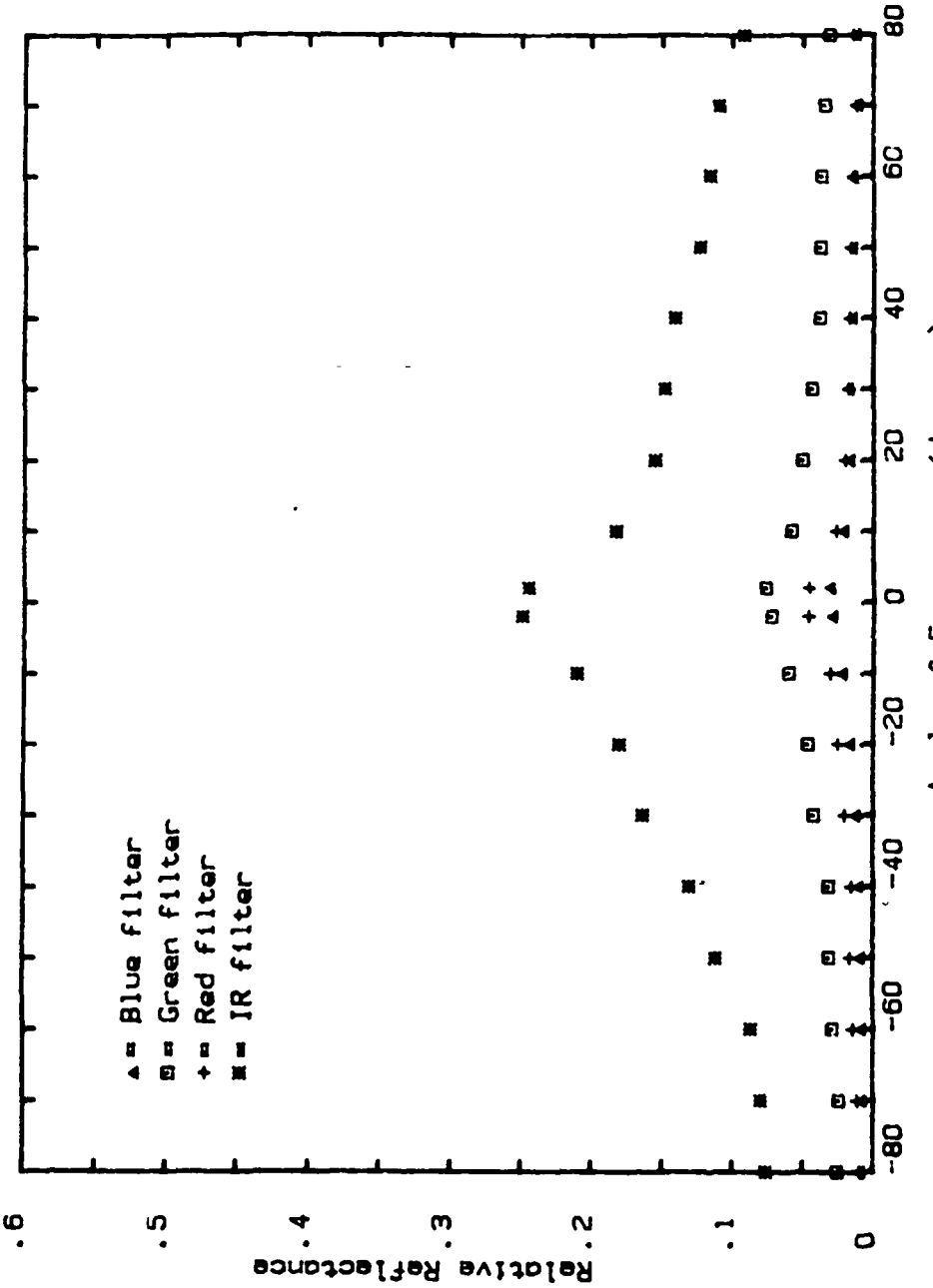

Figure 11a: Relative Reflectance vs. Angle of Emergence. Looking at a live patch of grass at i=0°.

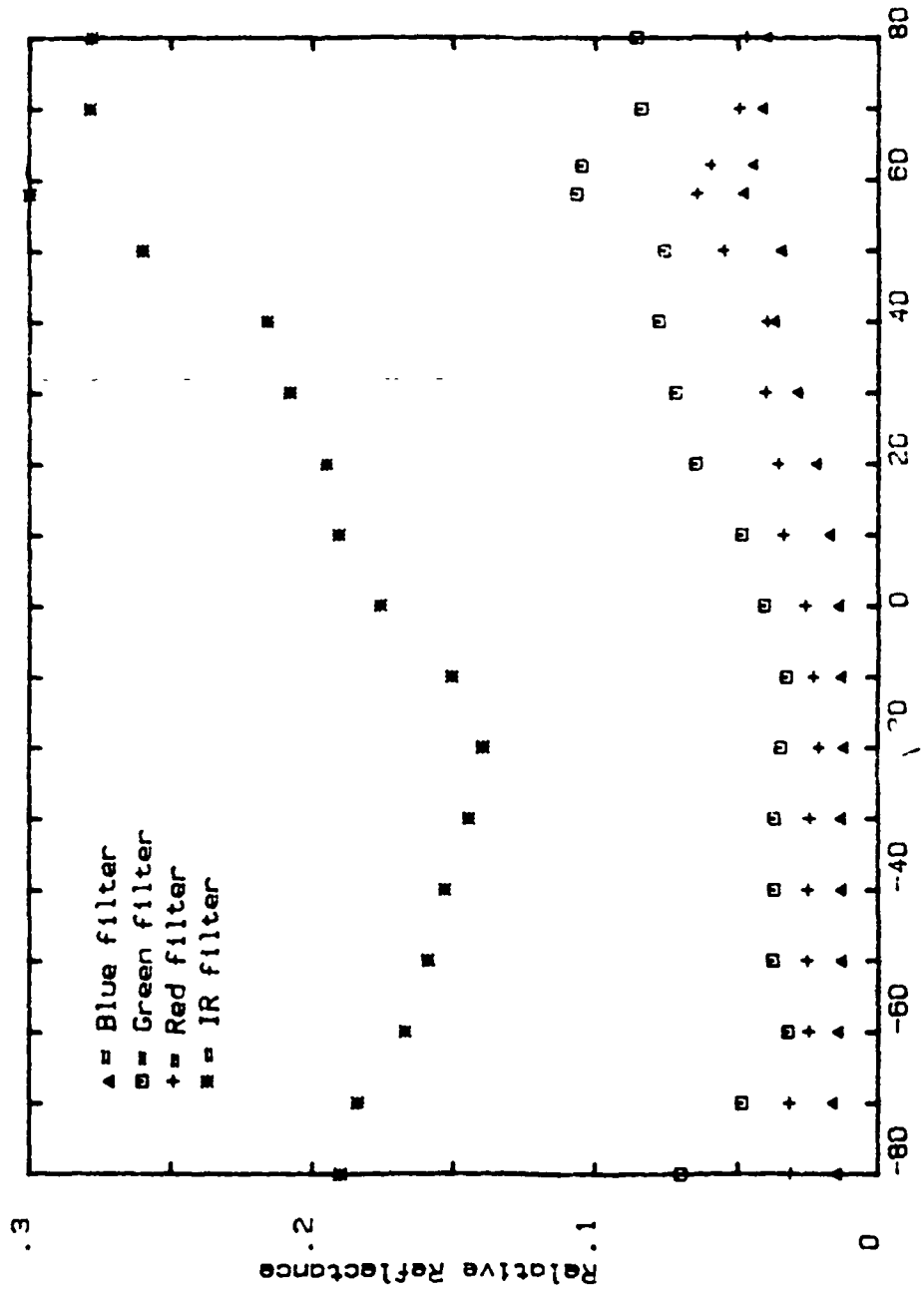

Figure 11b: Relative Reflectance vs. Angle of Emergence. Looking at a live patch of grass at i=60°.

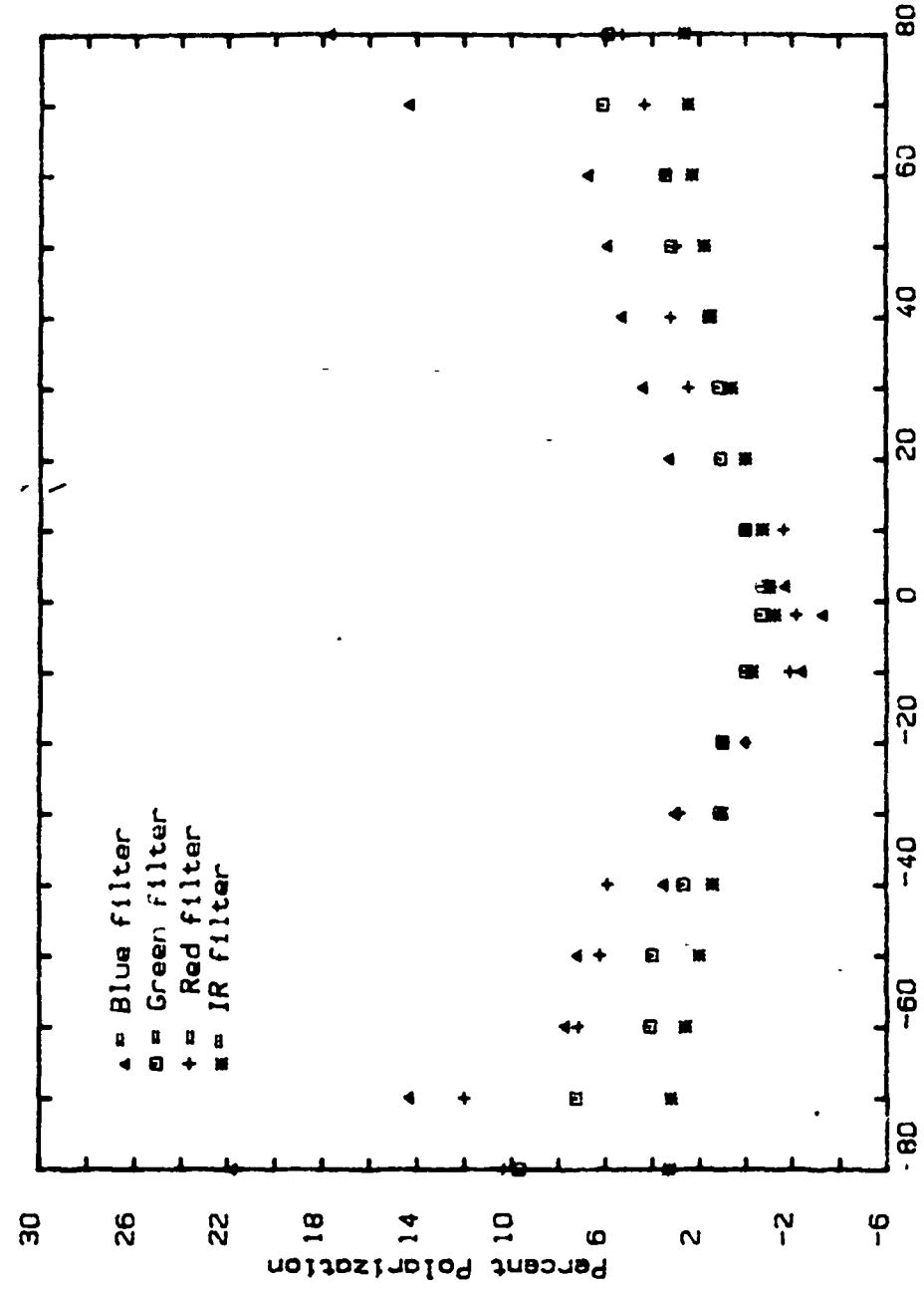

Figure 11c: Percent Polarization vs. Phase Angle. Looking at a live patch of grass at i=0°.

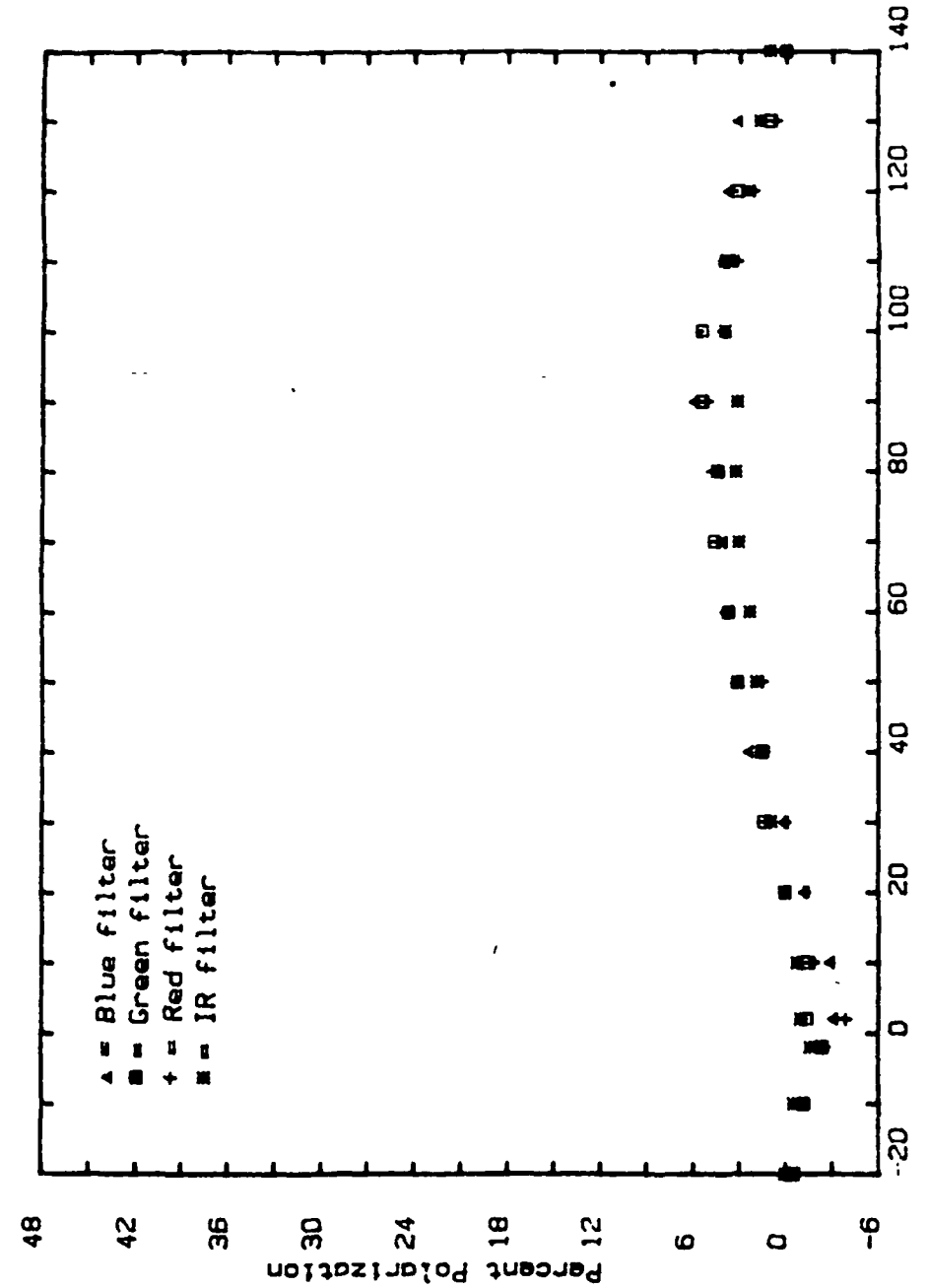

Figure 11d: Percent Polarization vs Phase Angle. Looking at a live patch of grass at i=61°.

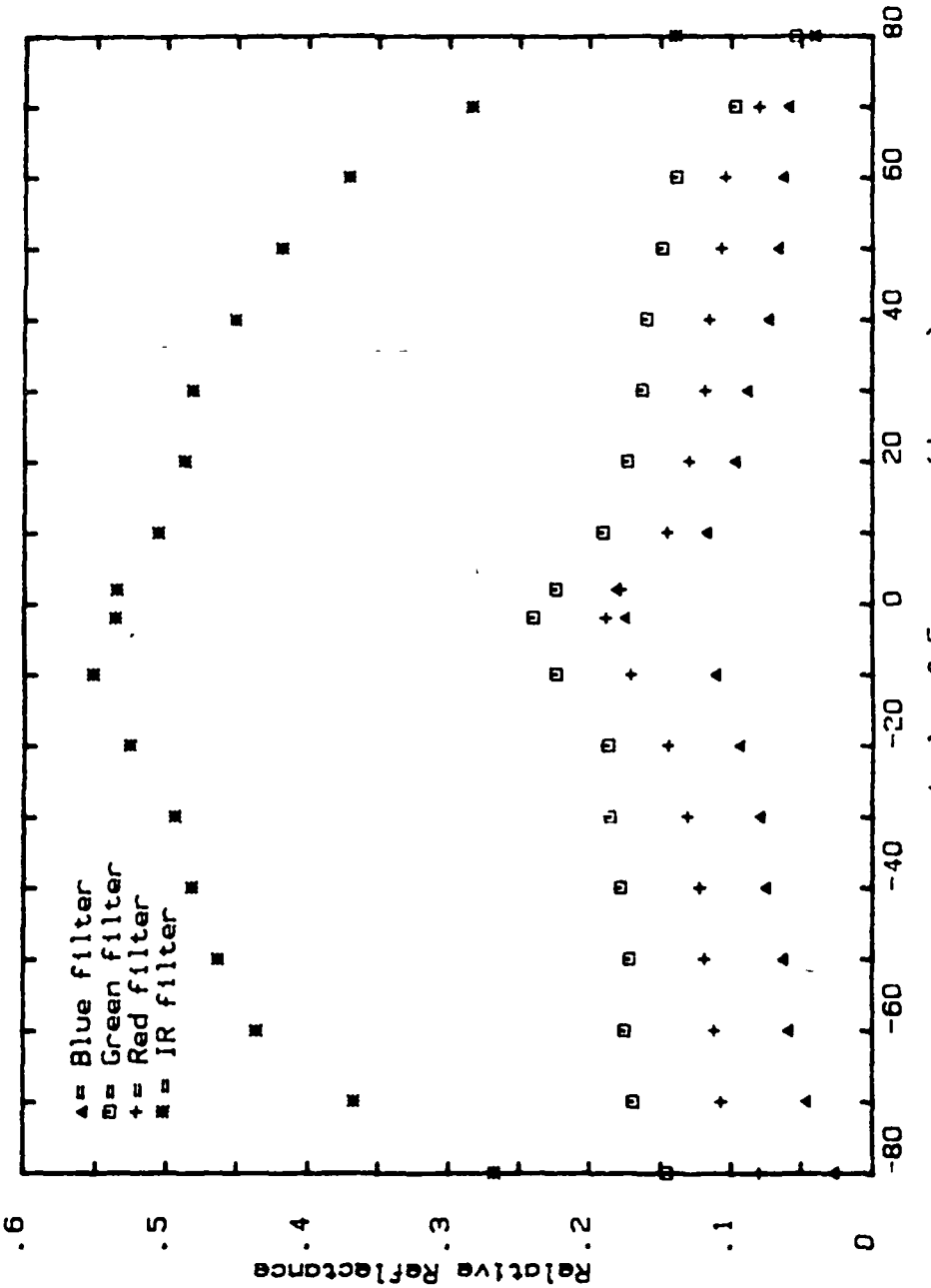

Figure 12a: Relative Reflectance vs. Angle of Emergence. Looking at a live corn leaf in the horizontal position at i=0°.

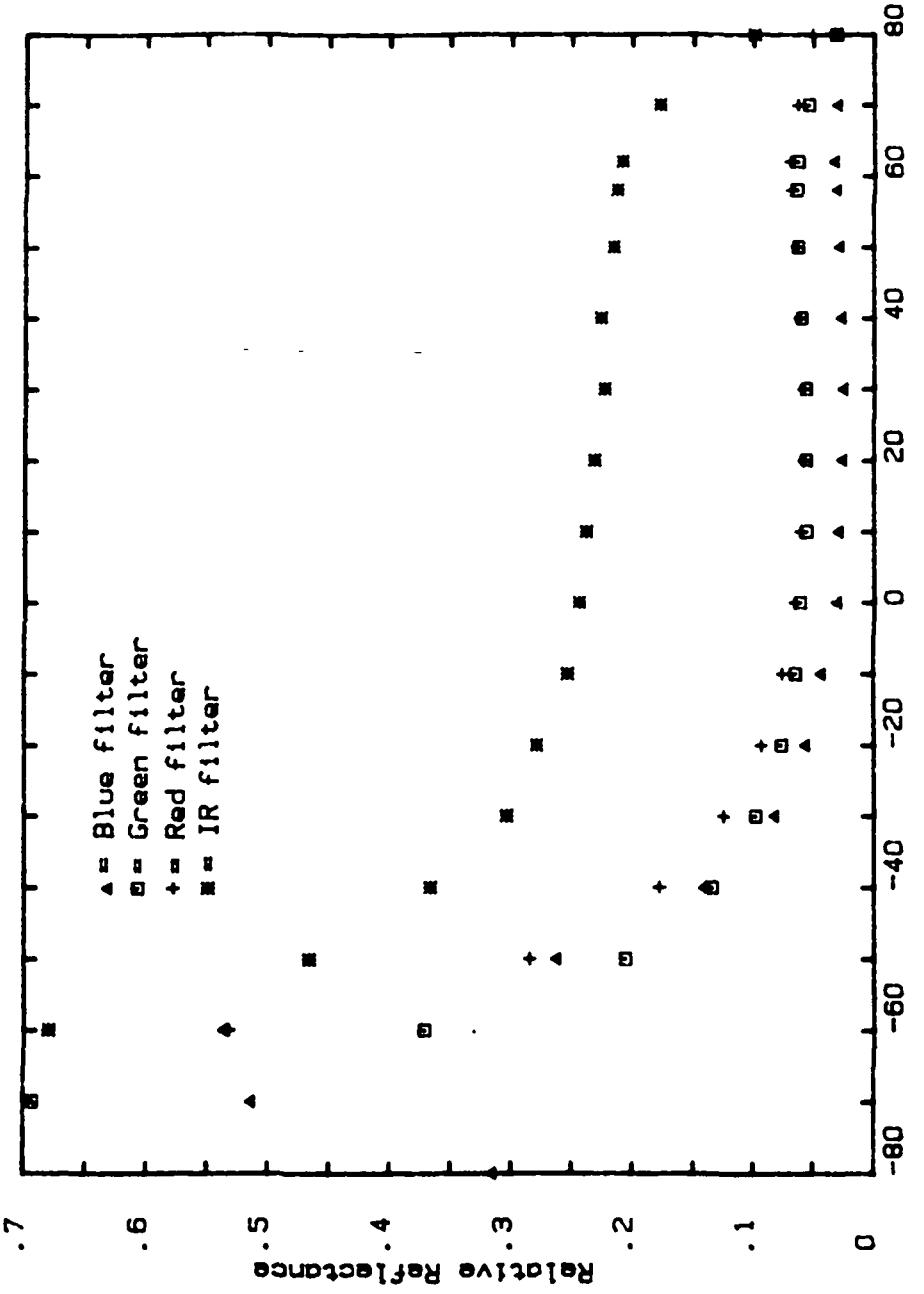

Figure 12. Relative Reflectance vs. Angle of Emergence. Looking at a live corn leaf in the horizontal position at i=60°.

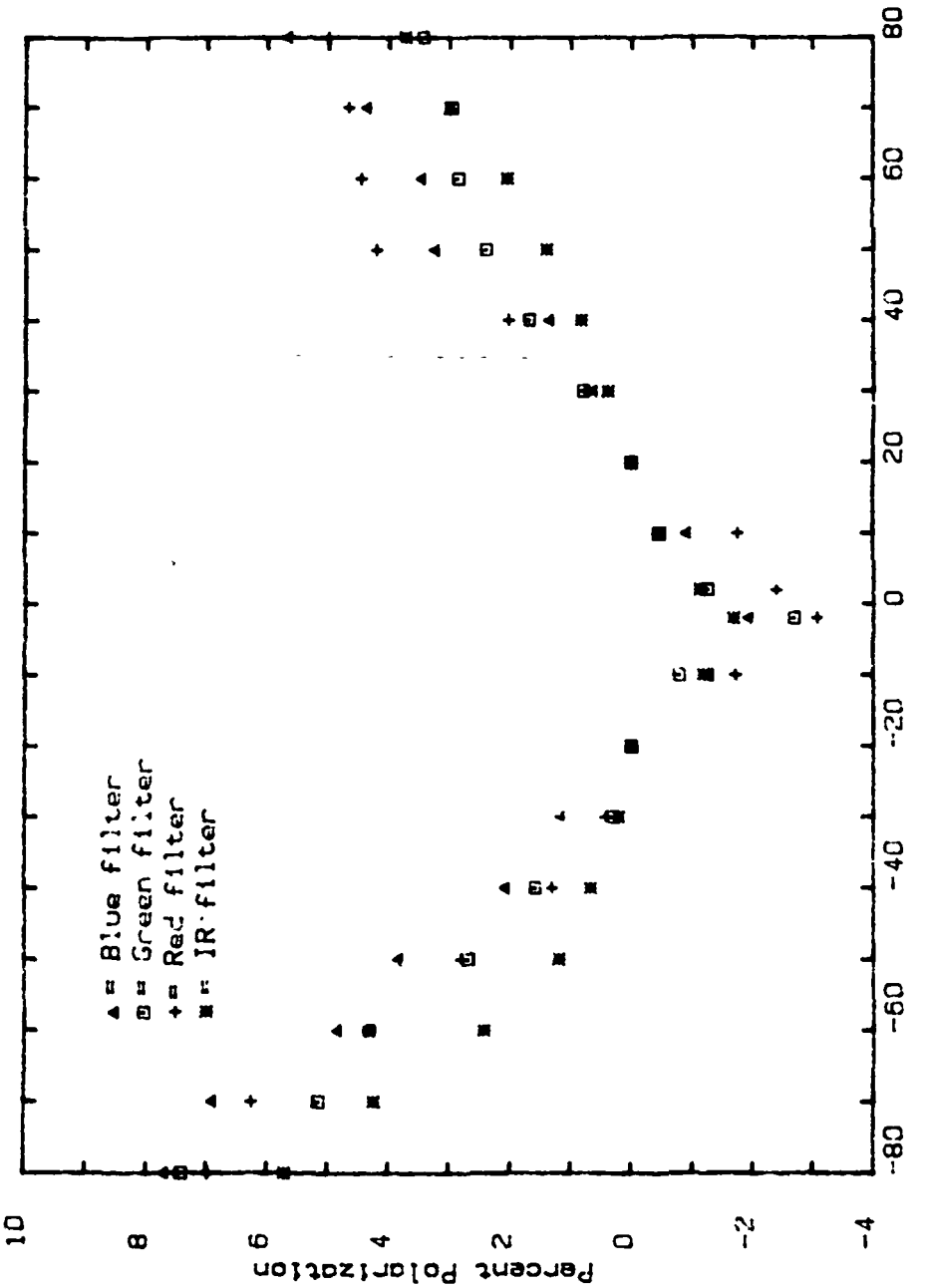

Figure 12c: Percent Polarization vs. Phase Angle. Looking at a live corn leaf in the horizontal position at i=0°.

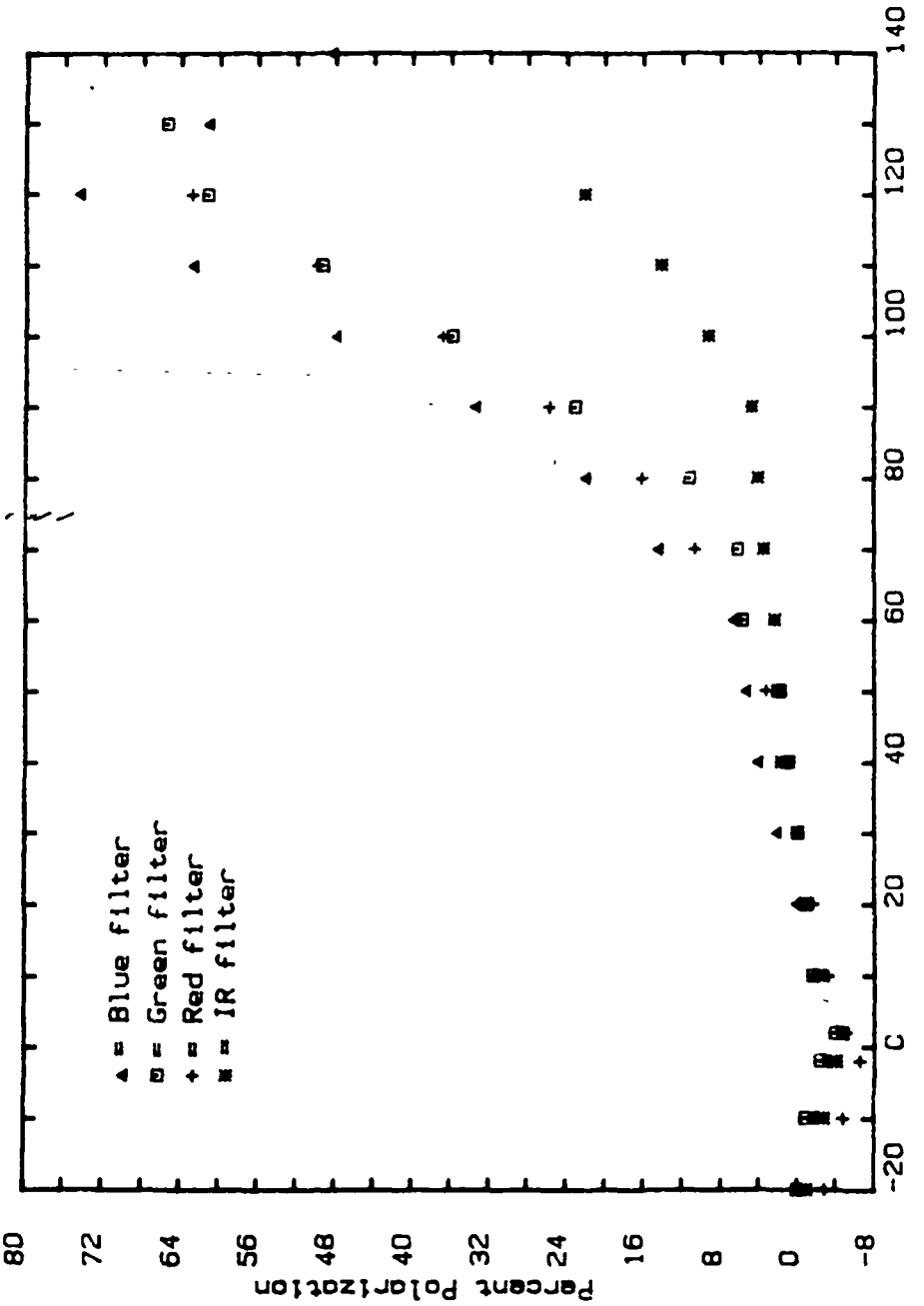

Figure 12d: Percent Polarization vs. Phase Angle. Looking at a live corn leaf in the horizontal position at i=60°.

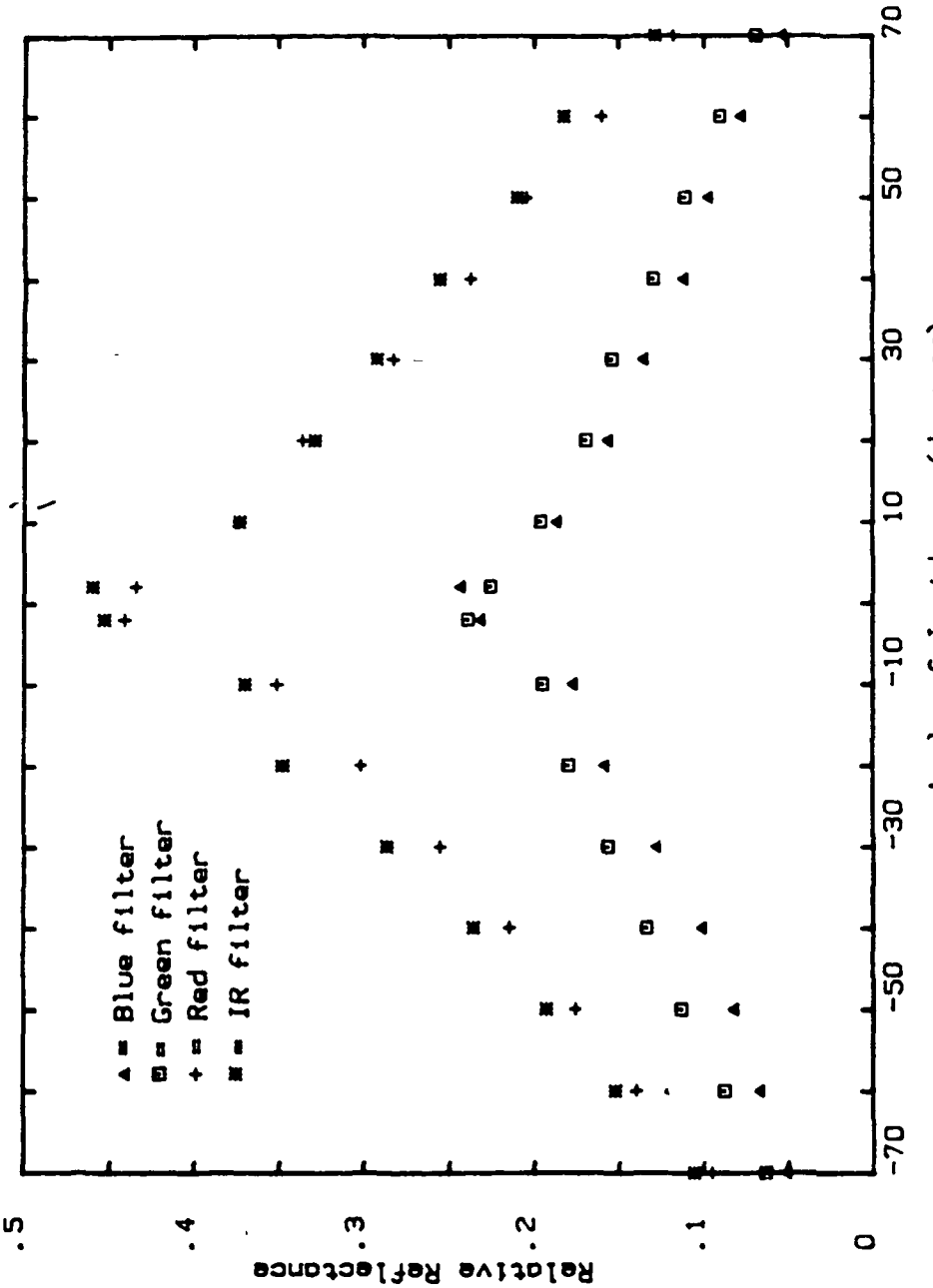

Figure 13a: Relative Reflectance vs. Angle of Incidence. Looking at the soil the clover grew in at e=0°.

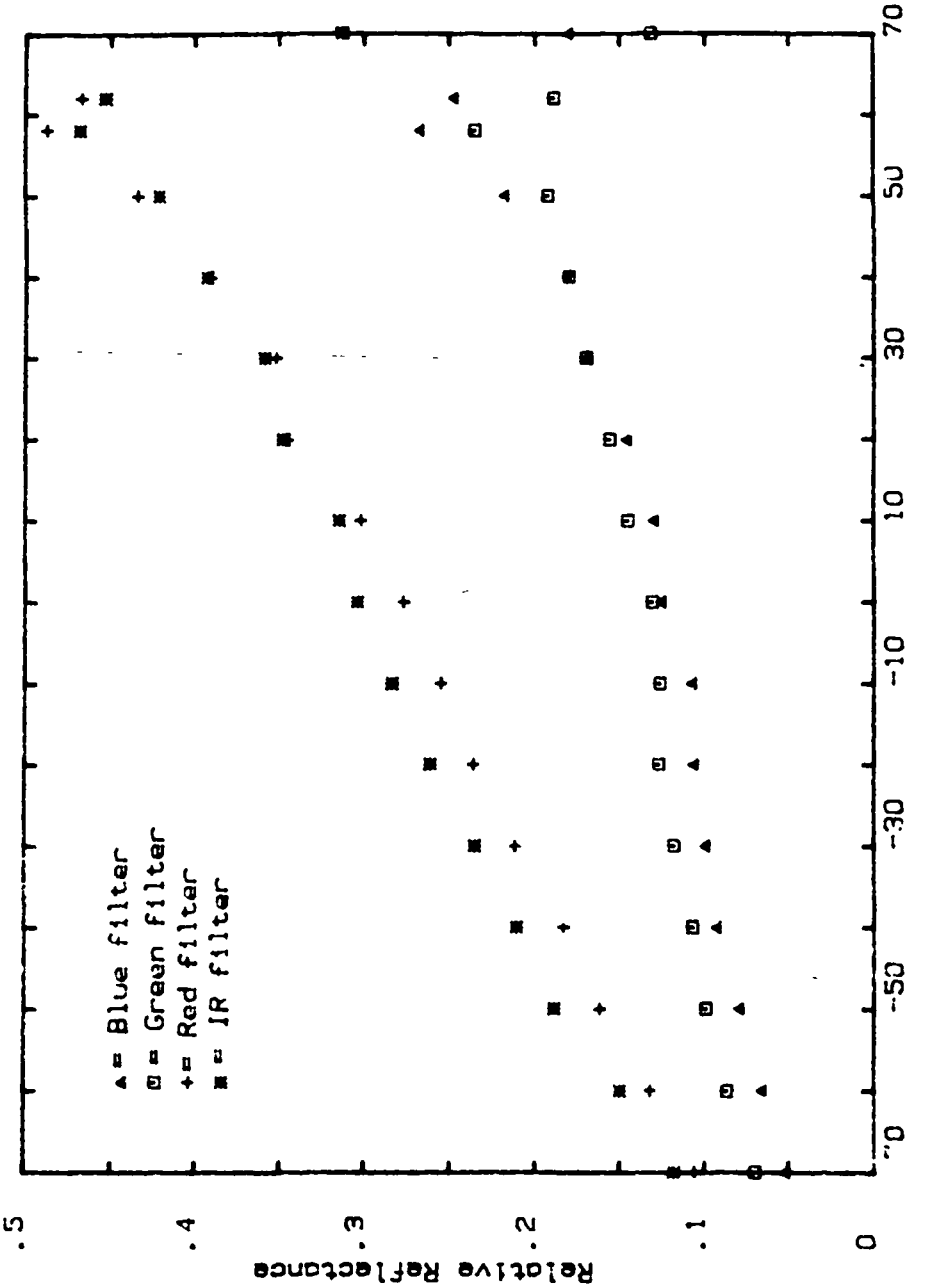

Figure 13b: Relative Reflectance vs. Angle of Incidence. Looking at the soil the clover grew in at e=50°.

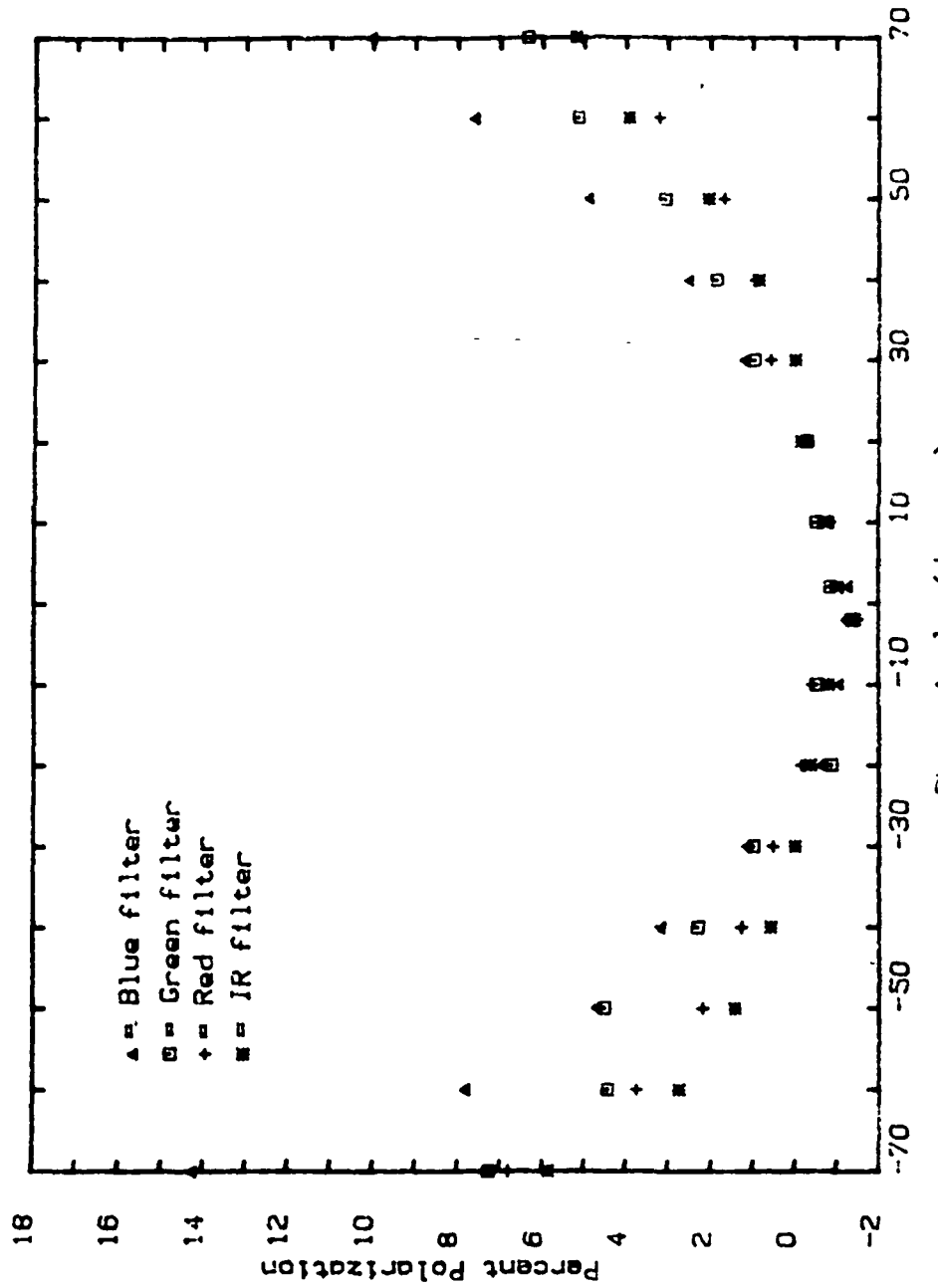

Figure 13c: Percent Polarization vs. Phase Angle. Looking at the soil the clover grew in at e=0°.

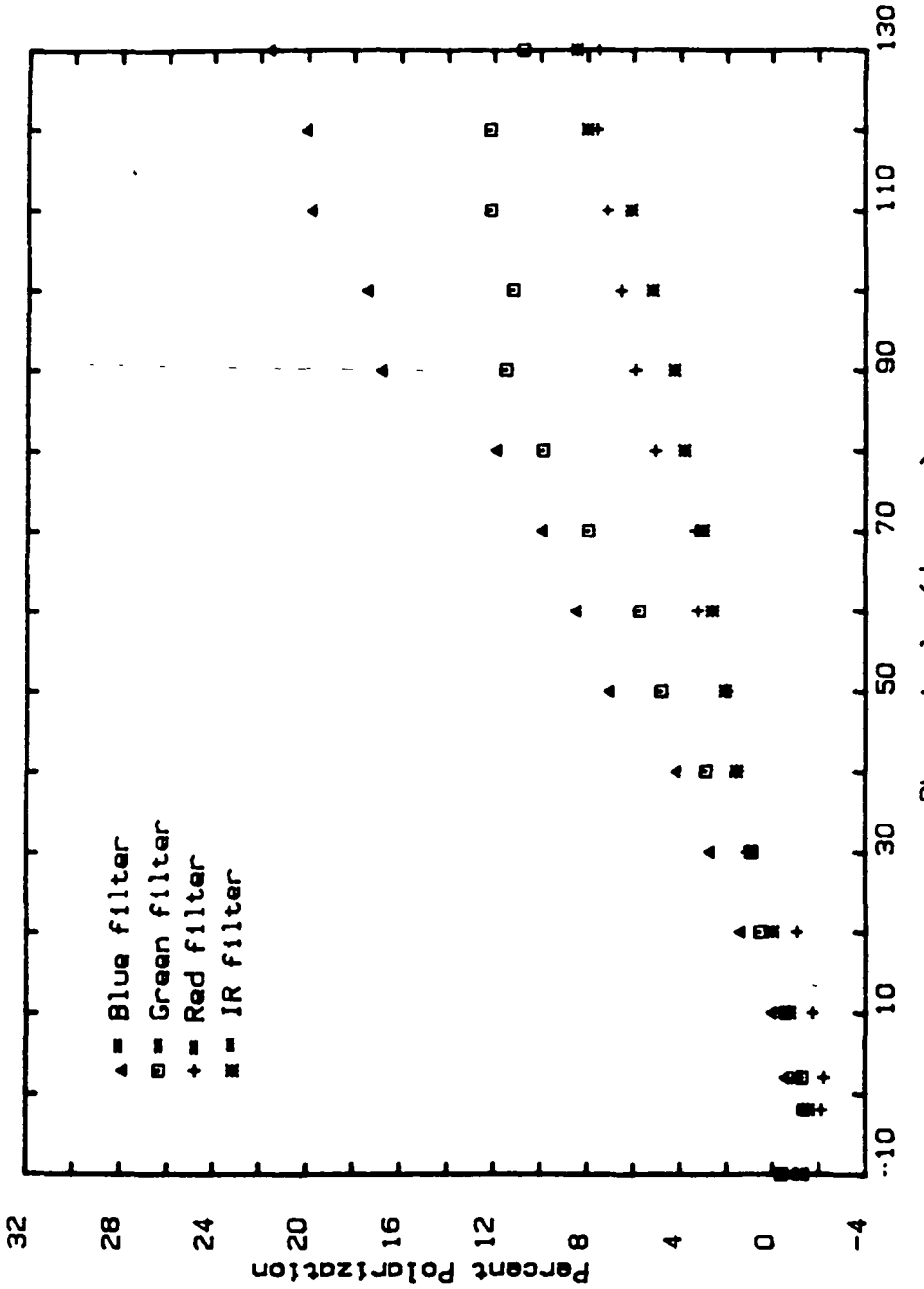

Figure 13d: Percent Polarization vs. Phase Angle. Looking at the soil the clover grew in at e=60°.

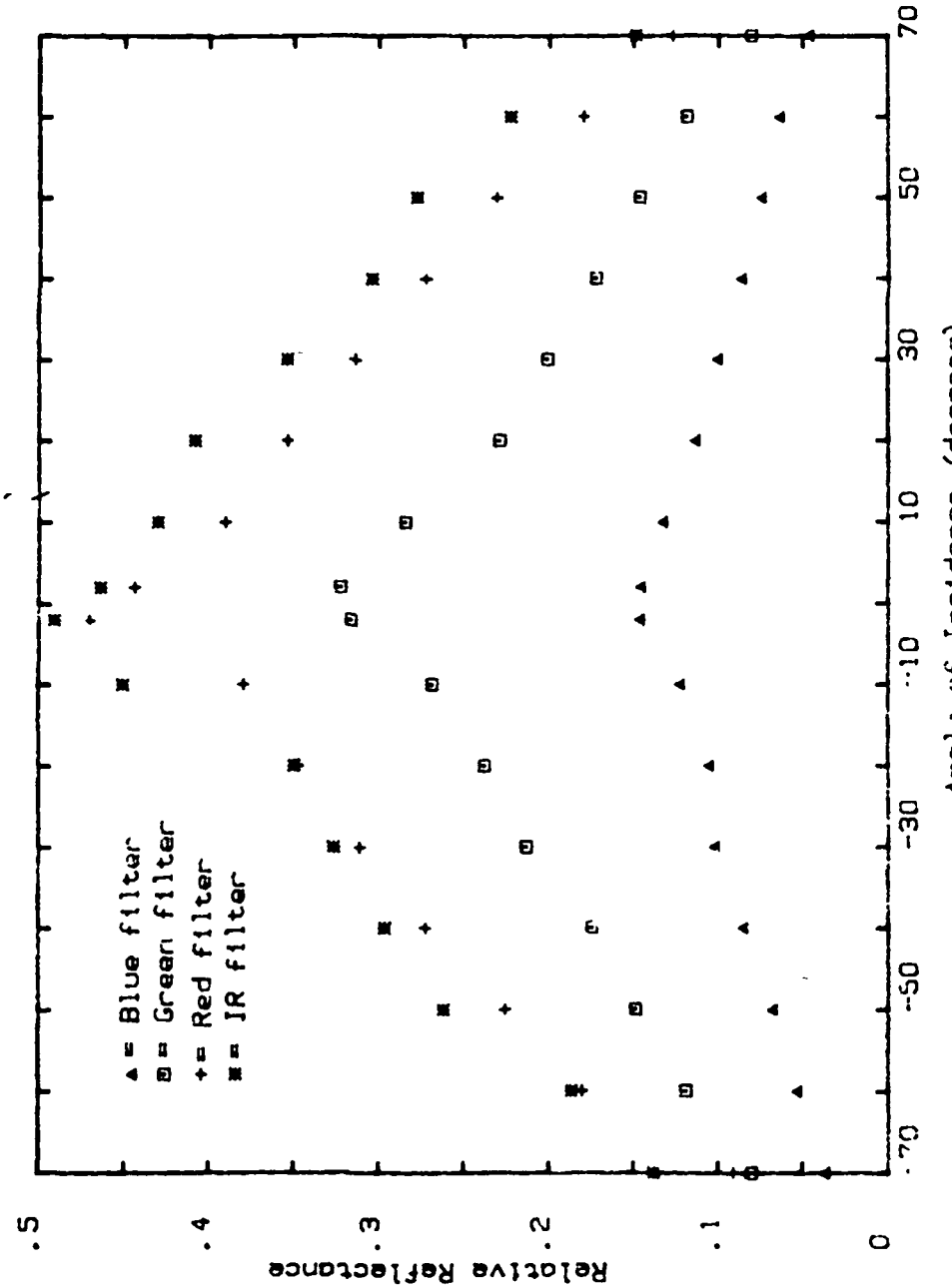

Figure 14a: Relative Reflectance vs. Angle of Incidence. Looking at the soil the clover grew in, baked between a temperature of 100-250°C, at e=0°.

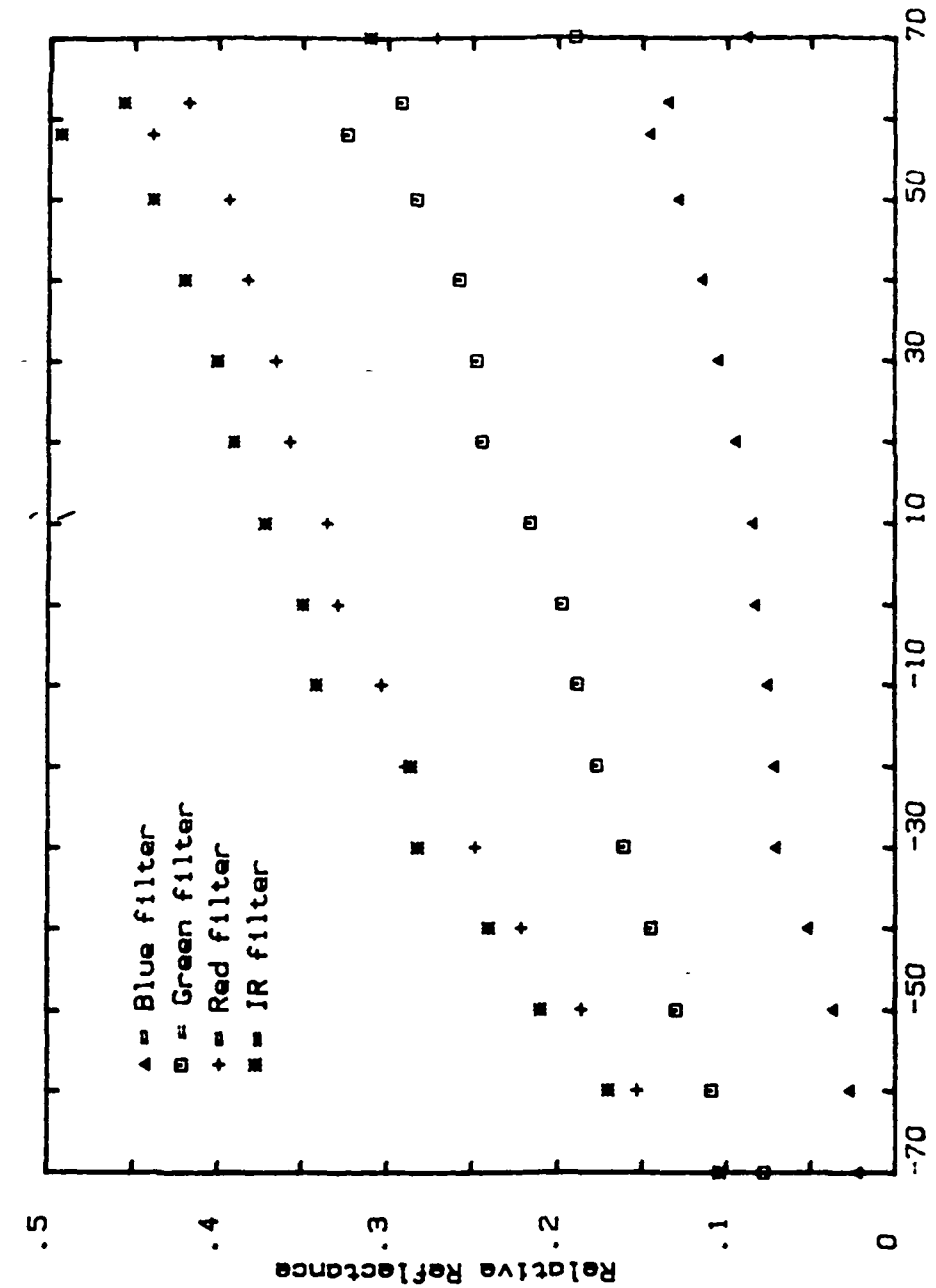

Figure 14b: Relative Reflectance vs. Angle of Incidence. Looking at the soil the clover grew in, baked between a temperature of 100-250°C, at e=60°.

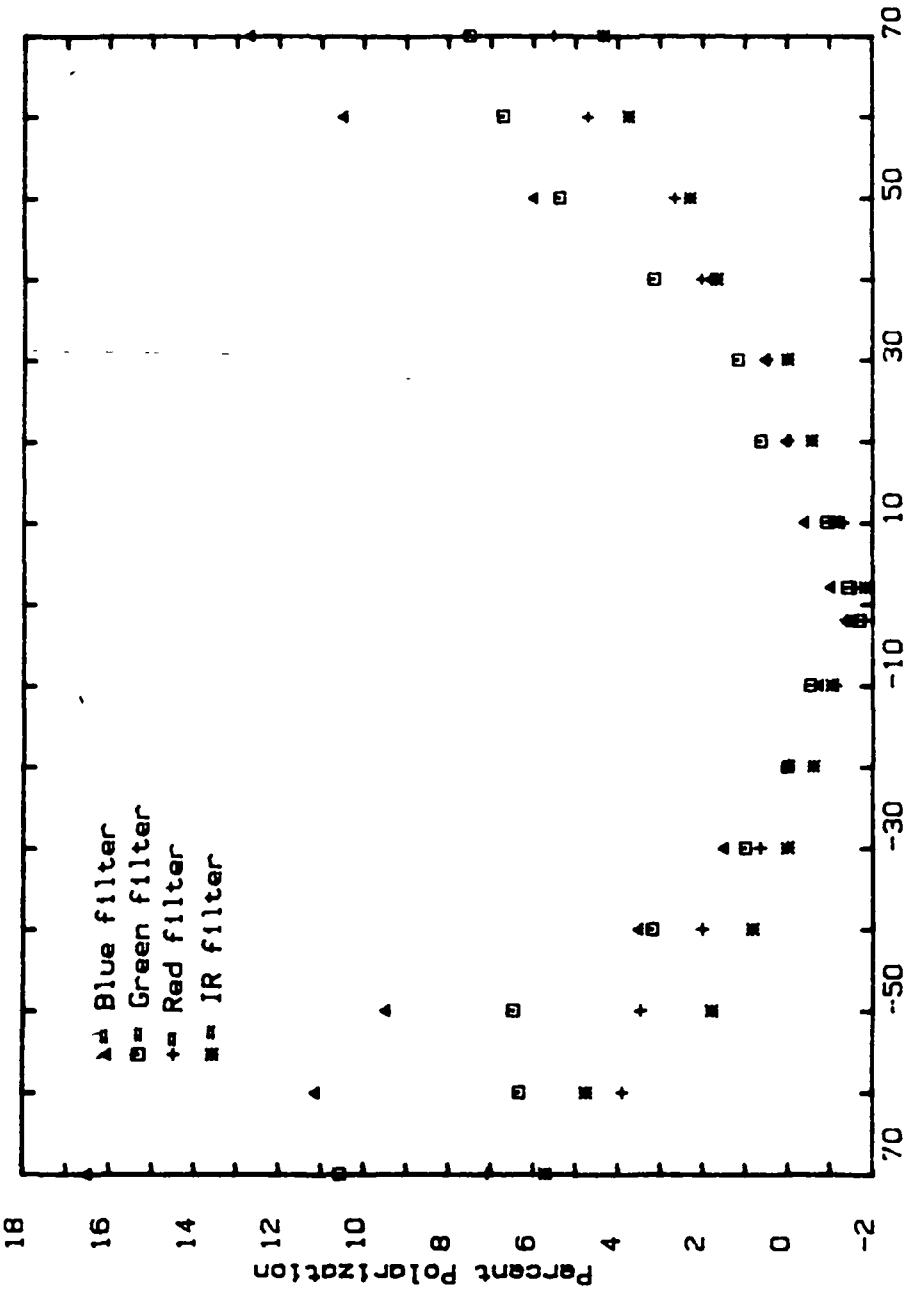

Figure 14c: Percent Polarization vs. Phase Angle. Looking at the soil the clover grew in, baked between a temperature of 100-250°C, at e=0°.

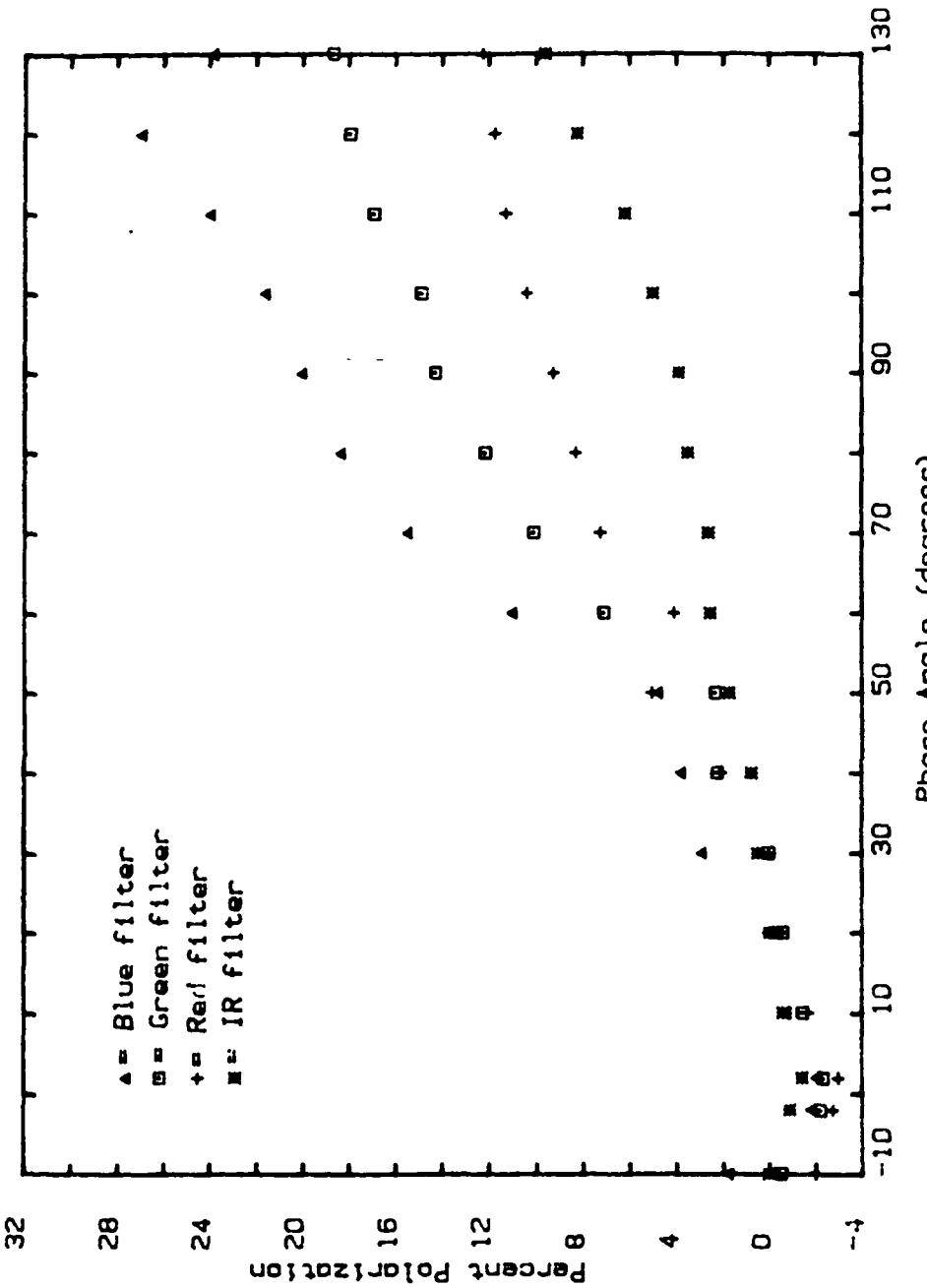

Figure 14d: Percent Polarization vs. Phase Angle. Looking at the soil the clover grew in, baked between a temperature of 100-250°C, at e=60°.

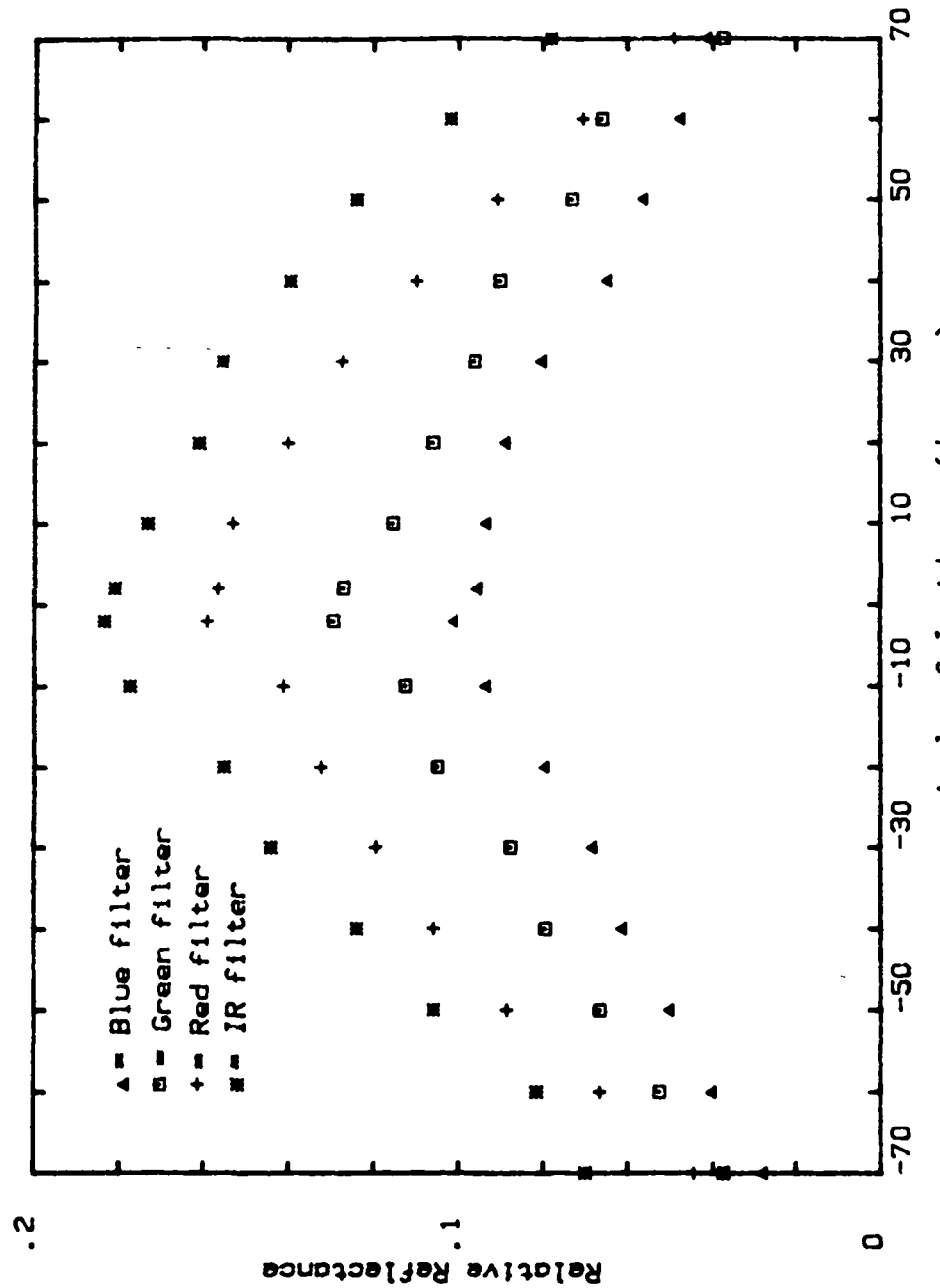

Figure 15a: Relative Reflectance vs. Angle of Incidence. Looking at the soil the clover grew in, moistened by water, at e=0°.

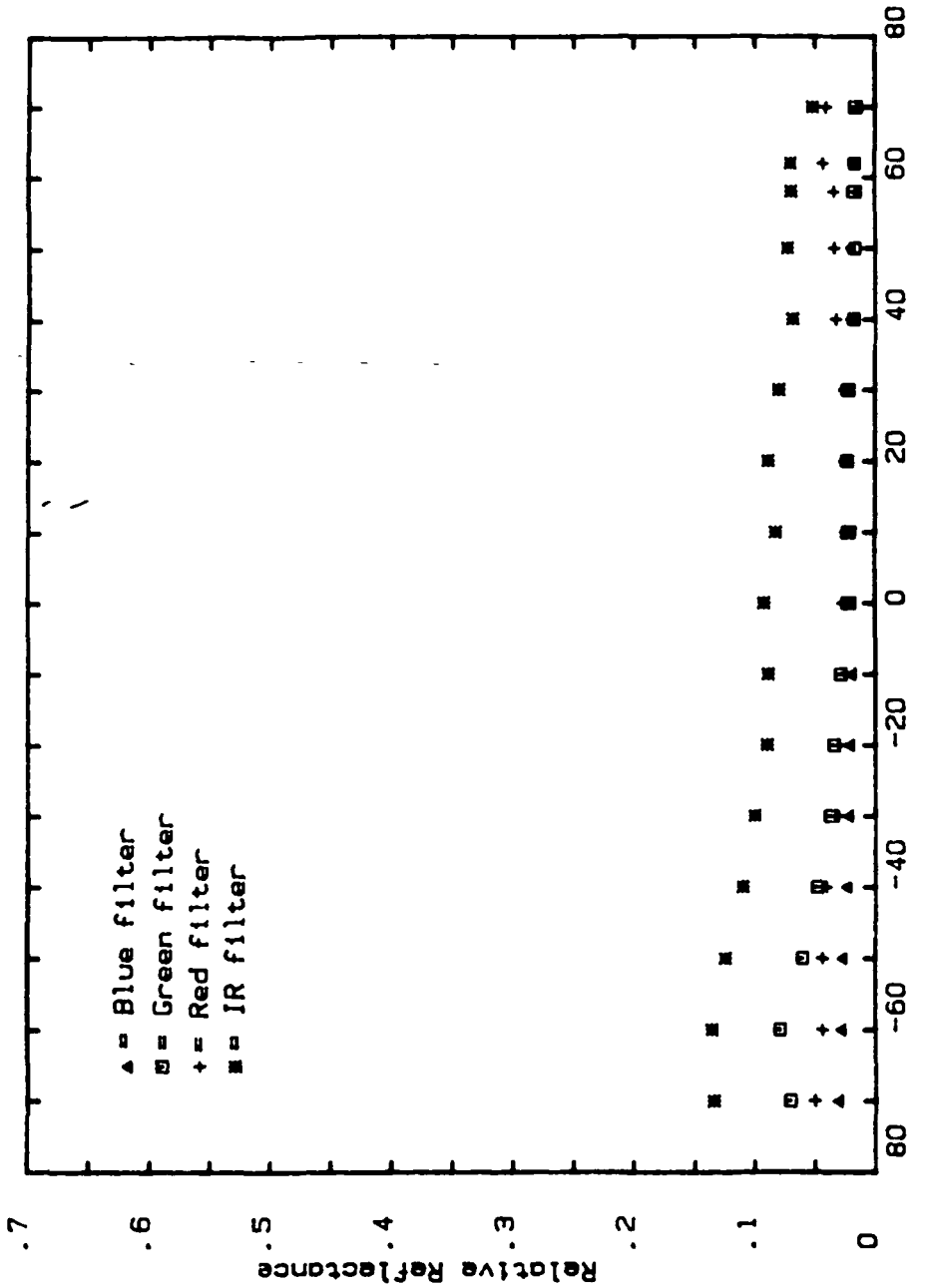

Figure 15b: Relative Reflectance vs Angle of Incidence. Looking at the soil the clover grew in, moistened by water, at e=60°.

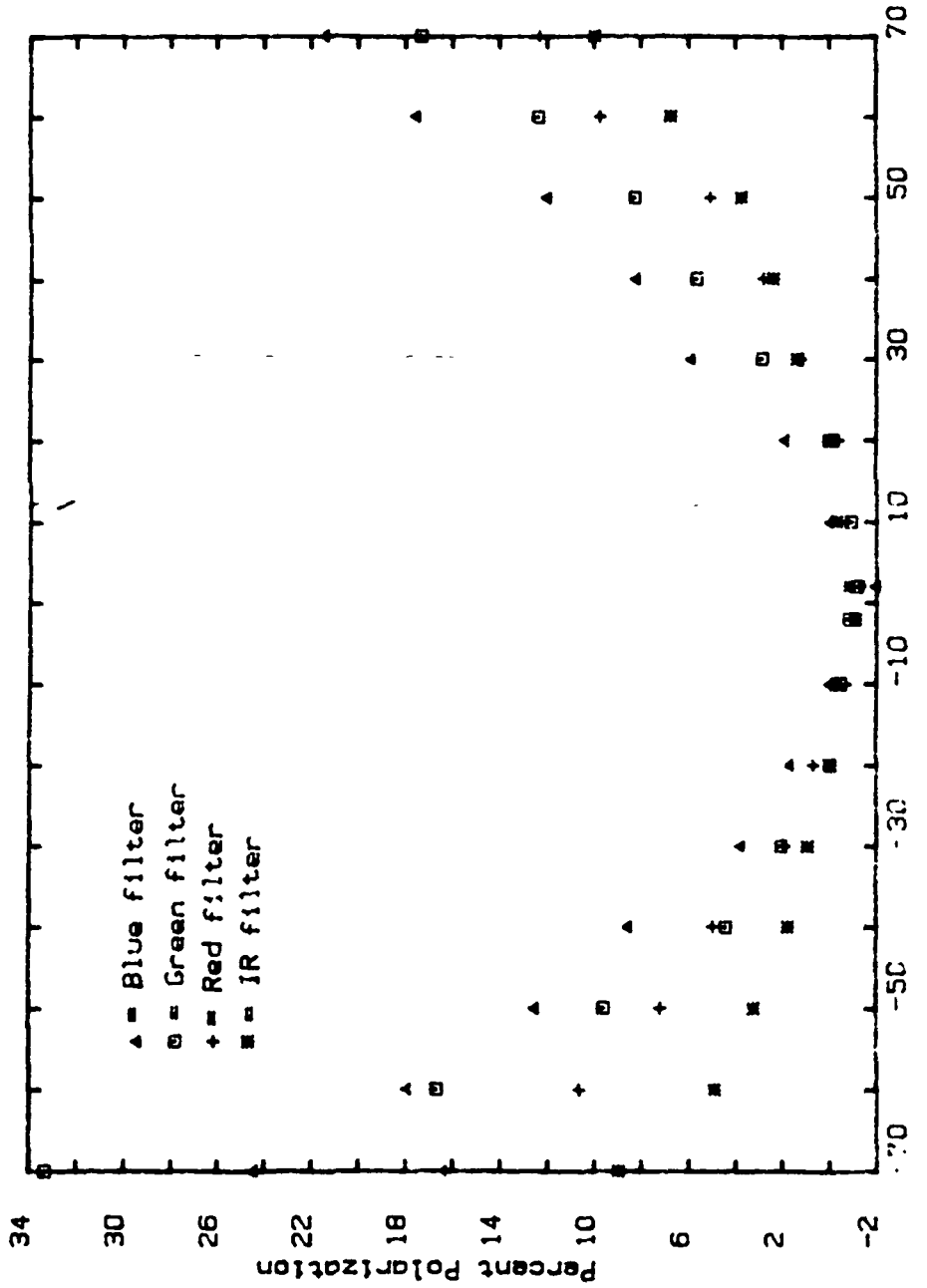

Figure 15c: Percent Polarization vs. Phase Angle. Looking at the soil the clover grew in, moistened by water, at e=0°

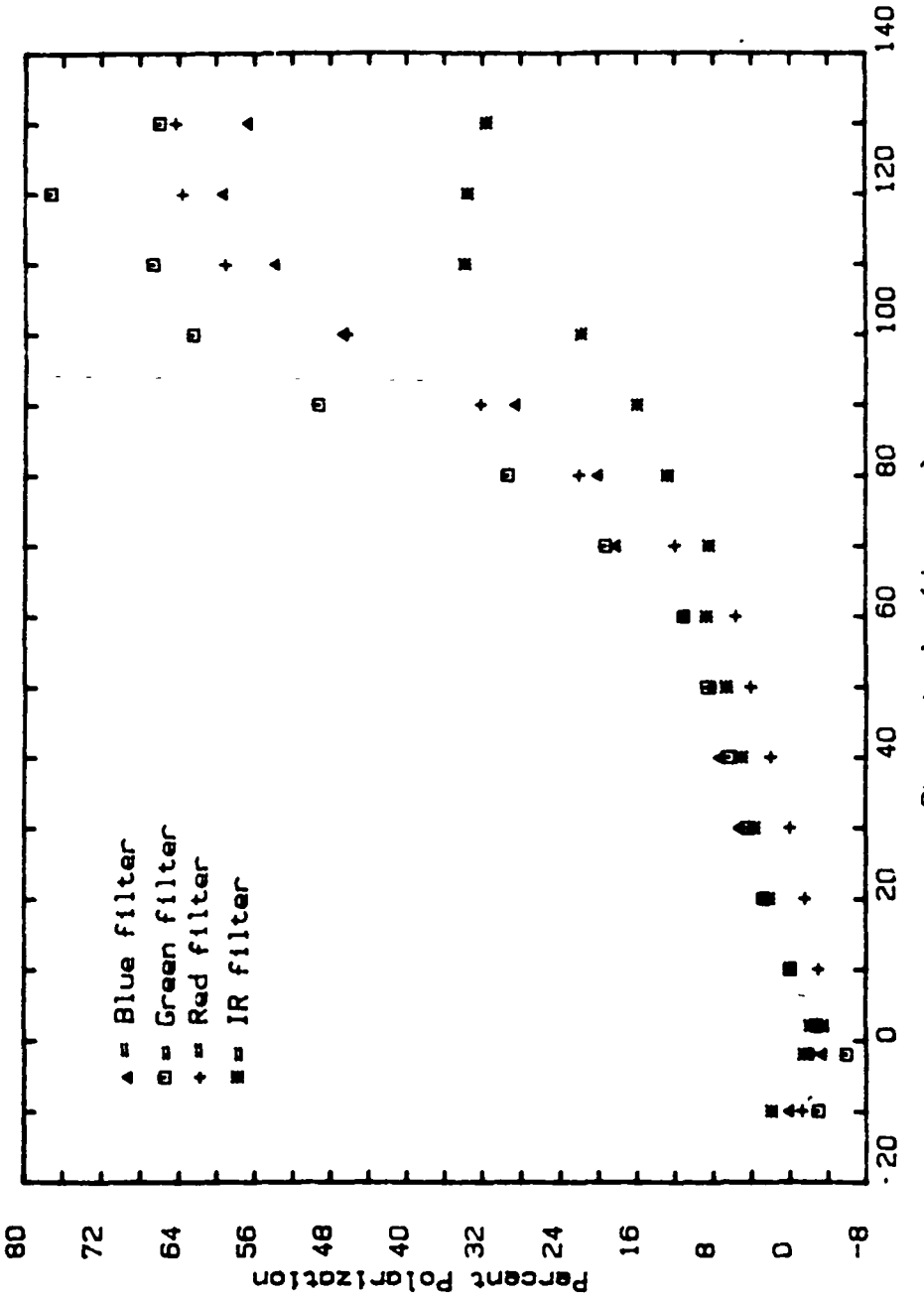

Figure 15d: Percent Polarization vs. Phase Angle. Looking at the soil the clover grew in, moistened by water, at e=60°.

and negative when on the opposite side. The following general observations can be made after examining the above data:

1) The reflectance curves of the vegetation data (figures 7-12) display the same general features as those for the soils (figures 13-15). This includes a sharp increase (cf. figures 9a,b) for patches in the reflectance near g=0°, which is indicative of the opposition effect, in which shadowing appears to play a major role (Hapke, 1971). Even the individual clover leaves have a small opposition effect.
2) The polarization curves of the vegetation data (figures 7-12) display the same general features as those for the soils (figures 13-15) and the planetary curve (figure 2). A negative branch is seen near g=0°, and the positive branch has a maximum near g=120°. The inversion angle is around g=10° to 20°, with little dependence on reflectance. The amplitude of the positive branch is inversely related to reflectance, consistent with the Umov effect. These results are similar to those of Egan and Hallock (1966).
3) Inversion angles are between 0°-30°, most commonly around 10°, 20° or 30°. Comparing with Egan and Hallock (1966) we see that pine is the only vegetation measured by them with a similar angle (10° in green, 38° in IR). However, several minerals have low inversion angles.
4) The angles e and g have as large or larger an effect on polarization as i. Thus, the conclusion of Vanderbilt et. al. (1982) that polarization is controlled by i is not substantiated.

5) By examining figure 8d (live clover leaf, vert.), it can be seen that the light scattered by the upper surface of the leaf ($g<90^\circ$) is positively polarized, but that transmitted through the leaf ($g>90^\circ$) is strongly negatively polarized. This is evidenced by a peak in the %P at $g=50^\circ$-70°, with a general decline thereafter, until it dips into the negative polarization region between $g=90^\circ$-120°.

6) In comparing the individual clover leaf data (figures 7-8) with the clover patch data (figure 9), we see that the individual leaf in the horizontal position (figure 7) has a higher reflectance and polarization (except at $i=0^\circ$ in the IR) than the patch (figure 9). However, the individual leaf in the vertical position (figures 8a,c) had a lower reflectance and polarization (except in the red) than the patch. Generally, the leaves in the aggregate have reflectances and polarizations which are intermediate between the individual leaf properties in the vertical and horizontal positions.

7) The clover patch and grass data are qualitatively, but not quantitatively, similar. The clover has higher %P and reflectance (except at $i=60^\circ$ in the red and IR bands). The polarization (figures 9d and 11d) of both show a peak at $g=90^\circ$-100°. The clover appears to have a small component of specular reflection, as evidenced by a small specular peak in figure 9b.

8) Figures 12b,d for corn and 15b,d for moist soil are similar, although the corn has a higher reflectance. This similarity

is due to the fact that the moist soil had numerous tiny "puddles" of standing water on it, thereby causing a significant specular reflection component. In the case of corn, the cutin layer, which is quite shiny, causes a significant specular reflection component.

9) Figures 13 and 14 for the natural and baked soil are similar. Soil curves are in general "smoother" than vegetation curves. We believe the reason for this is that when the vegetation was measured there were only a few leaves in the field of view of the detector, as opposed to the many soil grains seen. Thus, the vegetation sampling was incomplete. However, a spacecraft looking down would see many leaves and the vegetation curves would then be smoother. When examining the curves, the general trends are most important to note, not the detailed structure seen. In vegetation, the data taken through the blue and red filters is similar due to the chlorophyll absorption bands; i.e., reflectance is low and %P is high. In soil, the data taken through the blue and green filters are similar and that taken through red and IR are also similar. Reflectance is low and %P is high through the blue and green filters because soil contains ferric iron (Fe^{3+}) which absorbs at shorter wavelengths.

10) In comparing the dry clover leaf (figures 10a,b) with the live clover leaf (figures 7a,b), we see that Myers' statement (cf. sec. 2.4b) about reflectance increasing in the green wavelength region is incorrect. This may be because we

measured data for a dehydrated leaf, instead of one that had senesced. Our data may be more pertinent for plants that are found in areas that have been stricken by a drought. As my data shows: there is a decrease in the blue and green bands, an increase in red, while IR increases at i=0°, and decreases at i=60°. The reasons for this are not well understood, but may be related to an abundance of anthocyamin or carotene pigments, after the chlorophyll has been degraded (cf. Myers, 1983). The live and dry leaves both have a specular reflection component, as seen in figures 7b, 10b. This is evidenced by the reflectance peak occurring near -60° as opposed to 60°, and is due to the cutin layer on the leaf.

11) We examined the live clover patch (figure 9d) and the live grass patch (figure 11d) in order to determine the maximum polarization expected at each measured wavelength. In the blue filter, the clover patch peaked near 42%, while the grass peaked near 6%. In the green filter, the clover patch peaked near 14%, while the grass peaked near 6%. In the red filter, the clover patch peaked near 20%, while the grass peaked near 5%. Finally, in the IR filter, the clover patch peaked near 6%, while the grass peaked near 4%. We also wanted to estimate the polarization that would be expected for the clover and grass patches from a Landsat type of configuration (approximately e=0°, i=45°, g=45°). Through the blue filter, the polarization is approximately 11% for the clover patch

and 2.7% for the grass. Through the green filter, the polarization is approximately 5% for the clover and 2.3% for the grass. Through the red filter, the polarization is approximately 5.7% for the clover and 1.5% for the grass. Finally, through the IR filter, the polarization is approximately 2.2% for the clover patch and 1.7% for the grass.

4.2 Interpretation

In our first attempt to interpret the data we tried fitting the reflectance curves of the clover patch data (figures 9a, b) using the equation for the bidirectional reflectance of a particulate medium (Hapke, 1981), corrected for macroscopic roughness (Hapke, 1984). Relative to a Lambert surface, the reflectance is:

$$r=(w/4)[\cos i/(\cos i + \cos e)] \times \{[1+B(g)]p(g) + H(\cos i)H(\cos e) - 1\} \quad (1)$$

where,

$$B(g)= B_0/[1 + (1/h)\tan(g/2)], \quad (1a)$$

$$p(g)= 1 + b \cos g + c[(3\cos^2 g - 1)/2] \text{ and} \quad (1b)$$

$$H(x)= [(1+2x)/(1+2\sqrt{1-w}\, x)]. \quad (1c)$$

In addition, the roughness correction introduces a mathematically-complicated function of θ, the average surface roughness angle. The expression contains six parameters: w is the effective single-scattering albedo, B_0 and h are the amplitude and width, respectively, of the opposition effect, b and c are coefficients in the

Legendre polynomial expansion of the single-particle angular scattering function p(g), and the roughness angle θ. This form for B(g) is somewhat different from that given in (Hapke, 1981) and is an improved form based on unpublished work (Hapke, in preparation). The term [1+B(g)]p(g) describes the singly-scattered intensity, and H(cos i)H(cos e) - 1, the multiply-scattered light. We tried fitting the theoretical function to the data by first assigning trial values to w, B_0 and h. When a fairly close fit was found, we then assigned values to b, c and θ to fit the curve better. Next, we iterated all parameters until we had fit the curve as closely as possible.

Some of the theoretical curves are shown in figure 16, along with the best-fit values of the photometric parameters. Unfortunately, we could not get exact theoretical fits to all of the curves. We think this may be due to the fact that our field of view for the detector included only a few leaves. However, in general, the overall trends of the theory and data are similar, and the data appear to be described reasonably well by the theory.

Our working hypothesis was that the primary contribution to the positive branch of polarization was quasi-specular Fresnel reflection from portions of leaf surfaces that happen to be properly oriented for specular reflection of light from the source into the detector. To test this hypothesis we compared a quantity which we call the net polarized reflectance [R_+-R_] from the leaves with the

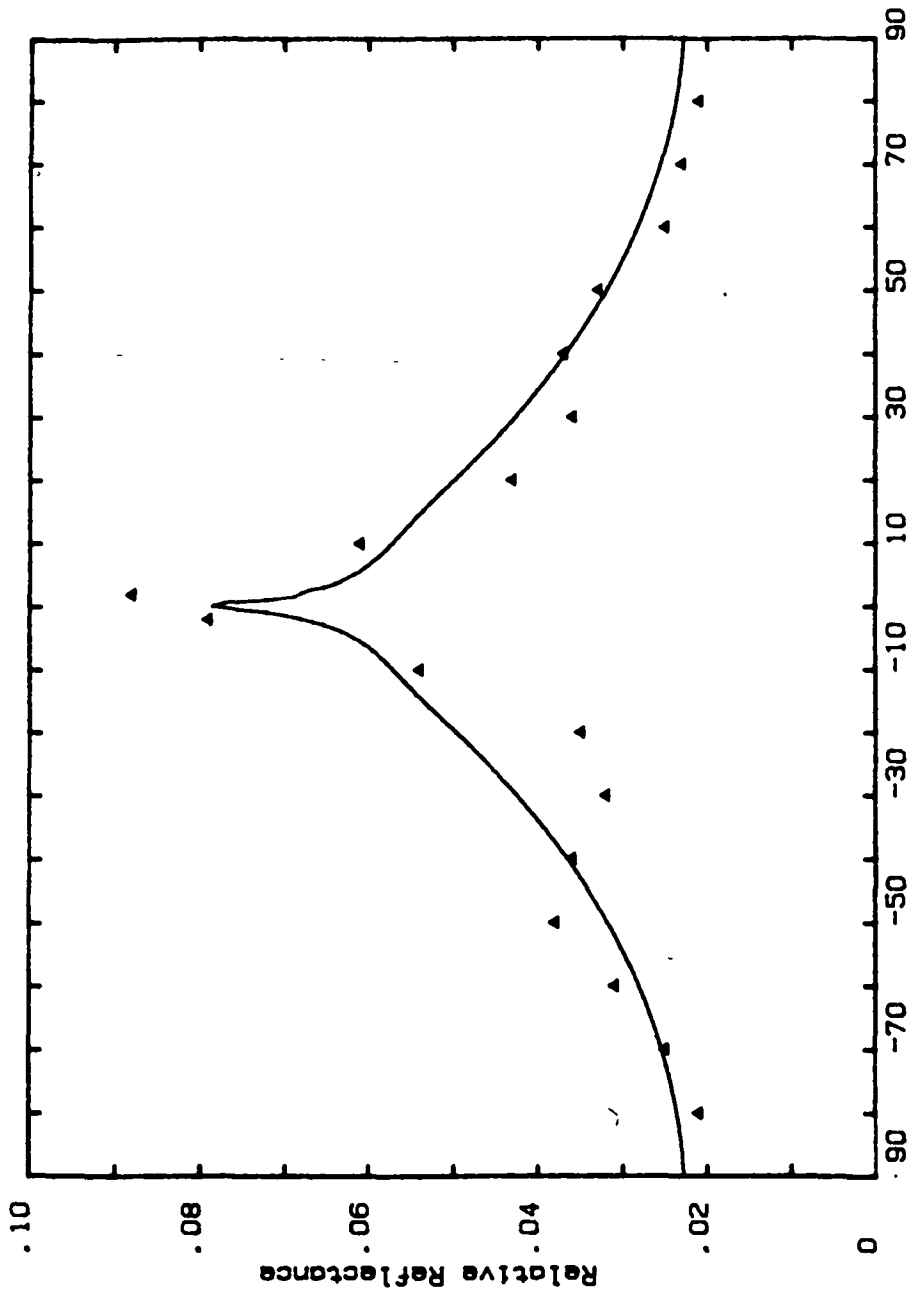

Figure 16a: Relative Reflectance vs. Angle of Emergence. Looking at a live clover patch, through the blue filter, at i=60°. The points represent the data. The solid line denotes the fit to the curve using the theoretical function (eq. 1), with the following parameters: w=.25, B =.6, h= 03, b=.2, c=.3 and θ_0=60°.

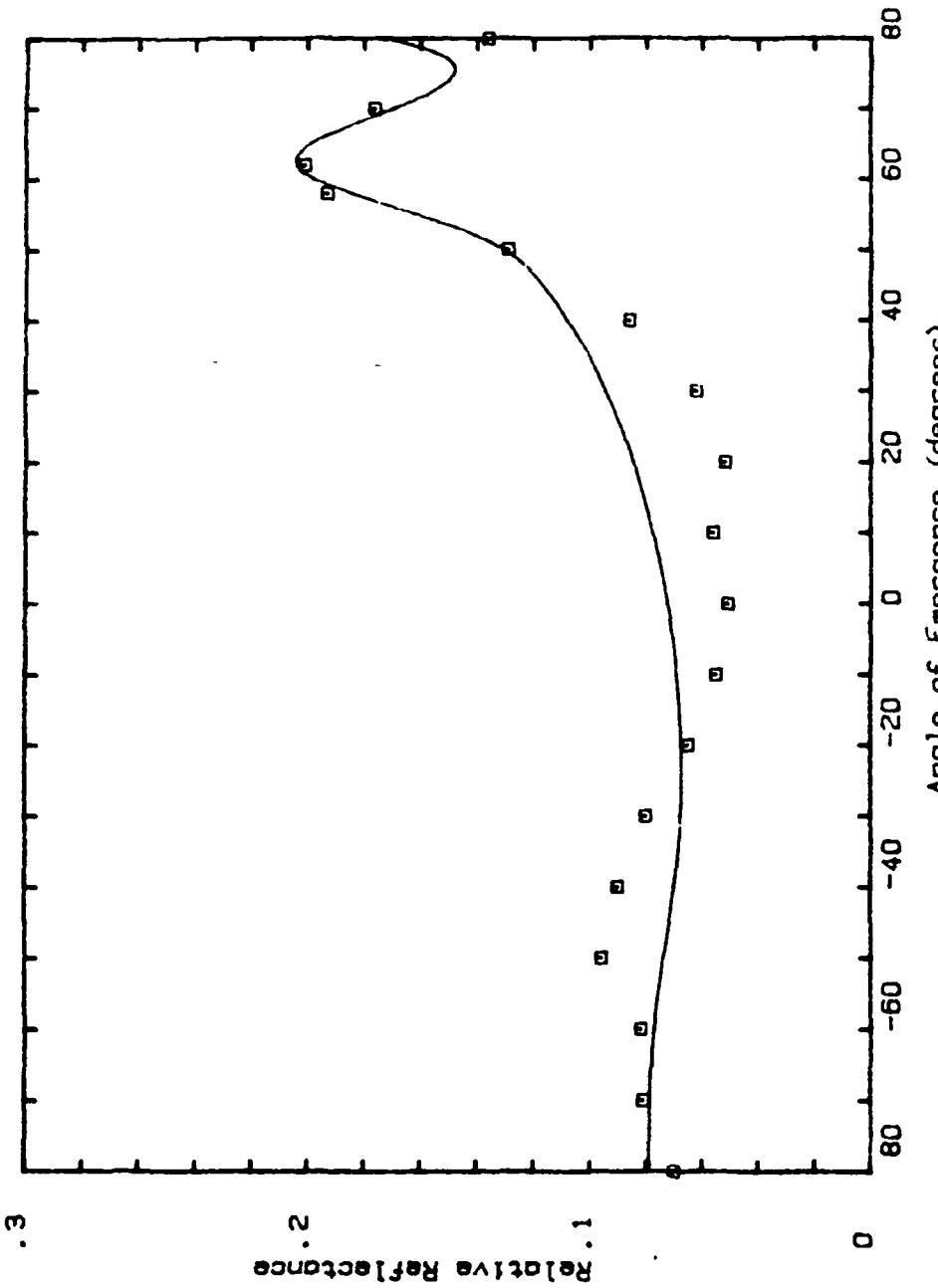

Figure 16b: Relative Reflectance vs. Angle of Emergence. Looking at a live clover patch, through the green filter, at i=60°. The points represent the data. The solid line denotes the fit to the curve using the theoretical function (eq. 1), with the following parameters: w=.54, B =.8, h=.05, b=.2, c= 2 and θ=15°.

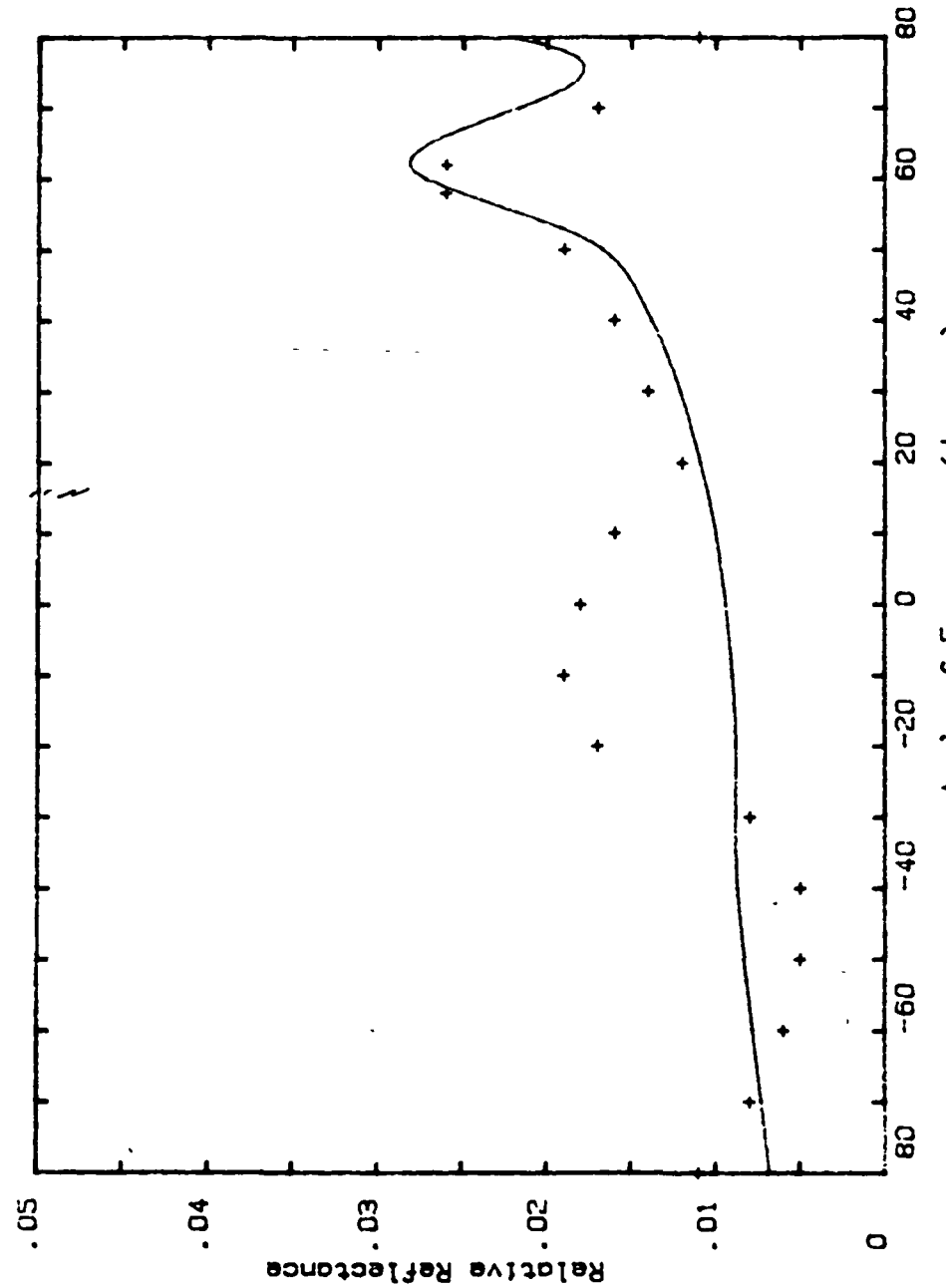

Figure 16c: Relative Reflectance vs. Angle of Emergence. Looking at a live clover patch, through the red filter, at ι=60°. The points represent the data. The solid line denotes the fit to the curve using the theoretical function (eq.1), with the following parameters: w=.11, B =.6, h=.03, b=.1, c=.1 and θ=25°.

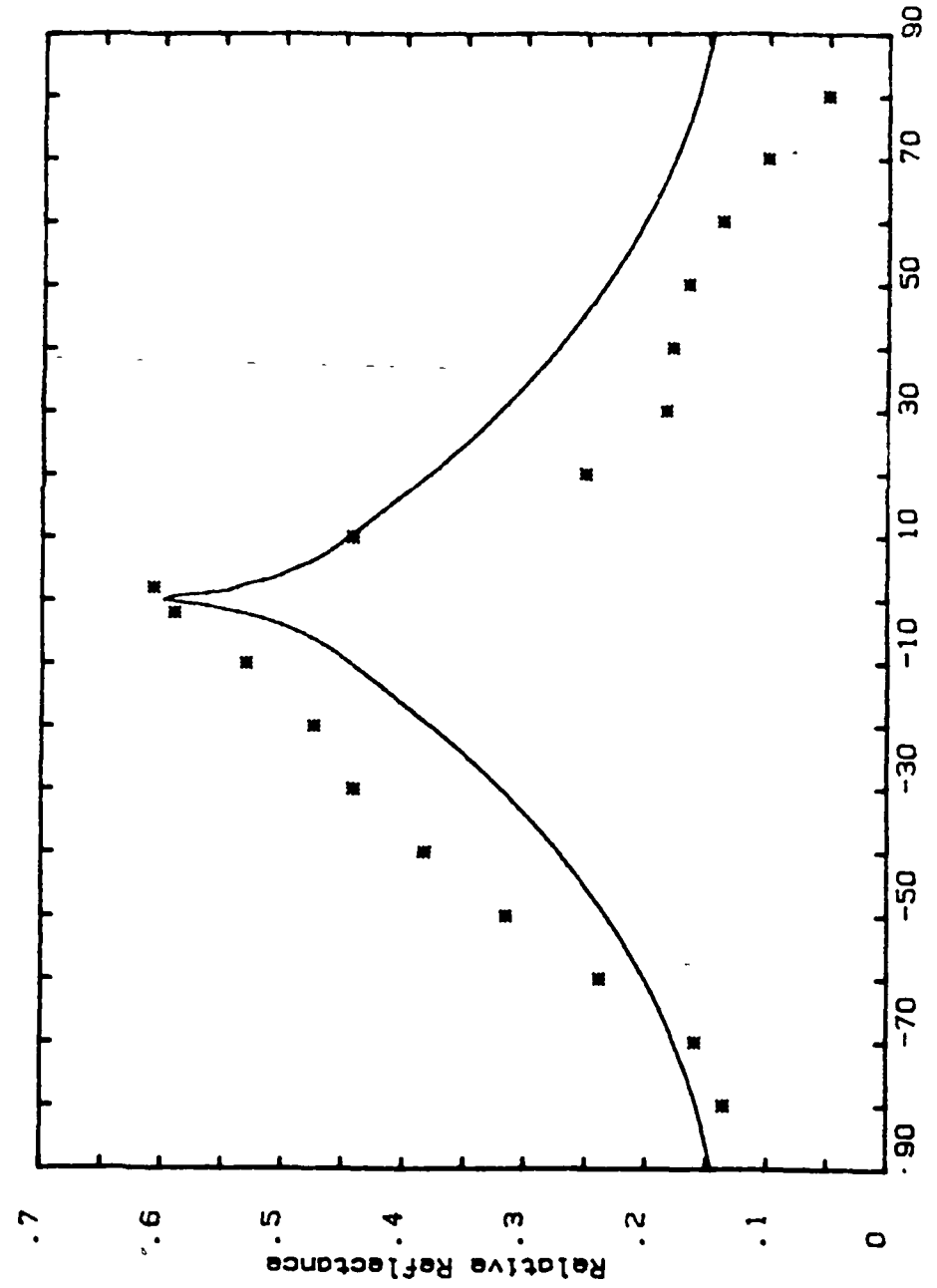

Figure 16d: Relative Reflectance vs. Angle of Emergence. Looking at a live clover patch, through the IR filter, at i=0°. The points represent the data. The solid line denotes the fit to the curve using the theoretical function (eq. 1), with the following parameters: w=.9, B =.87, h=.05, b=.7, c=.7 and θ=60°.

phase angle, g. The following derivation was used to define the net polarized reflectance:

$$I = Jr \qquad I_+ = J_+ r_+ \qquad I_- = J_- r_- \qquad J_+ = J_- = J/2 \qquad r = (r_+ + r_-)/2, \tag{2}$$

$$\begin{aligned} P &= [I_+ - I_-)/(I_+ + I_-)] \\ &= [(.5Jr_+ - .5Jr_-)/(.5Jr_+ + .5Jr_-)] \\ &= [(.5r_+ - .5r_-)/(.5r_+ + .5r_-)] \\ &= [(.5r_+ - .5r_-)/r] \end{aligned} \tag{3}$$

so,

$$2rP = r_+ - r_-, \text{ for a single particle (leaf).} \tag{4}$$

Now, a large number of solutions of the radiative transfer equation for the bidirectional reflectance from a semi-infinite particulate medium can be written in the form (Chandrasekhar, 1960):

$$r_+ = .25[\cos i/(\cos i + \cos e)]R_+ \text{ and}$$

$$r_- = .25[\cos i/(\cos i + \cos e)]R_- \tag{5}$$

where,

$$R_+ = w(\text{single particle} + \text{multiple scattering effects})_+,$$

$$R_- = w(\text{single particle} + \text{multiple scattering effects})_-. \tag{6}$$

For instance, using equation (1), we have: $R = w[1+B(g)]p(g) + w[H(\cos i)H(\cos e) - 1]$. If $g \gtrsim 20°$, then B(g) can be ignored. Therefore, for large phase angles:

$$8r[(\cos i + \cos e)/\cos i]P = R_+ - R_-. \tag{7}$$

We wished to test the hypothesis that the multiply-scattered radiance and the volume-scattered components of R_+ and R_- are essentially unpolarized, and that the only contribution to $R_+ - R_-$ will be that portion of wp(g) which describes specular scattering from the upper surfaces of the leaves. This portion should be approximately

equal to F_+-F_-, where F_+ and F_- are the Fresnel reflection coefficients for facets in a specular orientation with individual i=e=g/2:

$$F_+=[\sin(g/2-g'/2)/\sin(g/2+g'/2)]^2 \text{ and} \quad (8a)$$

$$F_-=[\tan(g/2-g'/2)/\tan(g/2+g'/2)]^2, \quad (8b)$$

where from Snell's law:

$$\sin(g/2)=n \sin(g'/2). \quad (8c)$$

The Brewster phase angle is given by:

$$n=\tan(g_B/2). \quad (8d)$$

Thus, if the above hypothesis is correct, from equation (8) we should have for patches of leaves:

$$x\equiv 8rP[1+(\cos e/\cos i)]=F+-F_-, \quad (9a)$$

where r and P are the measured reflectance and polarization of a "patch". Similarly for an individual leaf, from equation (4) we should have:

$$y\equiv 2rP=F_+-F_-. \quad (9b)$$

We computed the net polarized reflectance functions x and y versus g, and compared them with F_+-F_- for leaves, patches and soil.

The index of refraction, n, was measured for clover using the Becke line method. The method works as follows (Bloss, 1961). A grain in oil (or solution) viewed with the microscope objective focused slightly above the position of sharpest focus will usually display two thin lines (one dark and one bright) concentric with its border. The brighter of these (Becke line) is always closest to the material having the higher refractive index and, moreover, always moves toward the medium having the higher refractive index, if viewed as the microscope is racked steadily upward above correct focus. I used a solution of sucrose and water to determine n for

clover and a refractometer to determine n for the solution. Clover was found to have n=1.38 for visible light. For this value of n, $g_B=108°$.

The net polarized reflectance data is shown in figures 17-22. In most cases the points for i=0° and i=60° are close to one another on the x vs. g plots, showing that the dominant independent variable is g.

In the vegetation data, the Fresnel difference functions (F_+-F_-) peaked at phase angles which were 30° to 40° larger than the measured data. Thus the leaf surface obviously cannot be modelled as a large number of smooth plane facets oriented in various directions. However, if each surface facet (cf. figure 23) had roughness elements which caused shadowing, then F_+ and F_- would each be reduced by a shadowing factor, which in the first approximation is $(\cos i)(\cos e)=\cos^2(g/2)$. This gives us the following revised test equations for the clover patch or individual leaf:

$$x=(F_+-F_-)\cos^2(g/2) \qquad (10a)$$

or

$$y=(F_+-F_-)\cos^2(g/2). \qquad (10b)$$

When we plotted this modified net Fresnel reflectance difference on the graphs (figures 17-19), we found an improved fit: the theoretical function peaked at about the same phase angle as the data, but now had a significantly smaller magnitude. This finding implies that the positive polarization is not controlled only by first-surface scattering, as hypothesized; probably contributions by the volume-scattered and multiply-scattered components of light are more important than previously thought.

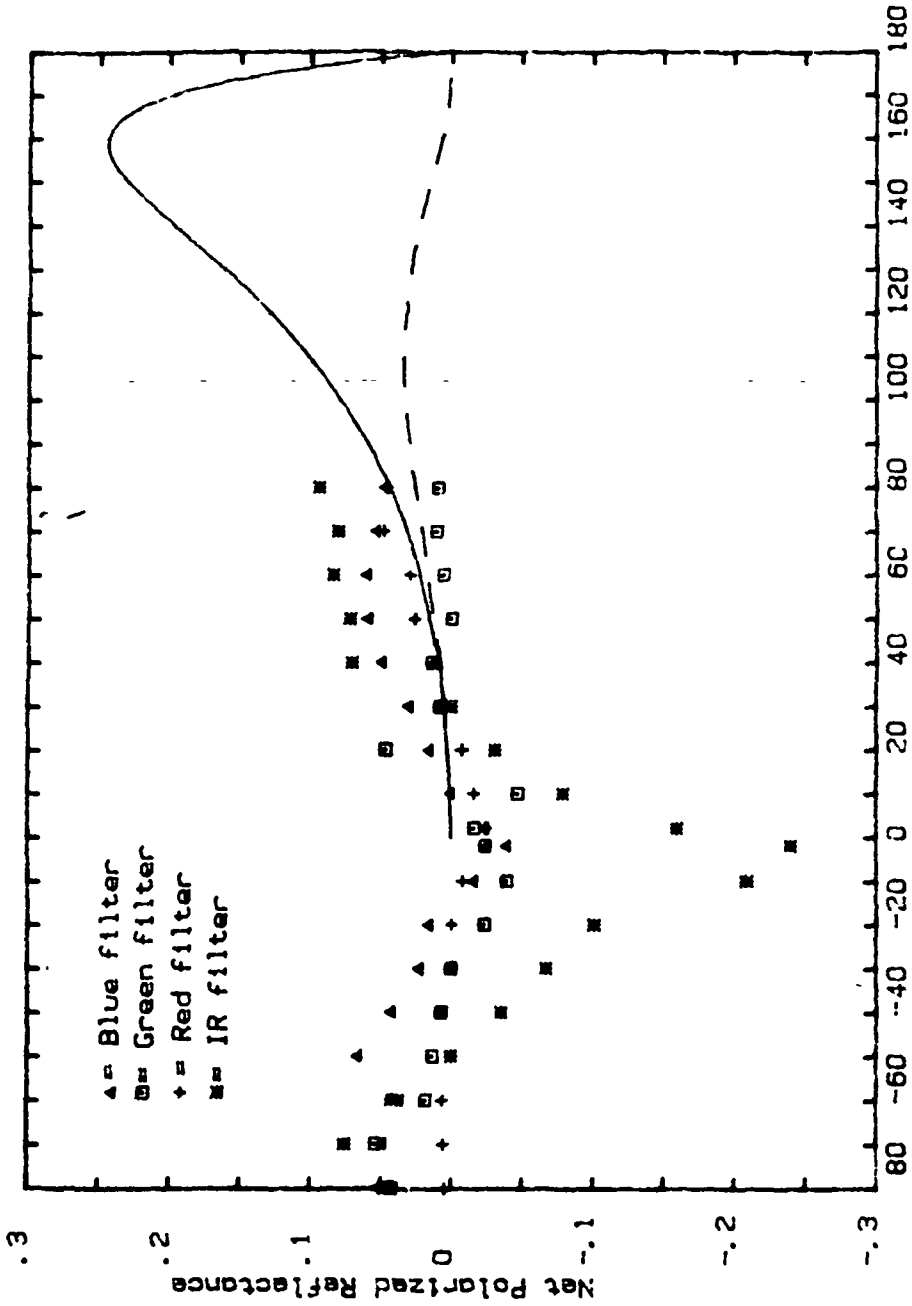

Figure 17a: Net Polarized Reflectance vs. Phase Angle. Looking at a live clover patch at i=0°. The solid line denotes the calculated Fresnel reflection coefficients (eq. 8), using n=1.38. The dashed line denotes the shadowed Fresnel reflectance difference (eq. 10).

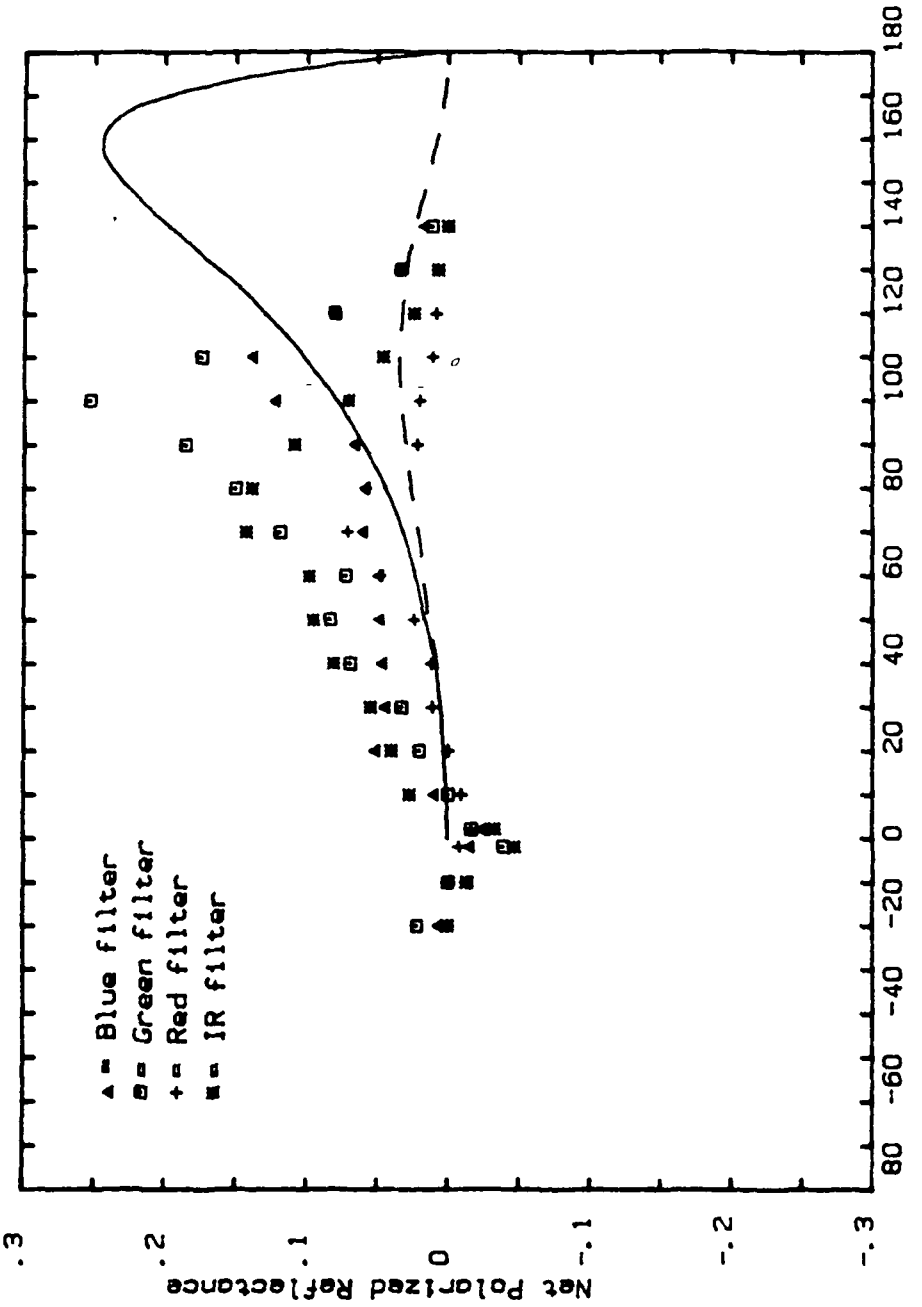

Figure 17b: Net Polarized Reflectance vs. Phase Angle. Looking at a live clover patch at i=60°. The solid line denotes the calculated Fresnel reflection coefficients (eq. 8), using n=1.38. The dashed line denotes the shadowed Fresnel reflectance difference (eq. 10)

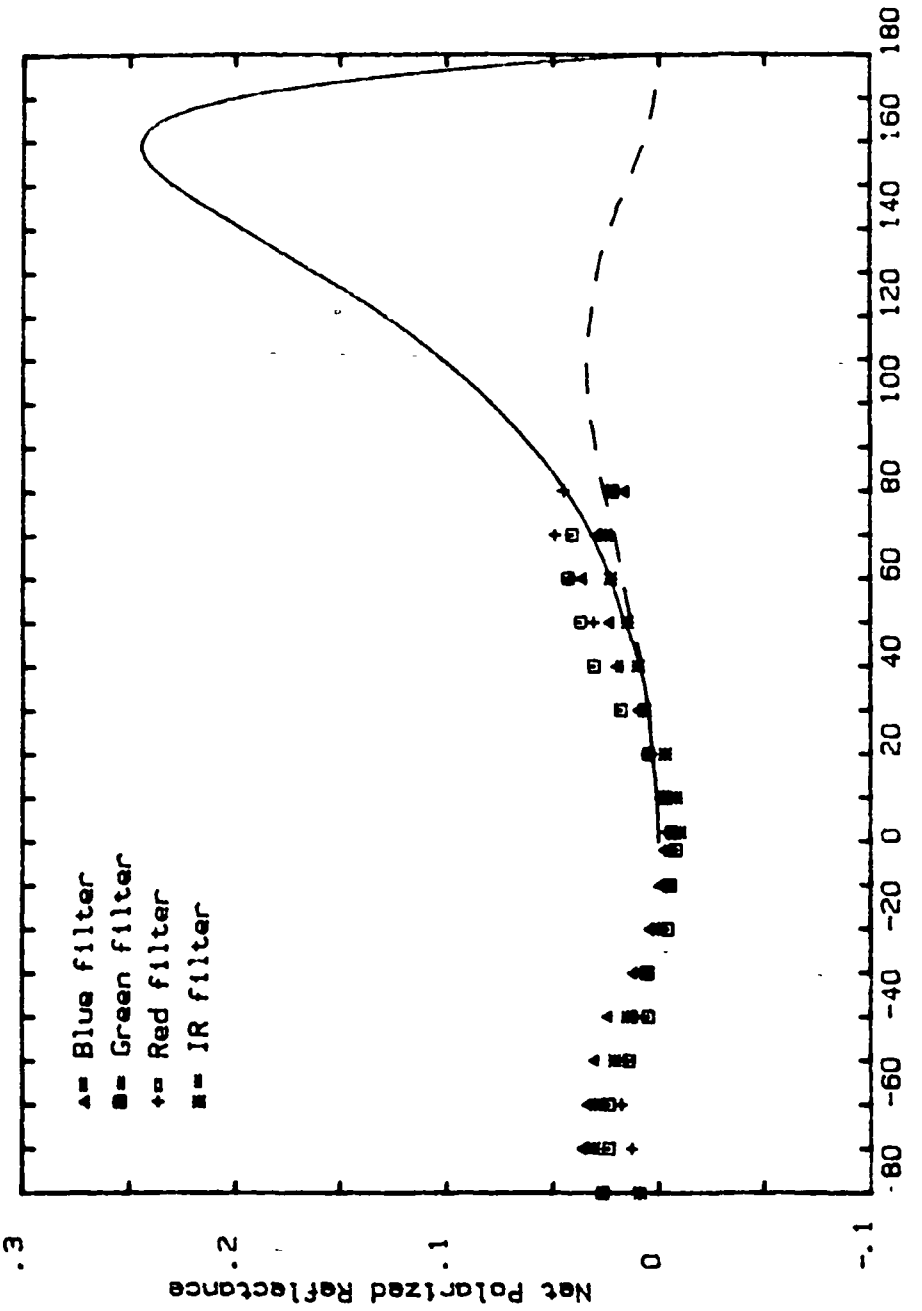

Figure 18a: Net Polarized Reflectance vs. Phase Angle. Looking at a live clover leaf in the horizontal position at $i=0^{o}$. The solid line denotes the calculated Fresnel reflection coefficients (eq. 8), using n=1.38. The dashed line denotes the shadowed Fresnel reflectance difference (eq. 10).

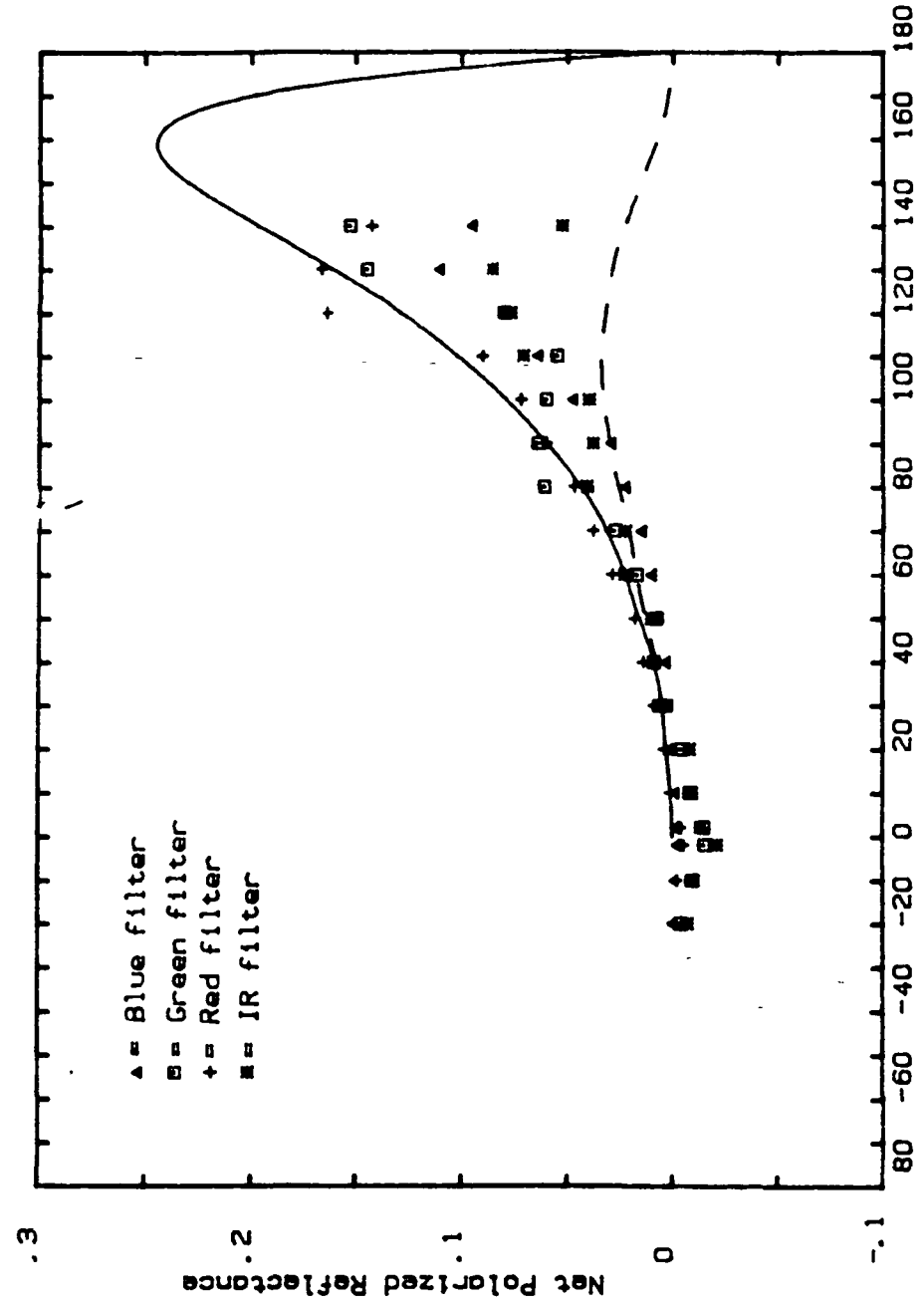

Figure 18b: Net Polarized Reflectance vs. Phase Angle. Looking at a live clover leaf in the horizontal position at i=60°. The solid line denotes the calculated Fresnel reflection coefficients (eq. 8), using n=1.38. The dashed line denotes the shadowed Fresnel reflectance difference (eq. 10).

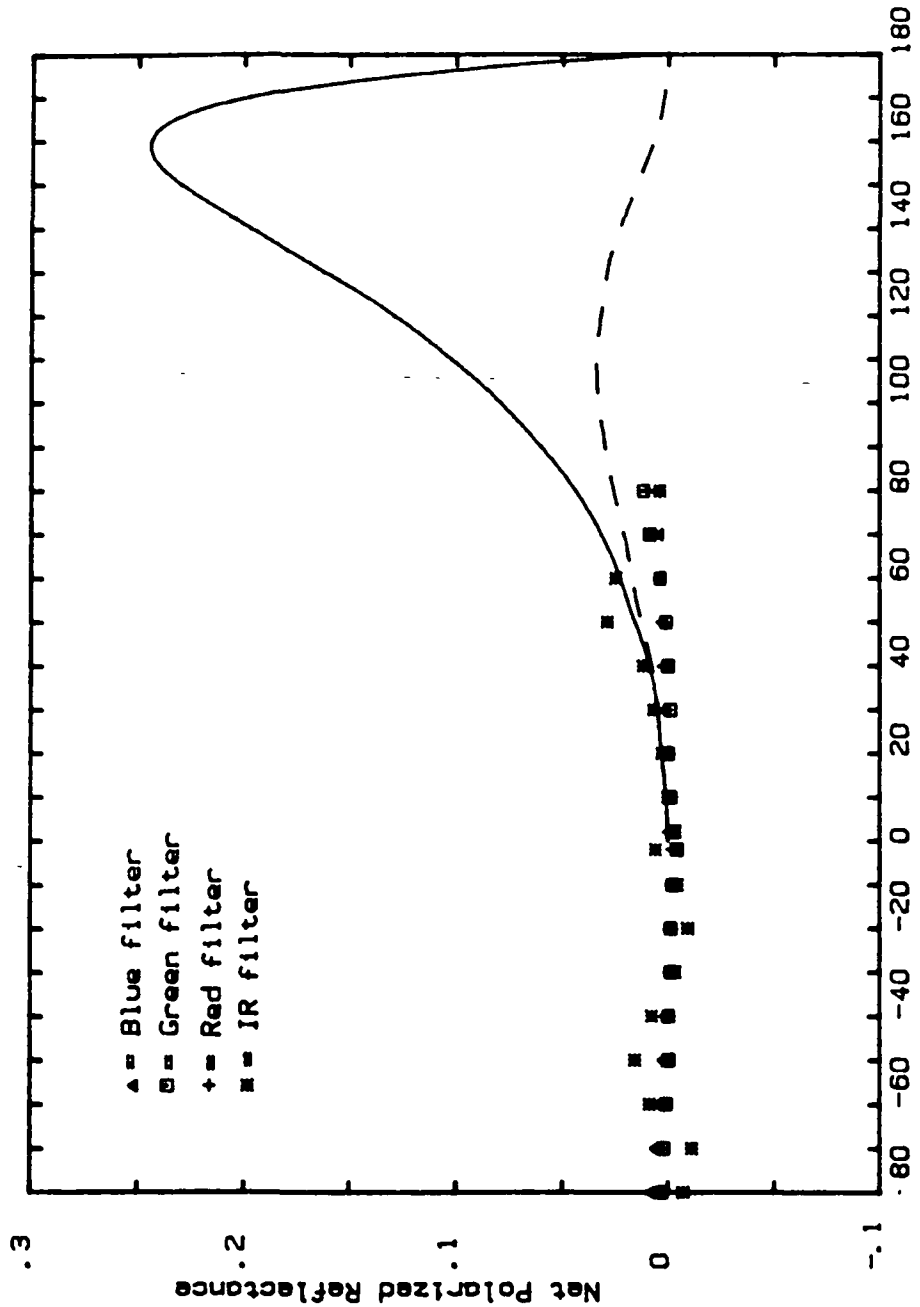

Figure 19a: Net Polarized Reflectance vs. Phase Angle. Looking at a live clover leaf in the vertical position at i=0°. The solid line denotes the calculated Fresnel reflection coefficients (eq. 8), using n=1.38. The dashed line denotes the shadowed Fresnel reflectance difference (eq. 10).

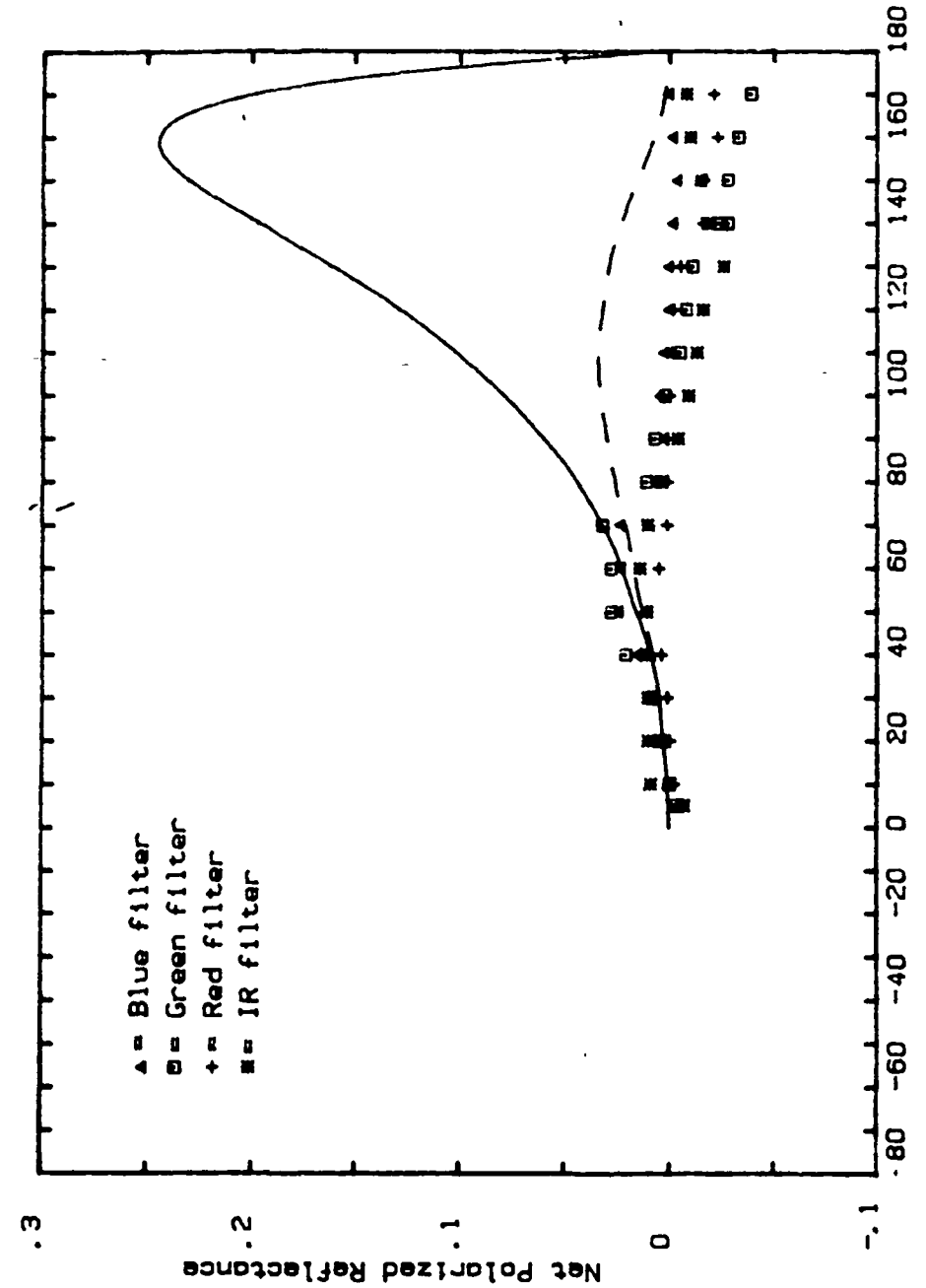

Figure 19b: Net Polarized Reflectance vs. Phase Angle. Looking at a live clover leaf in the vertical position at i=90°. The solid line denotes the calculated Fresnel reflection coefficients (eq. 8), using n=1.38. The dashed line denotes the shadowed Fresnel reflectance difference (eq. 10).

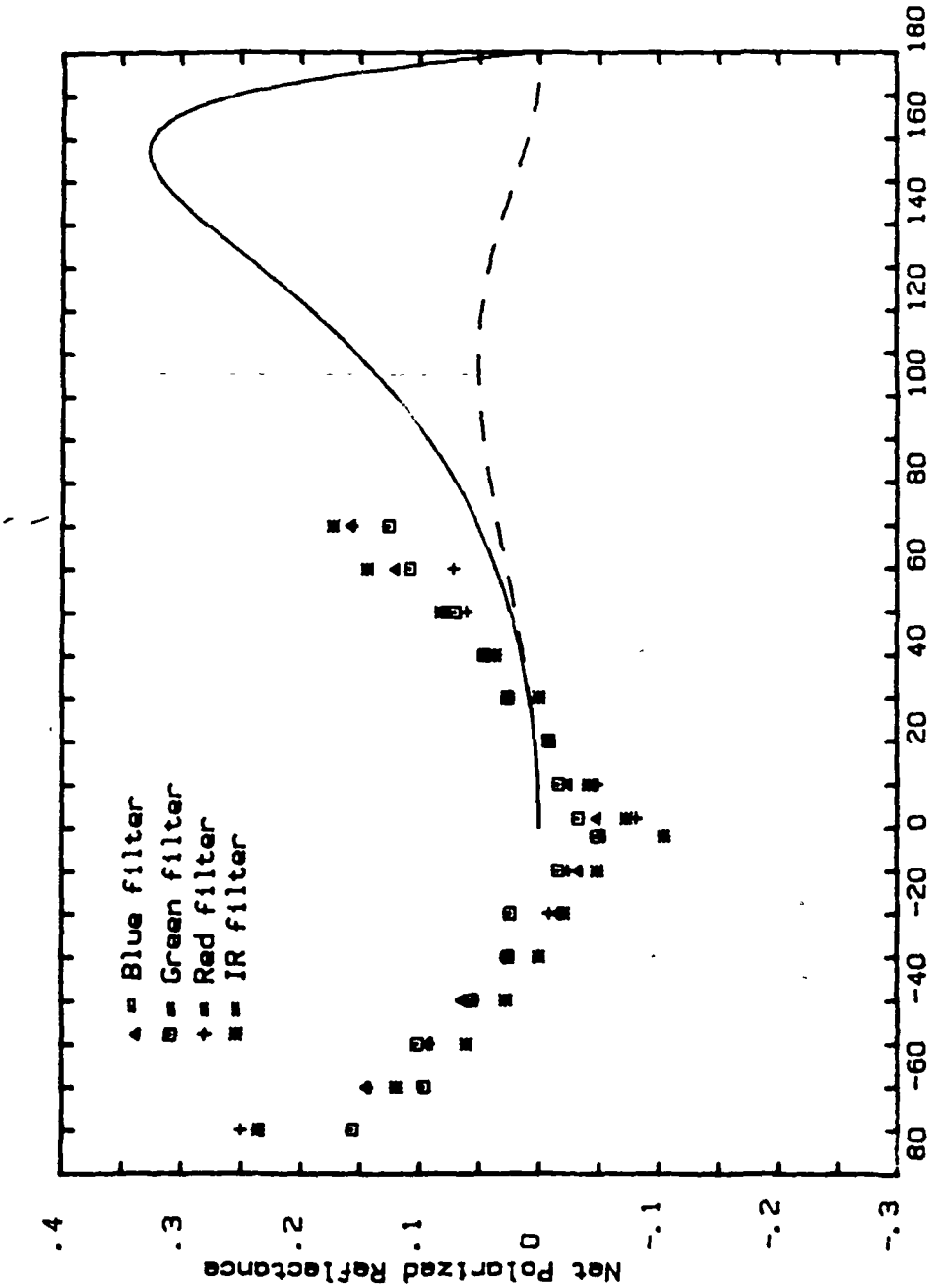

Figure 20a: Net Polarized Reflectance vs. Phase Angle. Looking at the soil the clover grew in at e=0°. The solid line denotes the calculated Fresnel reflection coefficients (eq 8), using n=1.55. The dashed line denotes the shadowed Fresnel reflectance difference (eq. 10).

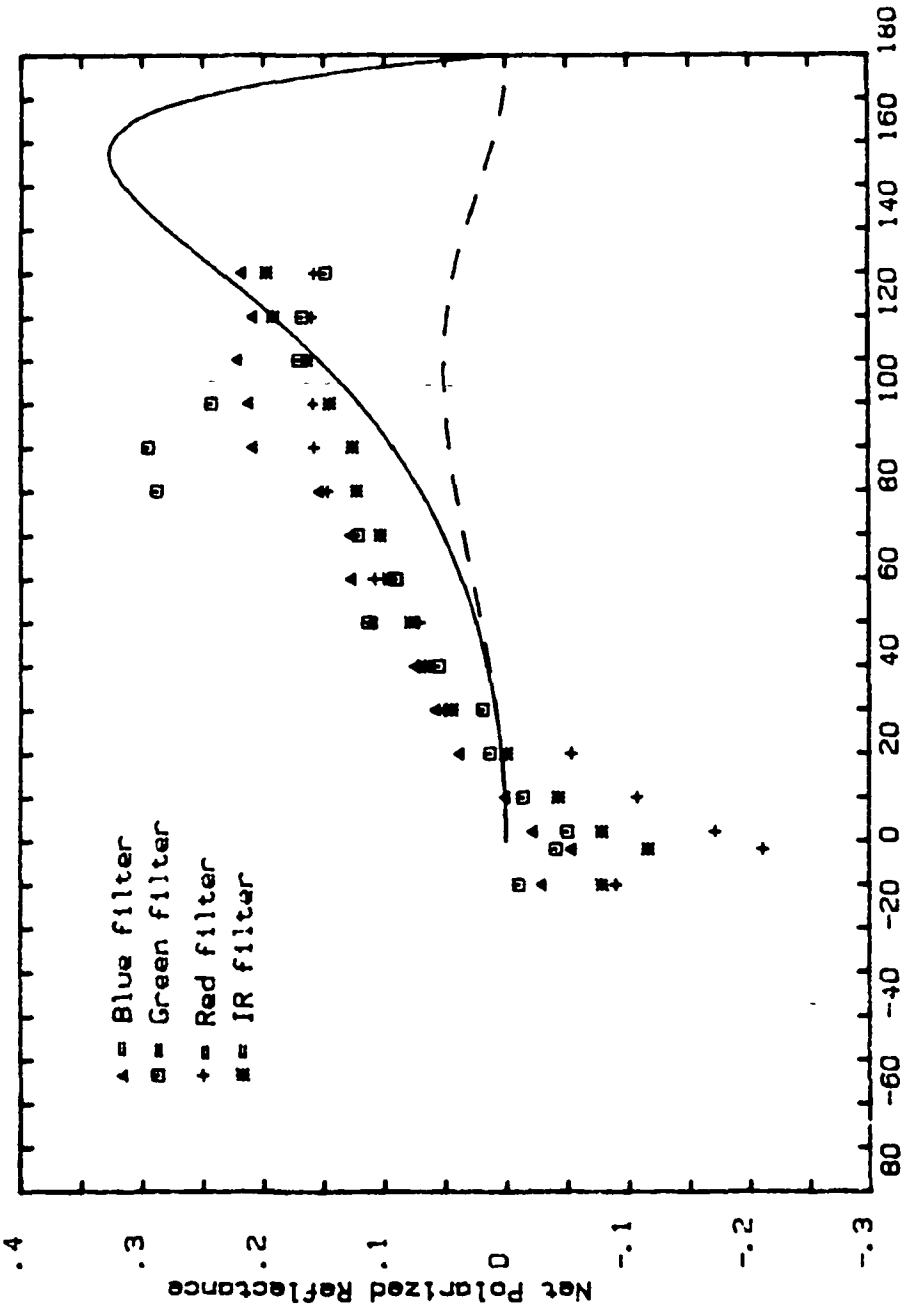

Figure 20b: Net Polarized Reflectance vs. Phase Angle.Looking at the soil the clover grew in at e=60°. The solid line denotes the calculated Fresnel reflection coefficients (eq. 8), using n=1.55. The dashed line denotes the shadowed Fresnel reflectance difference (eq. 10).

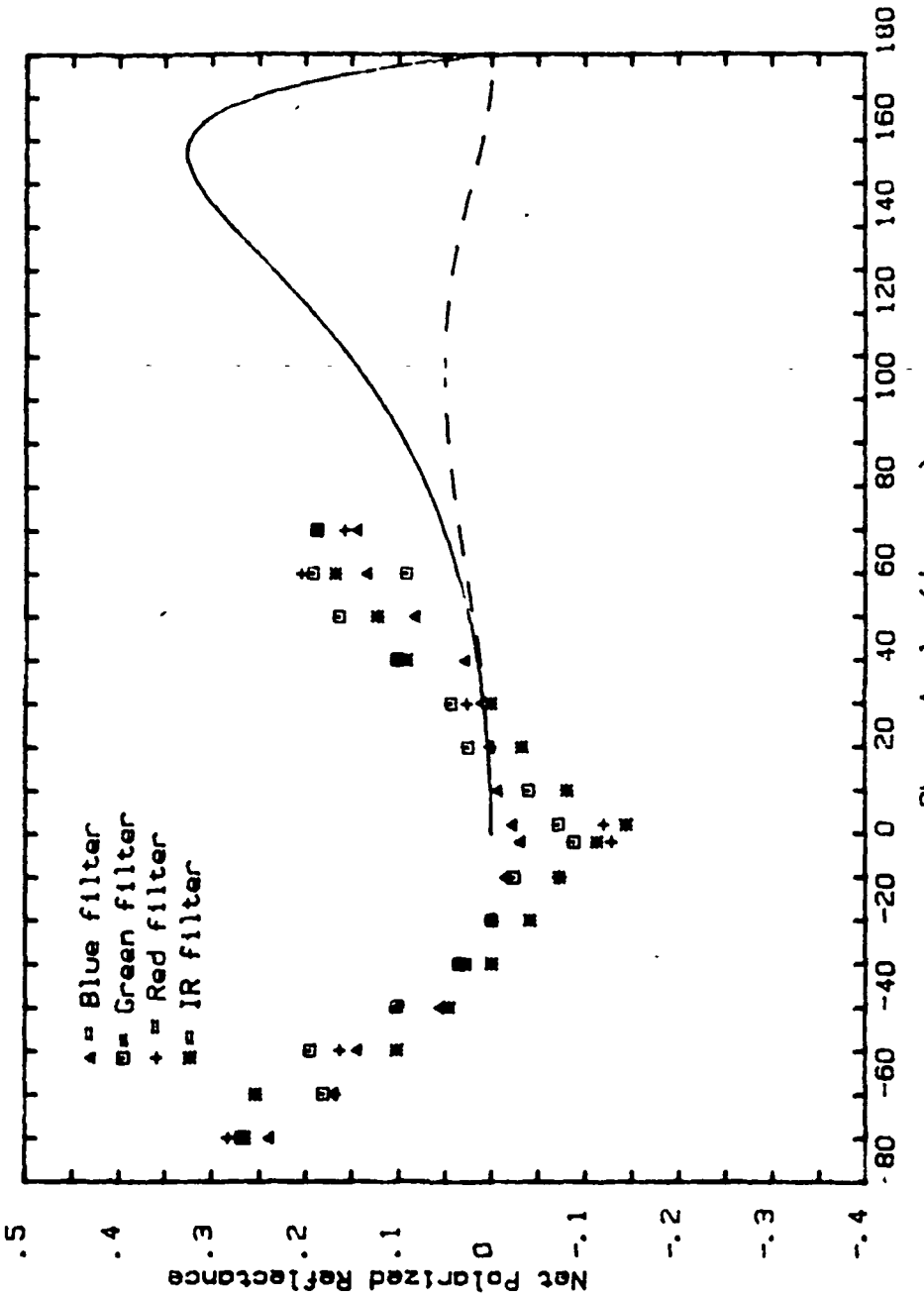

Figure 21a: Net Polarized Reflectance vs. Phase Angle. Looking at the soil the clover grew in, baked between a temperature of 100-250°C, at e=0. The solid line denotes the calculated Fresnel coefficients (eq. 8), using n=1.55. The dashed line denotes the shadowed Fresnel difference (eq.10).

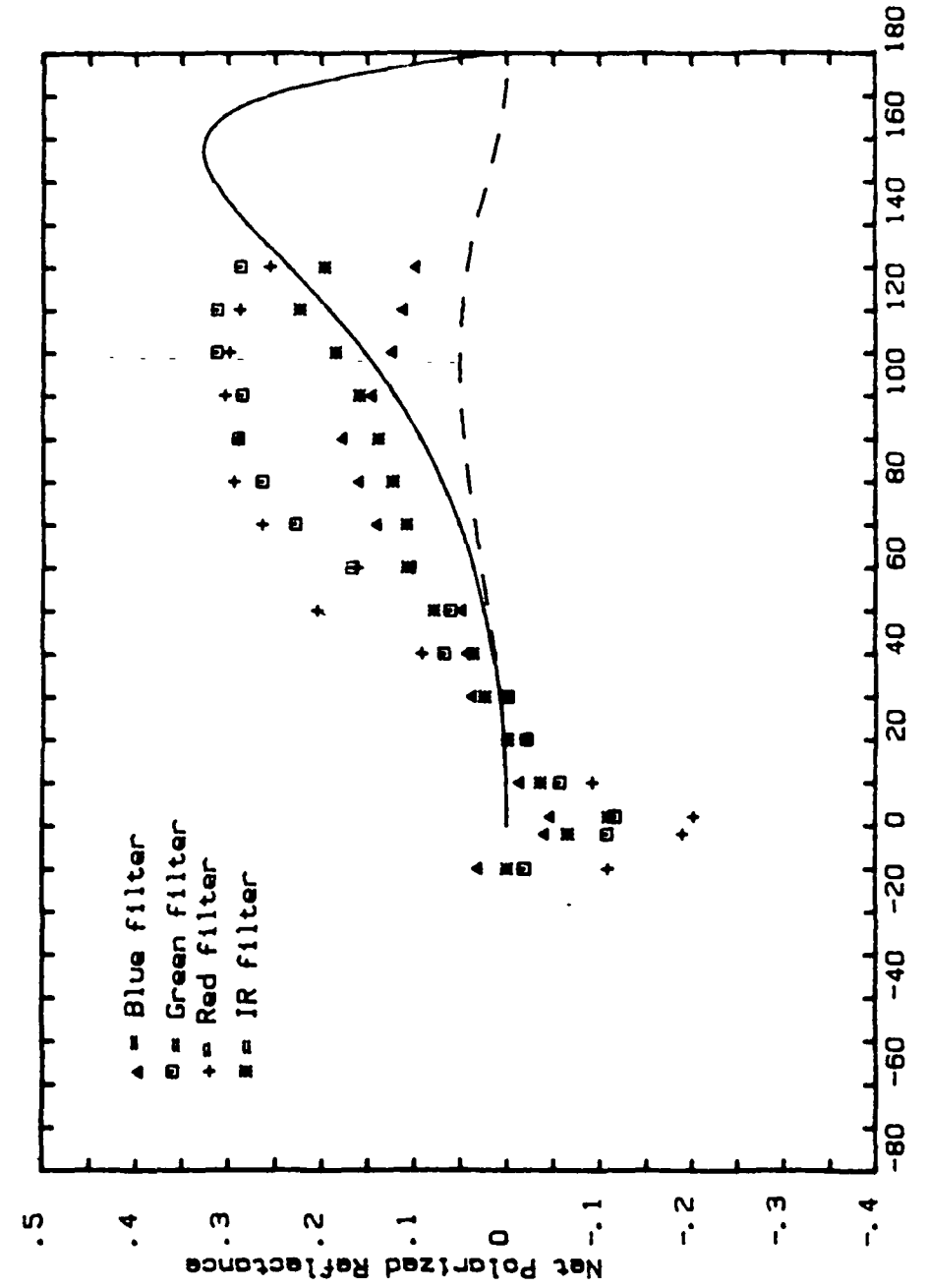

Figure 21b: Net Polarized Reflectance vs. Phase Angle. Looking at the soil the clover grew in, baked between a temperature of 100-250°C, at e=60°. The solid line denotes the calculated Fresnel reflection coefficients (eq.8), using n=1.55. The dashed line denotes the shadowed Fresnel reflectance difference (eq.10).

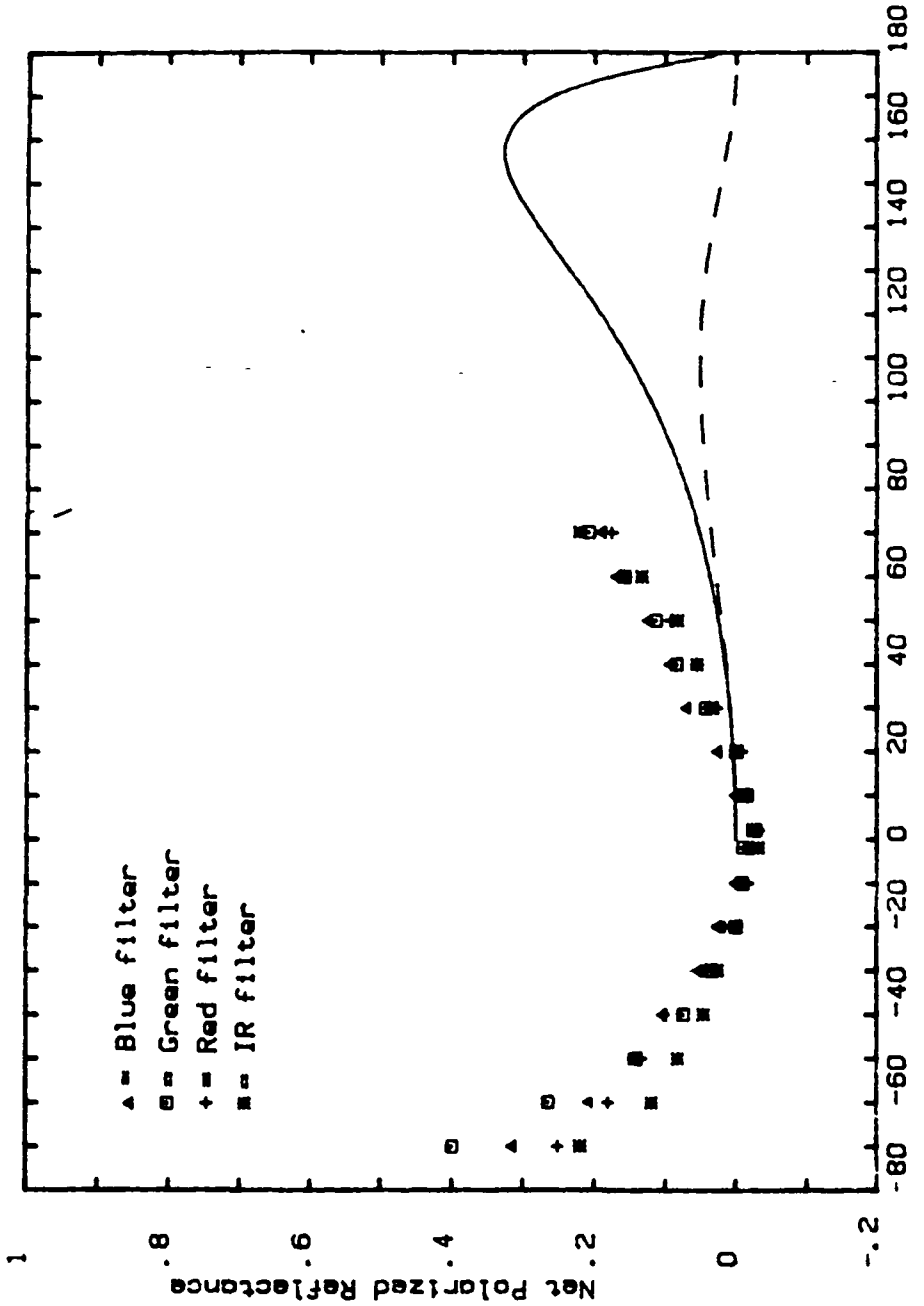

Figure 22d. Net Polarized Reflectance vs. Phase Angle. Looking at the soil the clover grew in moistened by water, at e=0°. The solid line denotes the calculated Fresnel reflection coefficients (eq 8), using n=1.55. The dashed line denotes the shadowed Fresnel reflectance difference (eq.10).

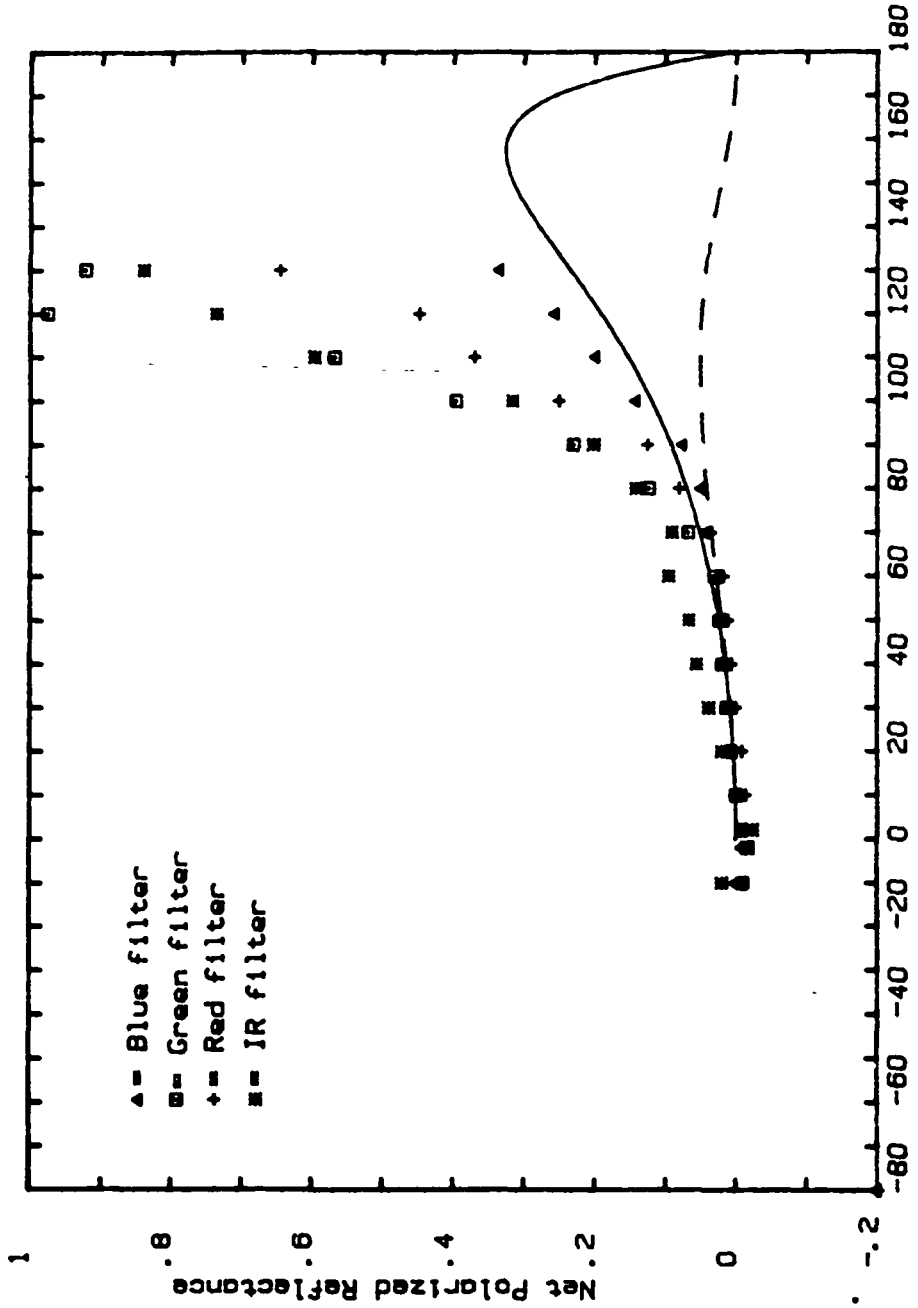

Figure 22b: Net Polarized Reflectance vs. Phase Angle. Looking at the soil the clover grew in, moistened by water, at e=60°. The solid line denotes the calculated Fresnel reflection coefficients (eq.8), using n=1.55. The dashed line denotes the shadowed Fresnel reflectance difference (eq 10).

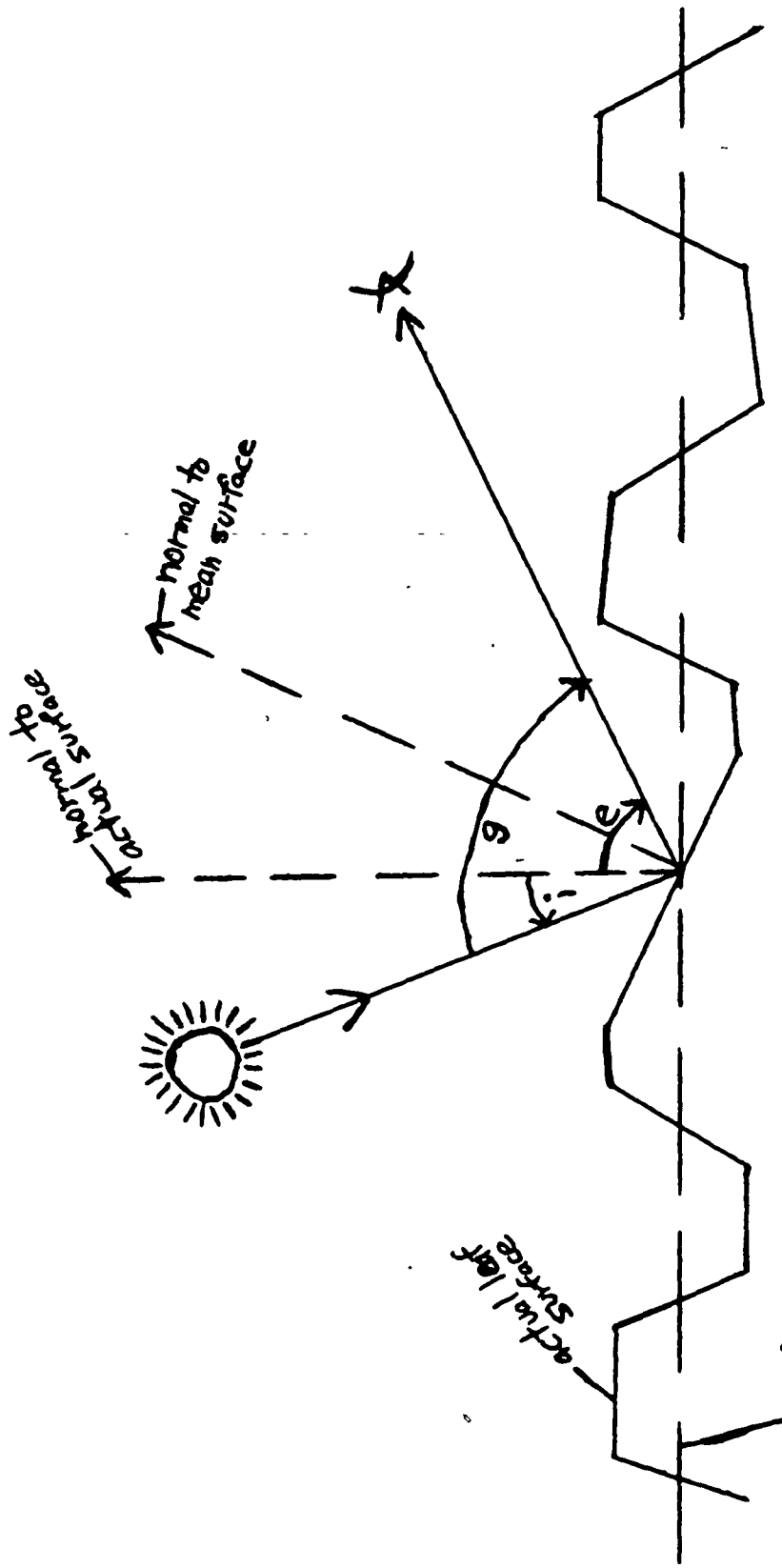

Figure 23: Specular reflection of light from the surface of a leaf.

We used a scanning electron microscope to examine the top and bottom surface of a leaf, and found that they were indeed rough, as predicted. The top surface is covered with shadow-casting structures that are approximately 9000 nm long, 1500 nm wide and 1500 nm high. The stomata on the bottom surface are approximately 1000 nm wide and 10,000 nm long.

5. Conclusions

From this work we drew the following conclusions:

1) Transmitted light is negatively polarized (cf. figures 8d and 19b). Therefore, its effects on polarization cannot be neglected.
2) Leaf surface roughness introduces shadowing factors which require the Fresnel reflection coefficients in the scattering from individual leaf surfaces to be multiplied by approximately $\cos^2(g/2)$.
3) As shown in figures 17-19 (except 19b) the measured values of x and y are significantly higher than $(F_+ - F_-)\cos^2(g/2)$. This result implies that when considering only light scattered into the upward hemisphere, the major contribution to the polarization is not only partially-shadowed Fresnel reflection from the upper leaf surfaces, as hypothesized, but also includes a significant contribution from the volume-scattered and multiply-scattered

components of light. Light transmitted through the leaf canopy is negatively polarized rather than unpolarized.

4) As shown in figures 18-19, negative polarization is intrinsic to the single leaf ("particle"). Negative polarization is not just due to double scattering between leaves ("particles").
5) The primary independent variable controlling the polarization is g, with i and e having only secondary effects.
6) The reflectance and polarization of patches are averages between those of individual leaves in vertical and horizontal positions.
7) The opposition effect is pronounced for the vegetation patches, while it is small or missing in the individual leaf.
8) If other vegetation has similar properties to clover and grass, then the polarization expected from a Landsat type of observation at the four wavelengths, is as follows. Through the blue filter, the polarization is approximately 11% for the clover patch and 2.7% for the grass. Through the green filter, the polarization is approximately 5% for the clover and 2.3% for the grass. Through the red filter, the polarization is approximately 5.7% for the clover and 1.5% for the grass. Finally, through the IR filter, the polarization is approximately 2.2% for the clover patch and 1.7% for the grass.

Acknowledgement

This research was supported by a grant from the National Aeronautics and Space Administration, Earth Survey Applications Division.

BIBLIOGRAPHY

Bibliography

Bloss, F. Donald, 1961, An Introduction to the Methods of Optical Crystallography, Holt, Rinehart and Winston, Inc.: Philadelphia, 294 p.

Chandrasekhar, S., 1960, Radiative Transfer, Dover: New York, 393 p.

Considine, Douglas M., ed., 1983, Van Nostrand's Scientific Encyclopedia (6th edition), Van Nostrand Reinhold Co.: New York, 3067 p.

Curtis, Helena, 1983, Biology (4th edition), Worth Publishers: New York, 1159 p.

Egan, W.G. and Hallock, H.B., 1966, Polarimetry Signature of Terrestrial and Planetary Materials: Proceedings of the Fourth International Symposium of Remote Sensing of the Environment, p. 671-689.

Gates, David M., Keegan, Harry J., Schleter, John C. and Weidner, Victor R., 1965, Spectral Properties of Plants: Applied Optics, v. 4, p. 11-20.

Hapke, Bruce, 1971, Optical Properties of the Lunar Surface in Kopal, Z., ed., Physics and Astronomy of the Moon (2nd edition): New York, Academic Press, p. 155-211.

Hapke, Bruce, 1981, Bidirectional Reflectance Spectroscopy 1. Theory: Journal of Geophysical Research, v. 86, p. 3039-3054.

Hapke, Bruce, 1984, Bidirectional Reflectance Spectroscopy 3. Correction for Macroscopic Roughness: Icarus, v. 59, p. 41-59.

Lintz, Joseph and Simonett, David S., 1976, Sensors for Spacecraft in Lintz, J. and Simonett, D.S., ed., Remote Sensing of the Environment: Reading, Mass., Addison-Wesley Publishing Co., p. 323-343.

Lyot, B., 1929, Research on the Polarization of Light from Planets and from Some Terrestrial Substances: Annales de l'Observatoire de Paris, Section de Meudon, v. 8, #1 (English Translation: NASA TT F-187, 1964).

Myers, Victor I., 1983, Remote Sensing Applications in Agriculture in Colwell, Robert N., ed., Manual of Remote Sensing: Falls Church, Va., American Society of Photogrammetry, p. 2111-2228.

Raines, Gary L. and Carey, Frank, 1980, Vegetation and Geology in Siegal, B.S. and Gillespie, A.R., ed., Remote Sensing in Geology: New York, John Wiley and Sons, p. 365-380.

Tucker, Compton J. and Garratt, Michael W., 1977, Leaf Optical System Modeled as a Stochastic Process: Applied Optics, v. 16, p. 635-642.

Vanderbilt, V.C., 1980, A Model of Plant Canopy Polarization Response: Sixth Annual Symposium on Machine Processing of Remotely Sensed Data, p. 98-108.

Vanderbilt, V.C., Biehl, L.L., Robinson, B.F., Bauer, M.E. and Vanderbilt, A.S., 1982, Linear Polarization of Light by Two Wheat Canopies Measured at Many View Angles: International Colloquium on Spectral Signatures of Objects in Remote Sensing, p. 217-224.

Weidner, V.L. and Hsia, J.J., 1981, Reflection Properties of Pressed Poly-tetrafluoroethylene Powder: Journal of the Optical Society of America, v. 71, p. 856-881.

Wolff, Milo, 1975, Polarization of Light Reflected from Rough Planetary Surface: Applied Optics, v. 14, p. 1395-1405.